OCS Study
MMS 96-0055

Ecosystem Analysis of the Louisiana Bight and Adjacent Shelf Environments

Volume I: The Fate of Organic Matter and Nutrients in the Sediments of the Louisiana Bight

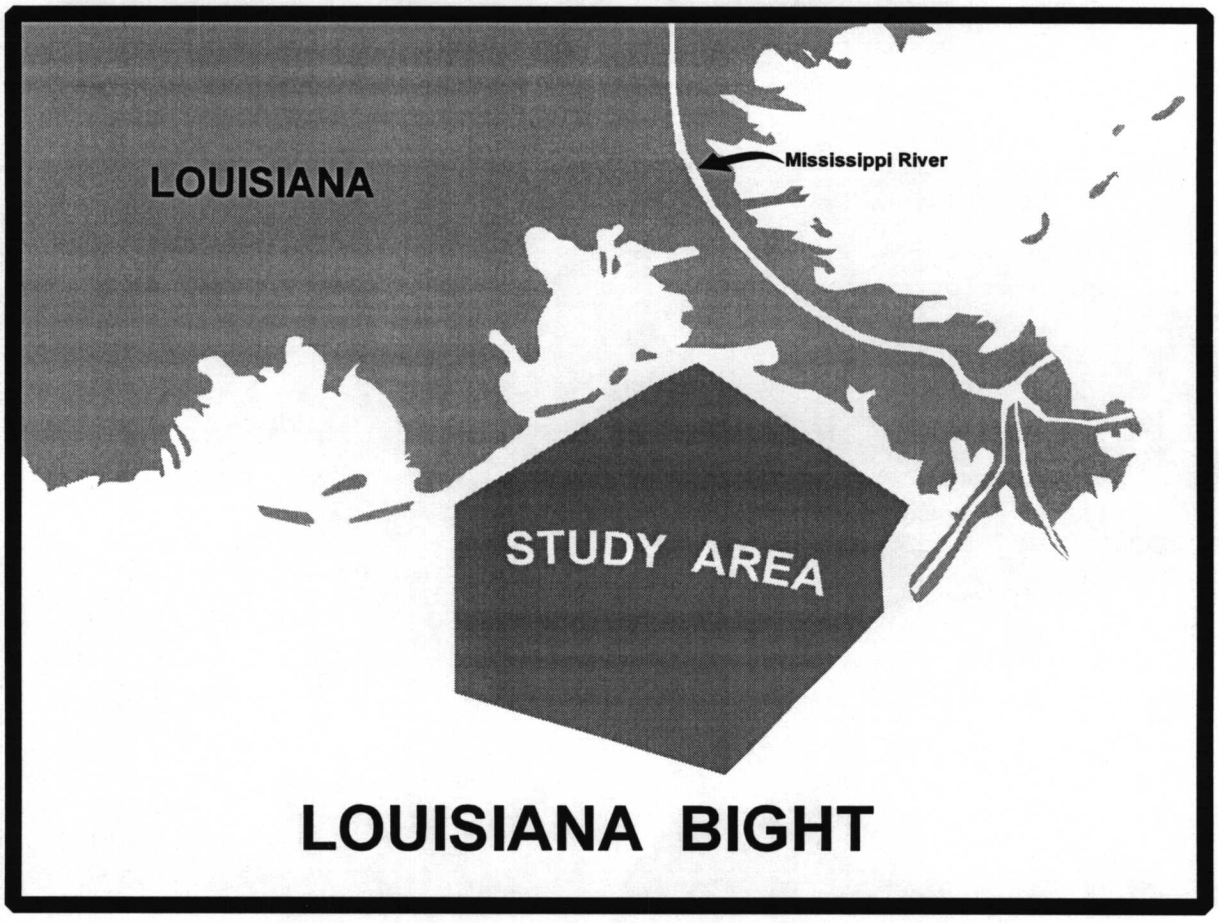

MMS U.S. Department of the Interior
Minerals Management Service
Gulf of Mexico OCS Region

OCS Study
MMS 96-0055

Ecosystem Analysis of the Louisiana Bight and Adjacent Shelf Environments

Volume I: The Fate of Organic Matter and Nutrients in the Sediments of the Louisiana Bight

Authors

Robert R. Twilley
Brent A. McKee

Prepared under MMS Cooperative Agreement
14-35-0001-30696
by
University of Southwestern Louisiana
Department of Biology
Lafayette, Louisiana 70506

Published by

U.S. Department of the Interior
Minerals Management Service
Gulf of Mexico OCS Region

New Orleans
November 1996

DISCLAIMER

This report was prepared under a cooperative agreement between the University of Southwestern Louisiana (USL) and the Minerals Management Service (MMS). This report has been technically reviewed by USL and MMS, and it has been approved for publication. Approval does not signify that the contents necessarily reflect the views and policies of the Service, nor does mention of trade names or commercial products constitute endorsement or recommendation for use. It is, however, exempt from review and compliance with MMS editorial standards.

REPORT AVAILABILITY

Extra copies of this report may be obtained from the Public Information Office (Mail Stop 5034) at the following address:

U.S. Department of the Interior
Minerals Management Service
Gulf of Mexico OCS Region
Attention: Public Information Office (MS 5034)
1201 Elmwood Park Boulevard
New Orleans, Louisiana 70123-2394

Telephone: (504) 736-2519 or
1-800-200-GULF

CITATION

Suggested citation:

Twilley, R.R. and B. McKee. 1996. Ecosystem Analysis of the Louisiana Bight and Adjacent Shelf Environments. Volume I: The Fate of Organic Matter and Nutrients in the Sediments of the Louisiana Bight. OCS Study MMS 96-0055. U.S. Dept. of the Interior, Minerals Mgmt. Service, Gulf of Mexico OCS Region, New Orleans, La. 129 pp.

CONTRIBUTORS

Greg Booth
Louisiana Universities Marine Center, Louisiana Universities Marine Consortium
Chauvin, LA 70344

John Bourgeois
University of Southwestern Louisiana, Department of Biology, Lafayette, LA 70504

Brent McKee
Louisiana Universities Marine Center, Louisiana Universities Marine Consortium
Chauvin, LA 70344

Tina Miller-Way
University of Southwestern Louisiana, Department of Biology, Lafayette, LA 70504

Robert R. Twilley
University of Southwestern Louisiana, Department of Biology, Lafayette, LA 70504

Peter Swarzenski
Louisiana Universities Marine Center, Louisiana Universities Marine Consortium
Chauvin, LA 70344

Terry Whitledge
University of Texas at Austin, Marine Science Institute, Port Aransas, TX 78373

PREFACE

The interrelationships among rates of material cycling through both benthic and water-column communities play an important role in the ultimate fate of inorganic nutrients and organic matter within coastal ecosystems (Figure 1). The coupling of benthic and pelagic processes contributes to elevated rates of primary productivity in coastal ecosystems by recycling nutrients in the water column and across the sediment-water interface. In the Louisiana Bight, high concentrations of suspended sediments and nutrients are introduced from the Mississippi River to a quiescent shallow shelf ecosystem and are thus either quickly deposited to the seabed in the near proximal zone of the plume region or utilized to support highly productive zones at the outer fringes of the front. Thus the seabed of the plume region may received high inputs of particulates of either terrigenous origin or from organic production in the water column. The fate of this particulate material that reaches the seabed of the Louisiana Bight is the focus of this report.

A research program at the University of Southwestern Louisiana and Louisiana Universities Marine Consortium Marine Center (LUMCON) was initiated to study the biogeochemistry of the Louisiana Bight. This research effort was initially funded by the Louisiana Board of Regents through a program entitled Louisiana Stimulus for Excellence in Research (LASER). A grant entitled "Development of a research emphasis in oceanographic processes on continental shelves influenced by large rivers" was funded in 1987 to LUMCON, USL, and LSU (Grant No. 86-LUM (1)-083-13; Dr. Mike Dagg, Principal Investigator) to develop an interdisciplinary study of the Mississippi River plume over the Louisiana Bight region. Robert Twilley was funded to study benthic nutrient regeneration in the initial LASER study, and when Brent McKee arrived at LUMCON, he was later added to the research effort to study sediment dynamics in the seabed of the region. These two individual efforts were gradually coordinated through the development of this 5-yr LASER program to study the deposition, burial and remineralization of nutrients at the sediment-water interface in the plume region.

The LASER program funded ship time, but had limited resources for analytical support for the research efforts to study benthic processes in the plume region of the Louisiana Bight. Additional ship time to the LASER program was provided by a grant from the National Science Foundation (R11-8820219) allowing a total of six cruises from August 1987 to October 1990. However, much of the sediment analyses, particularly the 42-station survey of geochronologies and nutrient concentration in the plume region, were not supported by the LASER program. This report provides the technical summary of information from the LASER program in addition to support by the Mineral Management Service (Cooperative Agreement No. 14-35-0001-30696) to complete analyses of sediment and pore-water samples that were collected during the LASER cruises. During the MMS grant period, we were also able to specifically test some ideas on the importance of selected sediment characteristics on benthic nutrient regeneration with funding from the National Science Foundation, Coastal Ocean Margin Uranium Study (COMUS), by providing ship time for two additional cruises to the study area. Thus, a total of eight cruises are summarized in this report of benthic processes in the plume region of the Louisiana Bight. The conceptual model that has guided this research program in the benthic biogeochemistry of the Louisiana Bight is described in Figure 1 and is provided as an overview of the ecological processes in this river-dominated shelf ecosystem.

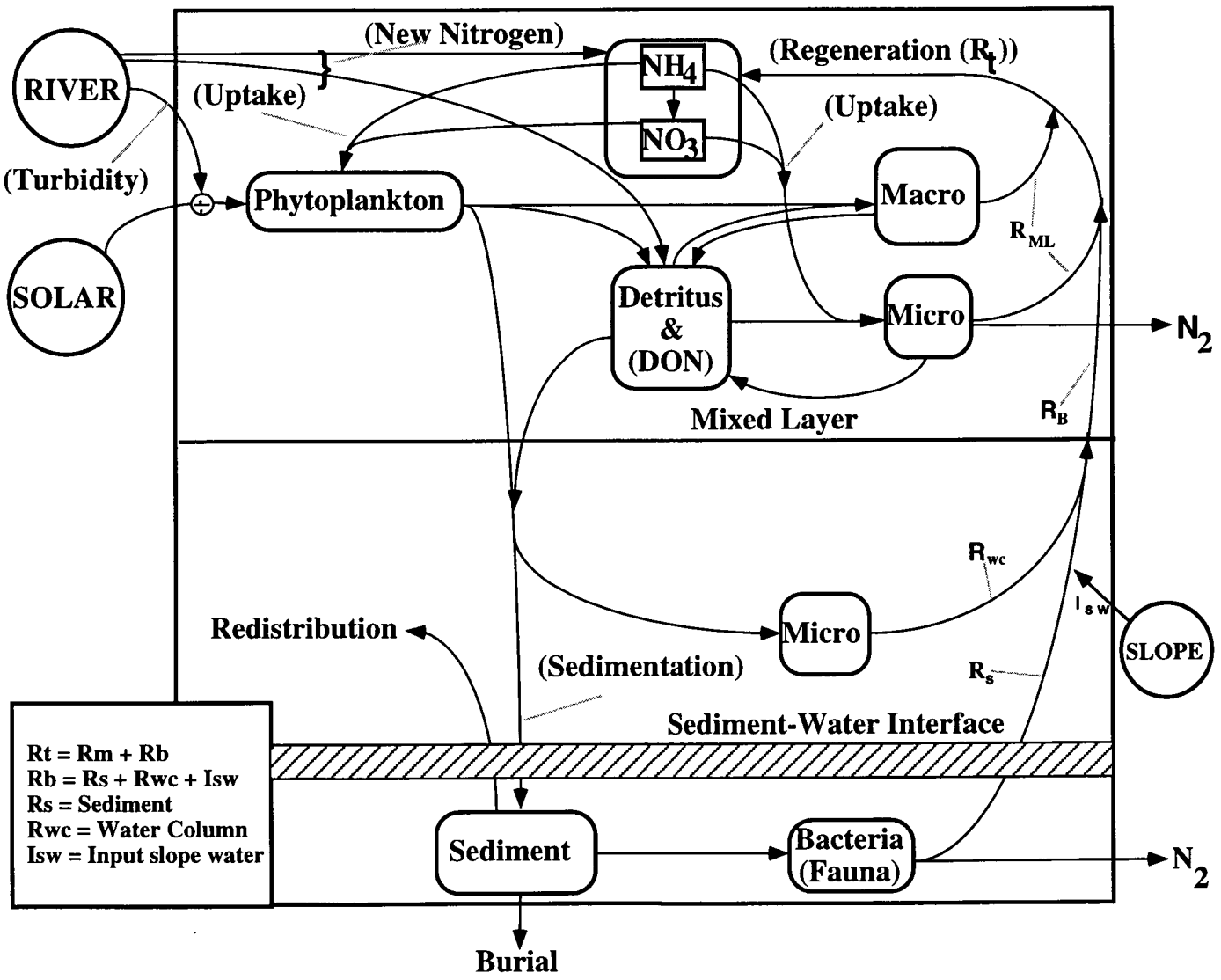

Figure 1 Conceptual diagram of the ecological processes of the Louisiana shelf ecosystem showing sources of new nutrients and pathways of regenerated nutrients. Sediments and nutrients from the pelagic zone are deposited to the seabed and either regenerated, redistributed, or buried in the sediments.

ABSTRACT

The major objective of the LASER and COMUS projects was to determine the role of benthic processes in affecting the fate of sediments and nutrients in a river dominated shelf ecosystem. This technical report describes studies to understand the coupling of the fifth largest river system in the world to coastal margin ecosystems in the plume region of the Louisiana Bight. Chapters in this technical summary describe the accumulation and regeneration of sediment, carbon, nitrogen, and phosphate from the seabed in the plume region of the Louisiana Bight. Strong variation in sedimentation and nutrient accumulation rates in 5417 km^2 plume region of the Louisiana Bight indicate the problem of accurately determining reliable estimates for these processes in river-dominated shelf ecosystems. The area-weighted sedimentation rate was 4,442 g m^{-2} yr^{-1}, carbon accumulation was 64, nitrogen 7.02 and phosphorus 2.89 g m^{-2} yr^{-1}. Results reveal that approximately 30% of the particulate organic carbon supplied by the Mississippi River to the adjacent shelf is remineralized within 4 months and an additional 40% is remineralized on a decadal time scale. Based on these results, combined with similar information from the Amazon, Changjiang and Huanghe Rivers, we conclude that only 30% of the particulate organic carbon supplied to the ocean by rivers is buried. Our area-weighted estimate of organic carbon burial in deltaic-shelf sediments is 75 gC m^{-2} yr^{-1} with less than 50% of the organic carbon buried being of terrestrial origin. The resulting global estimate for terrigenous POC burial is 0.05 PgC yr^{-1}, representing less than half the value currently used to constrain global CO_2 budgets (Sarmiento and Sundquist 1992).

Seasonal deposition of allochthonous organic matter during spring provides the predominant mechanism for sustaining peak rates of benthic regeneration in the plume region of the shelf. During April, ammonium regeneration in the plume region (station B50 and C50) may exceed 500 µmol m^{-2} h^{-1}, compared to fluxes of less than 200 µmol m^{-2} h^{-1} during low river discharge in September and October. Further downfield (stations D50 and E50), ammonium regeneration is generally less than 200 µmol m^{-2} h^{-1}. Seasonal differences in benthic regeneration are most evident nearest the mouth of the Mississippi River, while rates are more constant both temporally and spatially in more distant regions. The link between sediment deposition and benthic nutrient regeneration is clearly demonstrated in results of silicate flux at near and far - field stations on the Louisiana Bight. Fluxes of silicate across the sediment-water interface to the water column increase linearly with deposition rates from 0.3 to 2.5 cm/mo, reaching maximum silicate flux rates of 550 µmol m^{-2} h^{-1}. Above a deposition rate of 2.5 cm/mo, silicate flux was lower at less than half the maximum rates. However, there was no clear pattern in ammonium or phosphate regeneration with bulk deposition of sediments in the study area; suggesting that the quality of material must also be evaluated.

Rates of benthic nutrient flux tended to decrease with distance from the riverine source, and exhibited contours of rates similar to patterns of sedimentation and nutrient accumulation. Modeling nutrient fluxes from pore-water gradients showed little correlation to the actual measured nutrient flux; however these sediment characteristics do provide explanations for outliers in benthic regeneration rates. Benthic fluxes always showed a higher correlation to some qualitative index (input of carbon, nitrogen, phosphorus, or chlorophyll a) of deposition to the seabed than to the quantitative input of sediment. The combination of geochronologies on time scale of months and decades along with repeated measures of benthic nutrient regeneration provide spatial and temporal resolution of these benthic processes in this river-dominated continental shelf ecosystem.

TABLE OF CONTENTS

LIST OF FIGURES

LIST OF TABLES

ACKNOWLEDGMENTS

We would like to especially thank Ms. Claudia Muñoz for her skills in organizing and producing this technical report. This project supported John Bourgeois, Washington Cárdenas, and Jorge Espinoza that provided much of the technical and analytical work on the benthic samples. John and Washington both completed Master of Science degrees at USL during this project with significant contributions to understanding nutrient dynamics in continental margin ecosystems. Tina Miller-Way directed most of the benthic flux studies during LASER 4-6 and provided many of the calculations and statistical analyses of these flux rates. Terry Whitledge provided analytical support as nutrient assays with an autoanalyzer aboard the RV Pelican during all six of the LASER cruises. The National Science Foundation COMUS (Coastal Ocean Margin Uranium Study) program (Brent McKee, Principal Investigator) supported two additional cruises to the study region. The authors would like to thank J. Greg Booth, Laura Lawton, and Peter Schwarzenski for their help in the field and laboratory assistance during these projects. Many thanks also go out to the following for various degrees of technical and/or analytical support: Robert Bourgeois, Ronghua Chen, John Foret, Russell Garrett, Mike Radford, Patricia Rafferty, Victor Rivera-Monroy, and the captain and crew of the R/V Pelican.

Chapter 1

INVENTORY OF SEDIMENTATION AND NUTRIENT ACCUMULATION IN THE SEDIMENTS OF THE LOUISIANA BIGHT

1.1 Introduction

The interrelationships among rates of material cycling through both benthic and water-column communities play an important role in the ultimate fate of inorganic nutrients and organic matter within coastal ecosystems (Nixon 1981, Glibert 1982, Harrison et al. 1983, Kemp and Boynton 1984, Aller et al. 1985). The coupling of benthic and pelagic processes contributes to elevated rates of primary productivity in land margin ecosystems by sequestering nutrients in the coastal zone (Zeitzschel 1980, Boynton et al. 1982, Fisher et al. 1982, Klump and Martens 1983, Boynton and Kemp 1985). Rates of in situ nutrient remineralization may be equivalent to allochthonous inputs of inorganic and organic nutrients (Fisher et al. 1982, Nixon and Pilson 1983, Pennock 1987). Over short time scales, nitrogen remineralization from the sediments and water column may provide a significant proportion of the nitrogen required to support primary production. Over longer time periods, the balance between sediment deposition and remineralization rates determines the burial and loss of organic nutrients from the ecosystem (McKee et al. 1983, DeMaster et al. 1985). Quantifying the time and spatial scales of these major sediment processes that influence the availability of nitrogen and fate of carbon (e.g. mineralization and burial) are therefore essential to understanding the utilization of organic matter in the Louisiana shelf ecosystem (Dagg et al. 1991).

Nutrient concentration and production/sediment trap data indicate that nutrient inputs stimulate high rates of primary production and that these nutrients are quickly sequestered into organic matter in the water-column. Individual studies indicate that the fate of this organic matter appears to vary, at times fluxing to the sediments and undergoing remineralization or transport, while at other times appearing to be efficiently grazed and remineralized in the water column. Previous studies of deposition suggest that the proximal region of the Mississippi River plume is a zone of extreme input of allochthonous particulate material to the seabed. The fate of this organic matter is largely unknown in the Louisiana Bight west of the Mississippi River delta, as well as for other deltaic continental shelves. The objective of this chapter is to determine area weighted storage of sediments, carbon, nitrogen, and phosphorus in this region of the Gulf of Mexico.

These sedimentary processes in the Louisiana Bight give insights into the fate of carbon, nitrogen, and phosphorus in river-dominated continental shelves. The burial of nutrients in continental margins influenced by strong inputs of materials from the land may be significant to the global biogeochemistry of primary nutrients such as carbon, nitrogen, and phosphorus (Figure 1.1). The coupling of land and coastal waters is driven by the transport of rivers and includes detrital material that may be both inorganic sediments and nutrients (N in Figure 1.1) or consists of an organic matrix including dissolved and particulate matter (Organic C in Figure 1.1). The inorganic constituent may be deposited directly to the seabed (such as inorganic sediments) or enhance the production of organic matter in the shallow photic zone (such as nitrogen and phosphorus) in the vicinity of the river plume. At the fronts of river plumes in the region of the Louisiana Bight west of the Mississippi River delta there occurs high concentrations of phytoplankton biomass with rates of organic production exceeding 200 $gC\ m^{-2}\ yr^{-1}$ (Dagg et al. 1991). The deposition of material then is a combination of the river and coastal ocean processes that potentially contributes large loading of material to sediments of

the Louisiana Bight (Figure 1.1). Chapter 1 is an inventory of a survey of sediments and nutrients (carbon, nitrogen and phosphorus) in a study area west of the Mississippi River delta in a region referred to as the Louisiana Bight (Figure 1.2). Together with estimates of sedimentation rates in this region, the amounts of nutrient sequestration in shelf sediments in this region are estimated. In Chapter 2 the carbon burial estimates of this region are compared to loading rates and estimates of carbon remineralization and compared to other river-dominated shelf ecosystems.

1.2 Methods

Box core samples were collected from 42 stations in Mississippi River plume region of the Louisiana Bight (Figure 1.2) during the LASER 3 cruise in April 1989. The location and dates of collection are described in Table 1.1. Depths of water column ranged from 10 to 110 m and nearly 90 km from the mouth of Southwest Pass of the Mississippi River delta. Large diameter (16.5 cm) subcores were taken from box cores at each sampling station. Each core was carefully extruded and simultaneously subsectioned at precise 0.5-1.0 cm intervals. Yield tracers (^{208}Po) were added to the dried core samples, then leached with a combination HNO_3, HCl and $HClO_4$ solution. ^{210}Po is spontaneously deposited onto silver planchets and ^{210}Pb is measured via the polonium method (Nittrouer et al. 1979). Sediment subsamples were assayed for total carbon and nitrogen with a LECO Elemental Analyzer. Total phosphorus was determined by dissolving the ashed samples with HCl and determining PO_4 concentrations. The deposition and accumulation (burial) of carbon, nitrogen and phosphorus in bottom sediments was calculated from the following equation (Hatton et al. 1983): $A = Cd \times R \times D \times 104$ ($g\ m^{-2}\ yr^{-1}$); where A is the rate of nutrient deposition or burial, Cd is the dry mass nutrient concentration, D is bulk density, and R is the sedimentation rate (determined by ^{234}Th or ^{210}Pb).

1.3 Results and Discussion

The range in mean total carbon concentrations among the 42 stations was from 8.30 to 18.13 mg/gdm (Table 1.2 and 1.3). Total carbon concentrations were <10 mg/gdm at D10 and D20, whereas at stations along B, C, D, E, and F concentrations were >12 mg/gdm (Tables 1.2 and 1.3). The stations far-field from Southwest Pass including those along the G and H transect had concentrations <12 mg/gdm.

The range in mean total nitrogen concentrations in the stations of the study area was 0.48 to 2.02 mg/gdm (Tables 1.2 and 1.3). Total nitrogen concentrations followed a similar spatial pattern as total carbon. The near-field stations along the B,C, D, E, and F stations have concentrations > 1.5 mg/gdm, with the exceptions of D10 and D20 that have concentrations <0.8 mg/gdm (Tables 1.2 and 1.3). Total nitrogen concentrations along the G transect are <1.25 mg/gdm and along the H transect are <1.0 mg/gdm. The highest concentration of total nitrogen was 2.02 mg/gdm and occurred at C20 (Table 1.2).

The range in total phosphorus among the stations of the study area was less than for total carbon and total nitrogen at 0.45 to 0.78 mg/gdm (Tables 1.2 and 1.3). Total phosphorus concentrations are all >0.50 mg/gdm along all seven transects except for the D10 and D20 stations that have concentrations <0.5 mg/gdm (Tables 1.2 and 1.3). The highest concentration of total phosphate was 0.78 mg/gdm and recorded at E50.

Carbon:nitrogen ratios (atomic) ranged from 8.2 to 24.3 along the seven transects (Tables 1.2 and 1.3). Ratios <9 occurred at E20 to E60, whereas the higher ratios of 24.3 and 21.1 occurred at H27 and E110, respectively. Nitrogen:phosphorus ratios (atomic) ranged from 2.0 to 6.6 in the Louisiana Bight study area (Tables 1.2 and 1.3). Ratios were <4 at H10 to H50, with a ratio of only 2.0 at H27. Ratios were generally >5 along both the B and C transects.

A representative example of the distribution of Pb-210 near the mouth of Southwest Pass at B50 demonstrates the method of determining accretion rates in the study area (Figure 1.3). The concentrations of Pb-210 were ignored in the top 6-cm section of the core due to resuspension and high sediment turnover. This disturbance to Pb-210 geochronology in surface sediments was evident in the cores along the B and C transects, with much less variance in concentrations with depth at stations farther from the mouth of Southwest Pass.

Low accretion rates at <0.1 cm/yr occurred at only 3 stations including E10, E20, and G27 (Table 1.4). High rates >2.0 cm/yr occurred at 8 stations including all of the stations along the B and C transects, with the exception of C80. The highest rate recorded in the study area was 5.1 cm/yr at D50. The spatial rates in sedimentation in the Louisiana Bight study area followed the patterns of accretion (Table 1.4 and Figure 1.4). Low rates of <0.2 g cm^{-2} yr^{-1} occurred at E10 and E20; whereas highest rates >5.0 g cm^{-2} yr^{-1} occurred at B20, B50, C10, C20, C50, D50, D65, and D80. The contour of sedimentation rates for the study area (Figure 1.4) describe the location of each sampling station and include five zones: >1.6 g cm^{-2} yr^{-1}, 0.8-1.6 g cm^{-2} yr^{-1}, 0.4-0.8 g cm^{-2} yr^{-1}, 0.4-0.2 g cm^{-2} yr^{-1} and <0.2 g cm^{-2} yr^{-1}. The high deposition area is located in the mid-depth regions of the B and C transect near the mouth of Southwest Pass. There are two locations of the low deposition zone, one near the shore in the northeast region of the study area and the other region far-field from Southwest Pass and including most of transect H and the deeper sections of F and G transects.

Carbon accumulation among the 42 stations ranged from 493.6 to 1.4 gC m^{-2} yr^{-1} (Table 1.4) and followed patterns of sedimentation in the study area (Figure 1.5). The implications of this pattern of carbon accumulation to fate of carbon in this river-dominated shelf region is discussed in Chapter 2. Total nitrogen accumulation rates ranged from 54.4 to 0.2 gN m^{-2} yr^{-1} (Table 1.4). The pattern of nitrogen accumulation on the shelf includes a zone near the mouth of Southwest Pass with rates >30 gN m^{-2} yr^{-1} and two zones of lower rates <5 gN m^{-2} yr^{-1} along the northeast corner of the study area and along the western edge of the region (Figure 1.6). There is a sharp change in nitrogen accumulation rates from >30 to <5 gN m^{-2} yr^{-1} at the 50-80 m depths at the C to E transects. Total phosphate accumulation rates ranged from 21.7 to 0.1 gP m^{-2} yr^{-1} in the study area (Table 1.4). The contours of total phosphate burial rates are similar to Figure 1.6 for nitrogen.

The such strong variation in burial rates of sediment, carbon, nitrogen and phosphorus in the plume region of the Louisiana Bight requires some spatially weighed estimate of average accumulation. Single cores vary by several orders of magnitude in rates of sedimentation and nutrient accumulation within 40 km of Southwest Pass (Figures 1.4-1.6 and Table 1.4). We used five sections of the study area based on the magnitude of sedimentation rates to determine an area weighted estimate of total nutrient burial in the study area (Table 1.5). The section with highest rates of sedimentation (section A) had an area of 326 km^2 (6 % of total) compared to minimum rates that had an area of 2383 km^2 (44 % of total). More than 50% of the total study area of 5417 km^2 included the two lowest ranges in sedimentation rates (Table 1.5). The average sedimentation rate for the study area was 4,442 g m^{-2} yr^{-1}. The average carbon

accumulation rate was 64 gC m^{-2} yr^{-1} (Table 1.5). The area-weighted average nitrogen accumulation rate was 7.02 gN m^{-2} yr^{-1} and total phosphate was 2.89 gP m^{-2} yr^{-1} (Table 1.5).

Coastal and shelf sediments may be considered large reservoirs of deposited nutrients that are not regenerated to the water column. The relative magnitude of burial is controlled by the quantity and quality of particulate material supplied to bottom sediments (Zeitzschel 1980; Klump and Martens 1983). Annual rates of nitrogen accumulation in the plume region of the Louisiana Bight range from 0.16 to 57 gN m^{-2} yr^{-1} (Figure 3). Rates are highest along the 50-m depth contour near the mouth of southwest pass of the Mississippi River. The maximum rate of nitrogen burial is 465 µmol m^{-2} h^{-1}; equivalent to higher estimates of ammonium regeneration in this region of the shelf (Chapter 3).

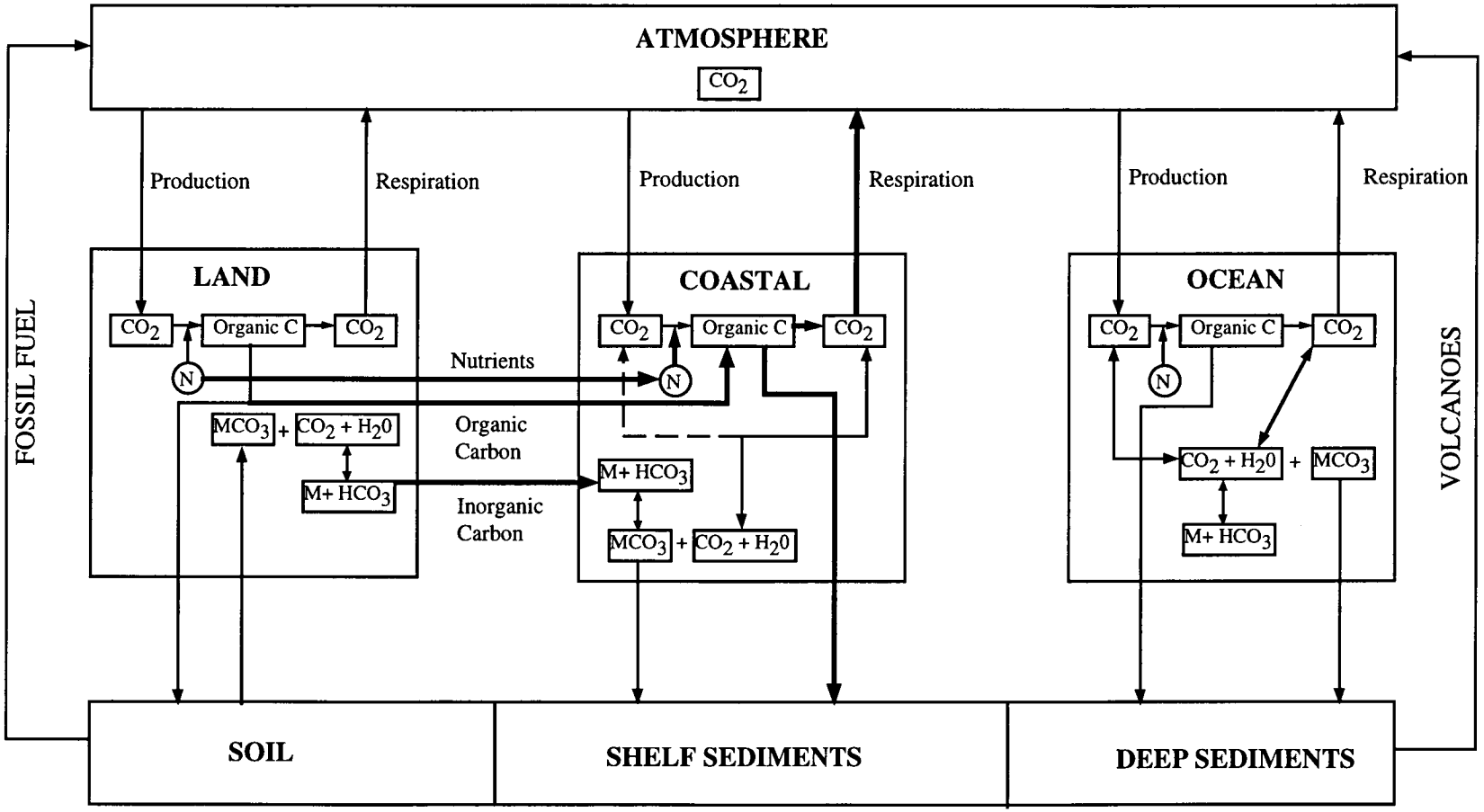

Figure 1.1. Diagram of the global carbon cycle between the atmosphere, biosphere, and lithosphere. The biosphere is separated into three subcompartments including land, coastal ocean, and deep ocean. Linkages between the land and coastal ocean include organic and inorganic carbon, as well as nutrients that stimulate photosynthesis in the sea.

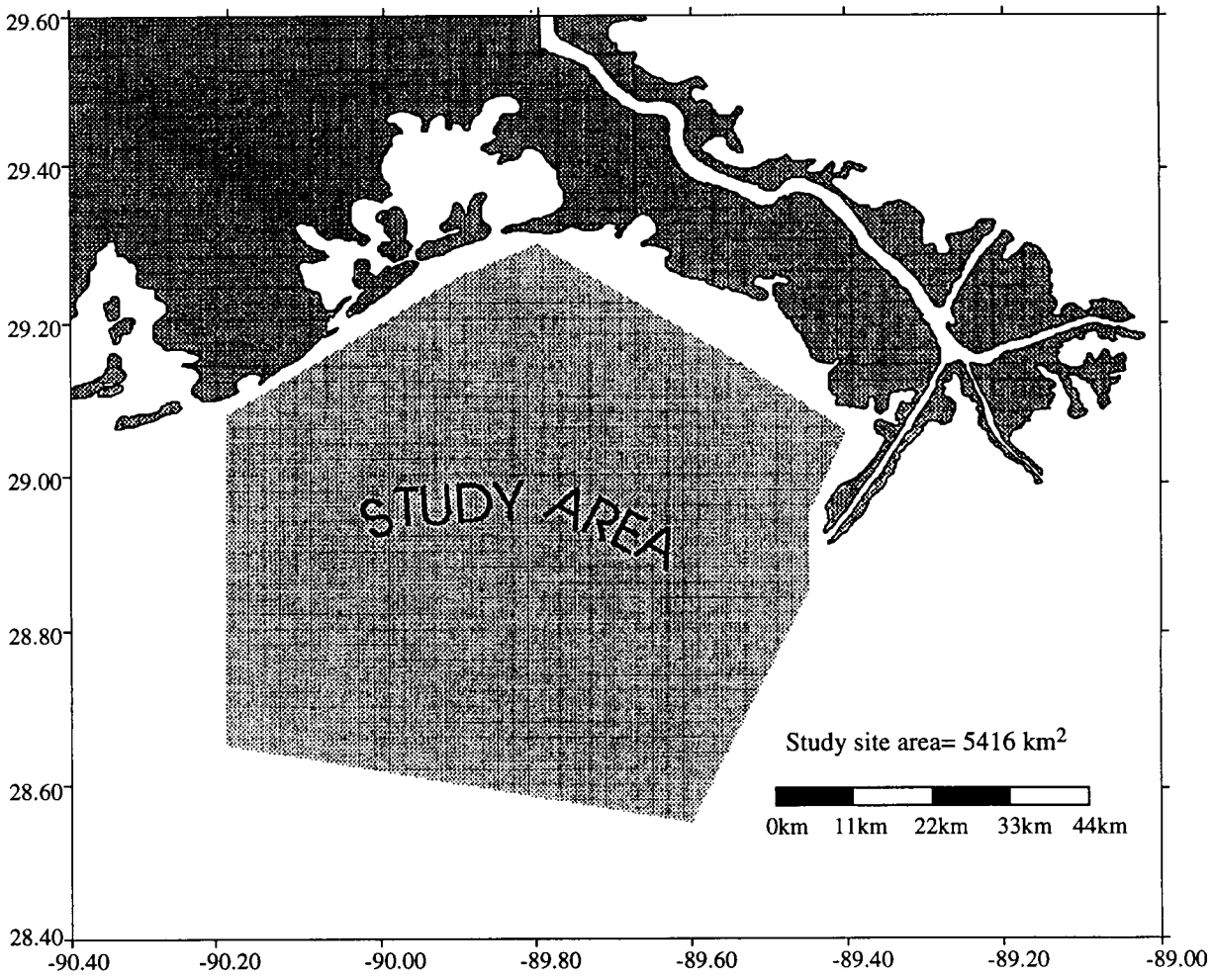

Figure 1.2. Region of the Louisiana Bight that was the study area for estimates of sediment and nutrient accumulation.

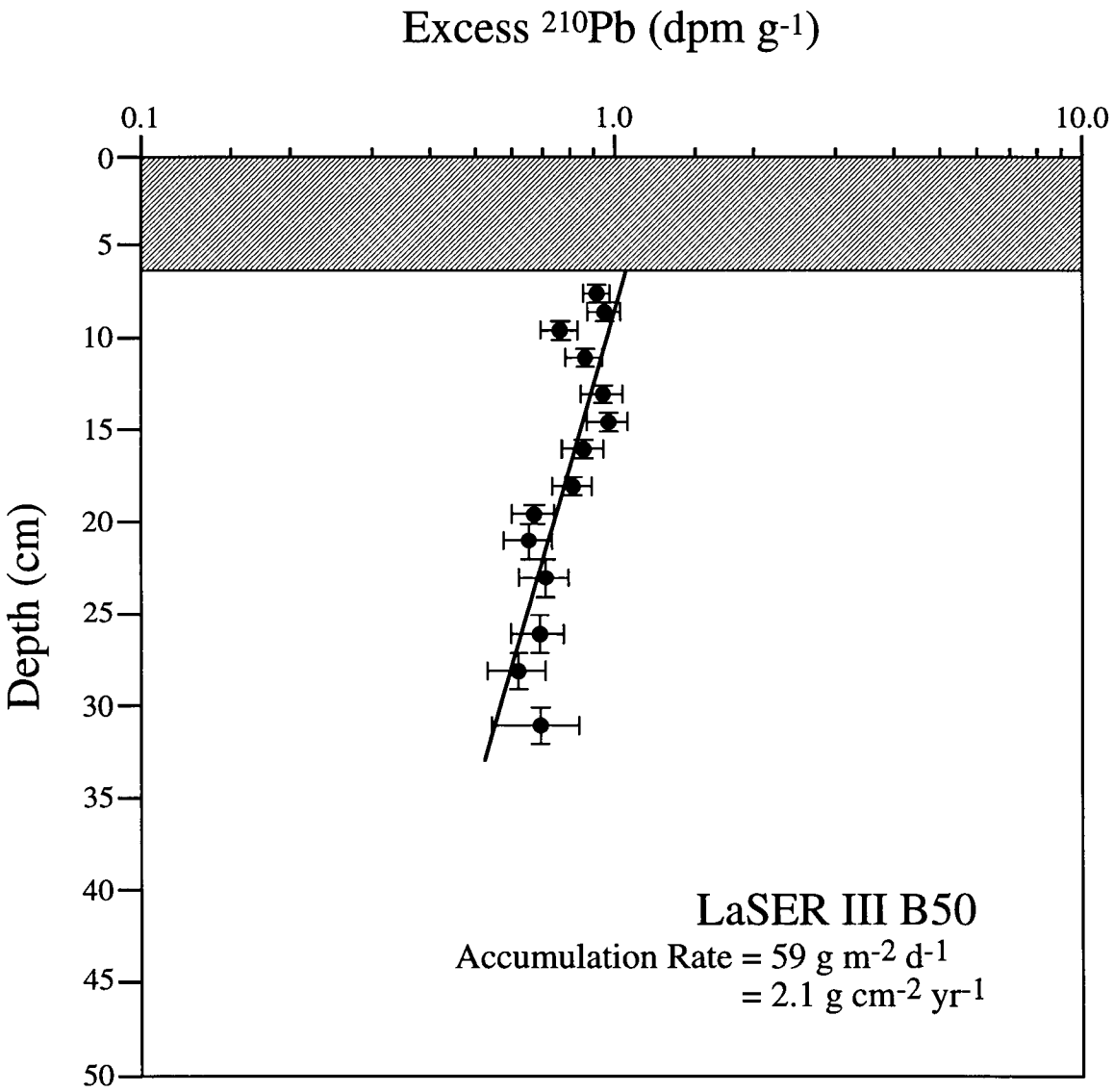

Figure 1.3. Diagram of Pb-210 distribution with depth in sediments of station B50 showing typical geochronology in high deposition area.

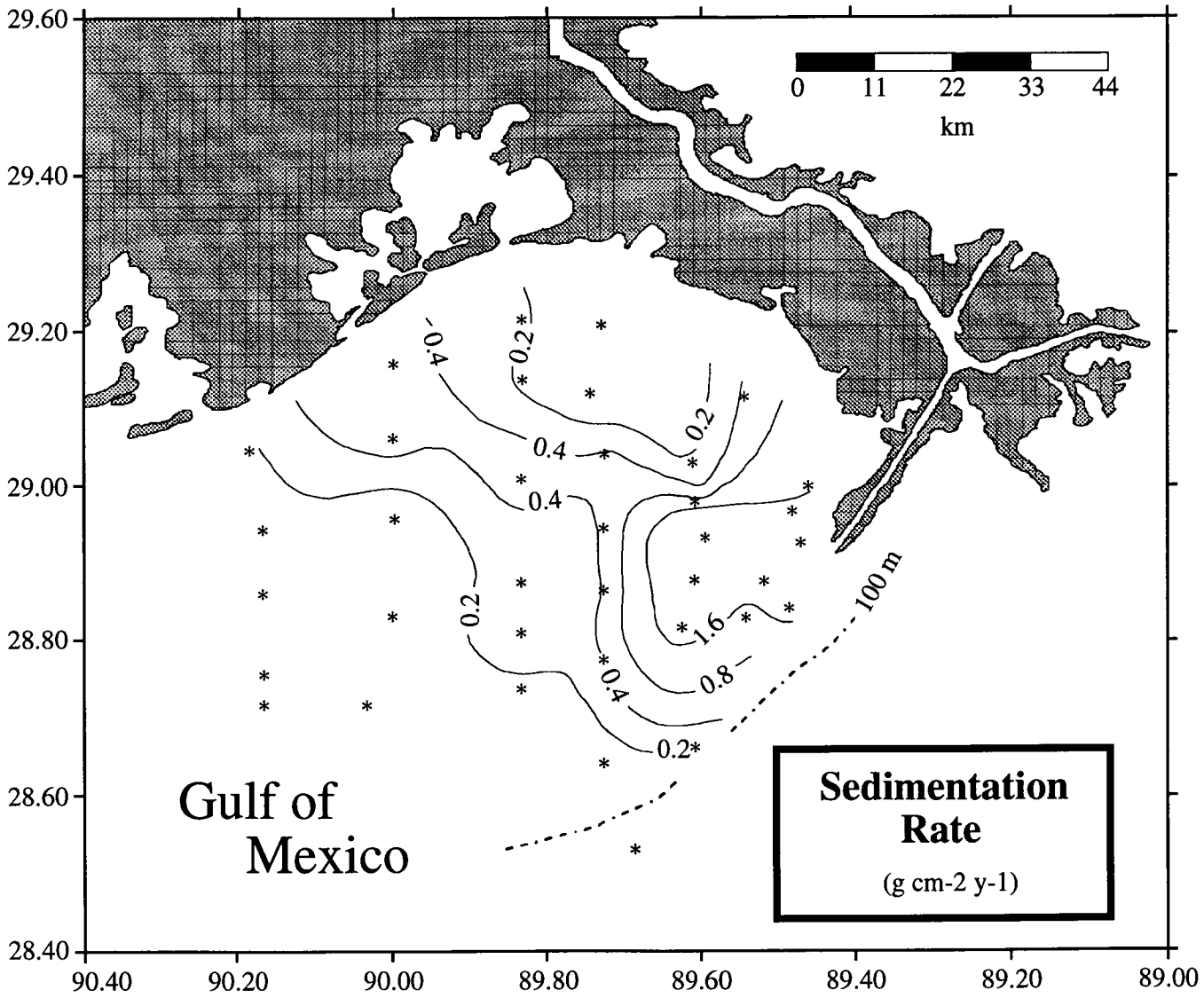

Figure 1.4. Contours of sedimentation rates in the study area of the Louisiana Bight.

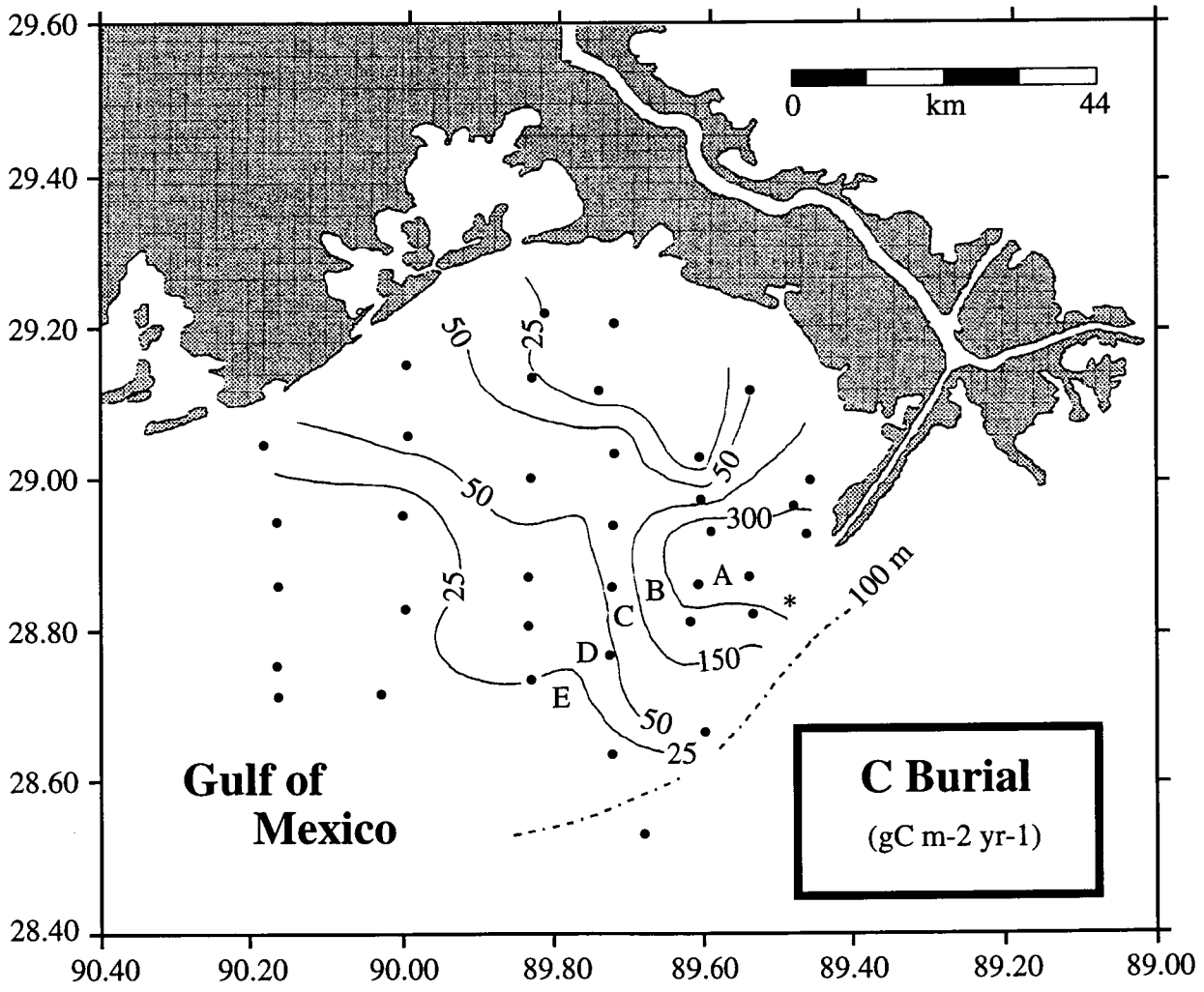

Figure 1.5. Contours of carbon accumulation rates in the study area of the Louisiana Bight.

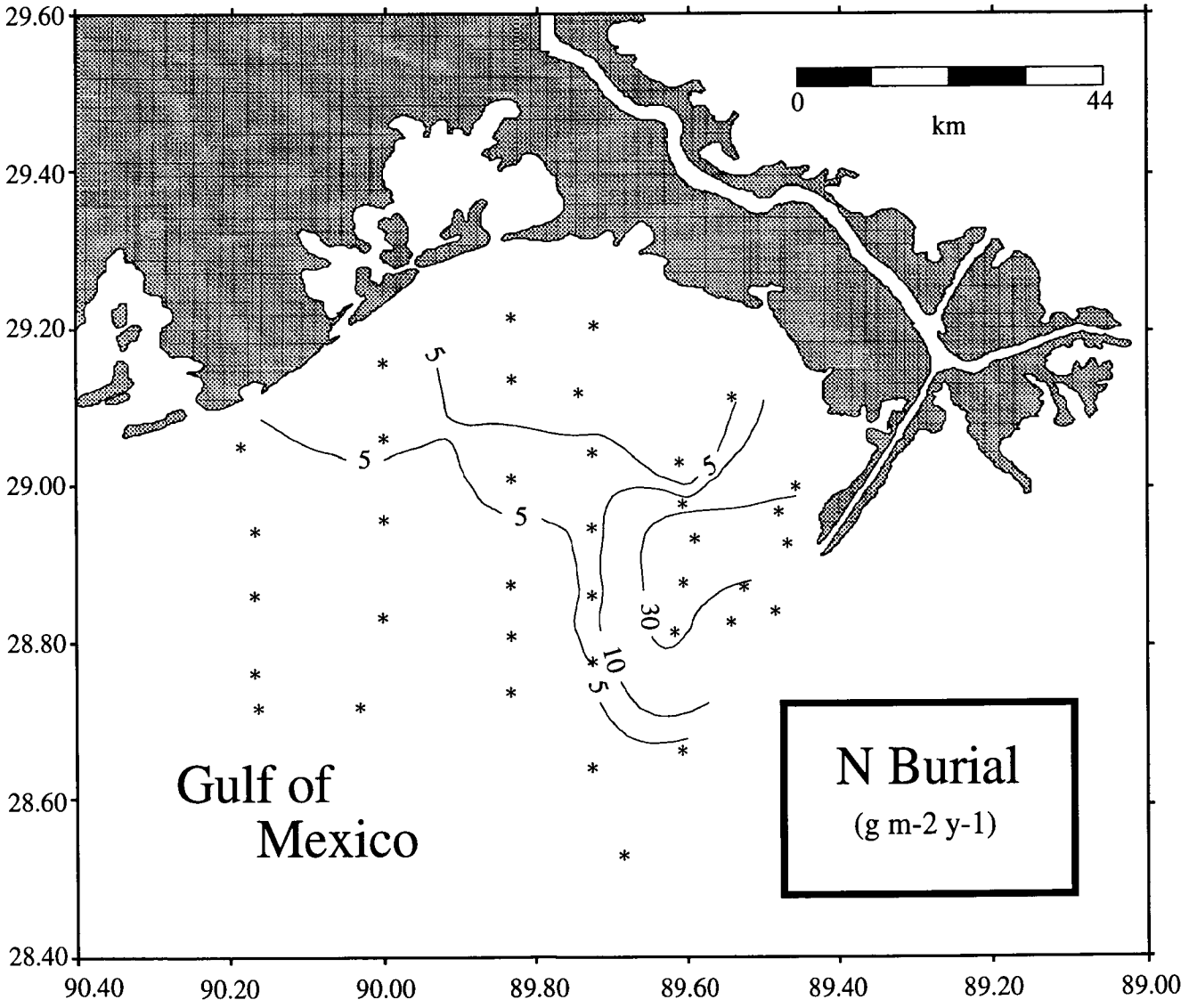

Figure 1.6. Contours of nitrogen accumulation rates in the study area of the Louisiana Bight.

Table 1.1. Organic carbon burial in the Mississippi deltaic-shelf environment.

Core	Latitude	Longitude	Date	Time	Core Length
B20	28 55.60	89 28.18	28 April 89	0700	45
B50	28 50.62	89 29.06	28 April 89	1400	35
C10	29 00.00	89 27.60	17 April 89	0457	37
C20	28 58.00	89 23.50	28 April 89	0725	39
C50	28 52.50	89 31.50	28 April 89	1100	35
C80	28 49.70	89 32.50	18 April 89	1144	32
D10	29 06.82	89 32.87	17 April 89	0220	30
D20	29 01.80	89 36.60	19 April 89	1135	30
D40	28 58.80	89 36.50	19 April 89	1430	35
D50	28 56.00	89 35.60	19 April 89	0709	41
D65	28 52.70	89 36.50	16 April 89	1753	25
D80	28 49.00	89 37.20	18 April 89	1515	32
D110	28 39.70	89 36.50	17 April 89	1800	33
E10	29 12.50	89 43.50	19 April 89	1936	21
E20	29 07.24	89 44.63	20 April 89	0709	27
E30	29 02.50	89 43.50	17 April 89	0105	35
E50	28 56.75	89 43.55	20 April 89	1201	39
E60	28 51.75	89 43.50	16 April 89	1930	33
E80	28 46.50	89 43.50	28 April 89	0710	29
E110	28 38.50	89 43.50	17 April 89	2246	31
E200	28 32.00	89 41.10	17 April 89	1935	36
F10	29 12.90	89 50.00	19 April 89	2055	31
F20	29 08.25	89 50.00	19 April 89	2148	27
F35	29 00.50	89 50.00	16 April 89	2400	33
F50	28 52.50	89 50.00	16 April 89	2245	35
F60	28 48.60	89 50.00	28 April 89	2056	31
F80	28 44.25	89 50.00	16 April 89	2100	31
G10	29 09.40	90 00.00	19 April 89	2355	23
G20	29 03.60	90 00.00	20 April 89	0056	32
G27	28 57.50	90 00.00	19 April 89	0215	30
G40	28 50.00	90 00.00	18 April 89	2055	17
G50	28 43.05	90 01.97	18 April 89	0105	15
H10	29 02.85	90 11.08	15 April 89	2005	17
H20	28 56.60	90 10.00	18 April 89	2345	19
H27	28 51.65	90 10.00	19 April 89	2240	19
H32	28 45.50	90 10.00	18 April 89	0344	18
H50	28 43.00	90 10.00	18 April 89	0250	16

Table 1.2. Concentrations of total carbon (C), nitrogen (N), and phosphorus (P) at respective depths of cores sampled in the Louisiana Bight.

Sample ID	Station	Depth (cm)	Total C mg/gdm	Total N mg/gdm	Total P mg/gdm	C:N atomic	N:P atomic
L3 B20 0-1	B20	0-1	17.40	2.25	0.84	9.0	5.9
L3 B20 2-3	B20	2-3	16.20	1.80	0.53	10.5	7.6
L3 B20 4-5	B20	4-5	21.25	2.20	1.03	11.3	4.7
L3 B20 9-10	B20	9-10	15.70	1.80	0.79	10.2	5.0
L3 B20 14-15	B20	14-15	15.85	1.60	0.69	11.6	5.2
L3 B20 19-20	B20	19-20	16.10	1.90	0.65	9.9	6.5
L3 B20 24-25	B20	24-25	16.45	1.90	0.64	10.1	6.6
L3 B20 29-30	B20	29-30	17.40	2.00	0.61	10.2	7.3
L3 B20 34-35	B20	34-35	15.60	1.80	0.73	10.1	5.5
L3 B20 39-40	B20	39-40	29.30	2.15	0.78	8.2	6.1
	Mean		18.13	1.94	0.73	10.10	6.03
	SD		4.27	0.21	0.14	0.96	0.95
L3 B50 0-1	B50	0-1	14.00	1.90	0.82	8.6	5.1
L3 B50 2-3	B50	2-3	13.35	1.75	0.71	8.9	5.5
L3 B50 4-5	B50	4-5	13.30	1.60	0.67	9.7	5.3
L3 B50 5-6	B50	5-6	13.60	1.55	0.55	10.2	6.3
L3 B50 7-8	B50	7-8	12.90	1.65	0.69	9.1	5.3
L3 B50 9-10	B50	9-10	18.60	2.10	0.84	10.3	5.6
L3 B50 14-15	B50	14-15	13.35	1.45	0.85	10.7	3.8
L3 B50 19-20	B50	19-20	13.35	1.80	0.75	8.7	5.3
L3 B50 29-30	B50	29-30	16.65	1.15	0.62	16.9	4.1
L3 B50 34-35	B50	34-35	15.70	1.35	0.66	13.6	4.6
	Mean		14.48	1.63	0.72	10.67	5.07
	SD		1.88	0.28	0.10	2.63	0.74
L3 C10 0-1	C10	0-1	16.85	1.90	0.78	10.3	5.4
L3 C10 2-3	C10	2-3	15.00	1.90	0.76	9.2	5.5
L3 C10 5-6	C10	5-6	15.35	1.95	0.57	9.2	7.6
L3 C10 8-9	C10	8-9	16.20	1.75	0.57	10.8	6.8
L3 C10 9-10	C10	9-10	16.20	1.45	0.62	13.0	5.2
L3 C10 14-15	C10	14-15	16.20	1.55	0.56	12.2	6.1
L3 C10 19-20	C10	19-20	15.80	1.50	0.55	12.3	6.1
L3 C10 24-25	C10	24-25	14.90	1.45	0.62	12.0	5.2
L3 C10 29-30	C10	29-30	14.50	1.50	0.51	11.3	6.5
L3 C10 34-35	C10	34-35	14.20	1.40	0.49	11.8	6.3
	Mean		15.52	1.64	0.60	11.22	6.07
	SD		0.86	0.22	0.10	1.31	0.77

Table 1.2. Concentrations of total carbon (C), nitrogen (N), and phosphorus (P) at respective depths of cores sampled in the Louisiana Bight.

Sample ID	Station	Depth (cm)	Total C mg/gdm	Total N mg/gdm	Total P mg/gdm	C:N atomic	N:P atomic
L3 C20 0-1	C20	0-1	15.75	1.60	0.87	11.5	4.1
L3 C20 2-3	C20	2-3	15.65	1.80	0.87	10.1	4.6
L3 C20 3-4	C20	3-4	16.55	2.05	0.97	9.4	4.7
L3 C20 4-5	C20	4-5	16.70	2.45	0.71	8.0	7.6
L3 C20 6-7	C20	6-7	17.75	1.80	0.71	11.5	5.6
L3 C20 9-10	C20	9-10	16.30	2.90	0.64	6.6	10.1
L3 C20 14-15	C20	14-15	16.40	1.60	0.64	12.0	5.5
L3 C20 19-20	C20	19-20	15.70	2.20	0.60	8.3	8.1
L3 C20 24-25	C20	24-25	16.35	2.10	0.64	9.1	7.3
L3 C20 29-30	C20	29-30	15.75	1.90	0.66	9.7	6.3
L3 C20 34-35	C20	34-35	16.30	1.80	0.69	10.6	5.8
	Mean		16.29	2.02	0.73	9.70	6.34
	SD		0.61	0.39	0.12	1.67	1.79
L3 C50 0-1	C50	0-1	17.00	2.15	0.79	9.2	6.0
L3 C50 4-5	C50	4-5	16.50	1.75	0.71	11.0	5.5
L3 C50 7-8	C50	7-8	14.85	1.60	0.67	10.8	5.3
L3 C50 9-10	C50	9-10	16.75	1.70	0.55	11.5	6.8
L3 C50 14-15	C50	14-15	16.00	1.55	0.81	12.0	4.3
L3 C50 19-20	C50	19-20	12.90	1.25	0.65	12.0	4.3
L3 C50 24-25	C50	24-25	16.10	1.60	0.78	11.7	4.5
L3 C50 29-30	C50	29-30	14.00	1.40	0.61	11.7	5.1
L3 C50 34-35	C50	34-35	17.50	2.25	0.68	9.1	7.3
	Mean		15.73	1.69	0.69	11.01	5.45
	SD		1.52	0.32	0.09	1.13	1.09
L3 C80 0-1	C80	0-1	15.90	1.75	0.76	10.6	5.1
L3 C80 4-5	C80	4-5	15.95	1.50	0.69	12.4	4.8
L3 C80 9-10	C80	9-10	16.15	1.60	0.68	11.8	5.2
L3 C80 14-15	C80	14-15	15.70	1.50	0.56	12.2	5.9
L3 C80 19-20	C80	19-20	15.35	1.50	0.58	11.9	5.7
L3 C80 24-25	C80	24-25	14.70	1.30	0.61	13.2	4.7
	Mean		15.63	1.53	0.65	12.02	5.24
	SD		0.53	0.15	0.08	0.85	0.49

Table 1.2. Concentrations of total carbon (C), nitrogen (N), and phosphorus (P) at respective depths of cores sampled in the Louisiana Bight.

Sample ID	Station	Depth (cm)	Total C mg/gdm	Total N mg/gdm	Total P mg/gdm	C:N atomic	N:P atomic
L3 D10 0-1	D10	0-1	9.30	0.85	0.56	12.8	3.3
L3 D10 3-4	D10	3-4	9.50	1.25	0.51	8.9	5.4
L3 D10 4-5	D10	4-5	8.70	0.70	0.49	14.5	3.1
L3 D10 5-6	D10	5-6	7.80	0.70	0.47	13.0	3.3
L3 D10 6-7	D10	6-7	8.75	0.80	0.46	12.8	3.9
L3 D10 8-9	D10	8-9	8.35	0.70	0.48	13.9	3.2
L3 D10 9-10	D10	9-10	8.55	0.65	0.42	15.3	3.4
L3 D10 14-15	D10	14-15	9.85	1.05	0.47	10.9	4.9
L3 D10 19-20	D10	19-20	10.25	0.85	0.53	14.1	3.6
L3 D10 24-25	D10	24-25	9.70	1.05	0.40	10.8	5.8
L3 D10 29-30	D10	29-30	10.95	0.95	0.48	13.4	4.4
	Mean		9.25	0.87	0.48	12.76	4.04
	SD		0.92	0.19	0.05	1.89	0.96
L3 D20 0-1	D20	0-1	9.45	0.95	0.44	11.6	4.8
L3 D20 1-2	D20	1-2	8.60	0.85	0.49	11.8	3.8
L3 D20 2-3	D20	2-3	8.55	0.80	0.42	12.5	4.2
L3 D20 3-4	D20	3-4	8.35	0.85	0.45	11.5	4.2
L3 D20 5-6	D20	5-6	8.70	0.80	0.43	12.7	4.1
L3 D20 6-7	D20	6-7	8.05	0.70	0.45	13.4	3.4
L3 D20 7-8	D20	7-8	8.00	0.80	0.53	11.7	3.3
L3 D20 8-9	D20	8-9	8.80	0.70	0.42	14.7	3.7
L3 D20 9-10	D20	9-10	8.65	0.75	0.42	13.5	4.0
L3 D20 14-15	D20	14-15	8.35	0.40	0.44	24.4	2.0
L3 D20 19-20	D20	19-20	8.30	0.35	0.48	27.7	1.6
L3 D20 24-25	D20	24-25	8.05	0.60	0.45	15.7	3.0
L3 D20 29-30	D20	29-30	8.00	0.45	0.41	20.7	2.4
	Mean		8.45	0.69	0.45	15.51	3.42
	SD		0.41	0.19	0.03	5.32	0.93
L3 D40 0-1	D40	0-1	17.50	1.80	0.79	11.3	5.1
L3 D40 1-2	D40	1-2	14.70	1.65	0.61	10.4	6.0
L3 D40 2-3	D40	2-3	14.80	1.70	0.40	10.2	9.4
L3 D40 3-4	D40	3-4	15.95	2.00	0.75	9.3	5.9
L3 D40 4-5	D40	4-5	16.30	1.65	0.62	11.5	5.9
L3 D40 17-18	D40	17-18	14.40	1.20	0.51	14.0	5.3
L3 D40 34-35	D40	34-35	12.15	0.80	0.51	17.7	3.5
	Mean		15.11	1.54	0.60	12.06	5.86
	SD		1.70	0.41	0.14	2.90	1.79

Table 1.2. Concentrations of total carbon (C), nitrogen (N), and phosphorus (P) at respective depths of cores sampled in the Louisiana Bight.

Sample ID	Station	Depth (cm)	Total C mg/gdm	Total N mg/gdm	Total P mg/gdm	C:N atomic	N:P atomic
L3 D50 0-1	D50	0-1					
L3 D50 1-2	D50	1-2	13.15	1.80	0.44	8.5	9.1
L3 D50 2-3	D50	2-3	13.85	1.65	0.78	9.8	4.7
L3 D50 3-4	D50	3-4	16.05	2.45	0.72	7.6	7.6
L3 D50 4-5	D50	4-5	15.80	1.75	0.65	10.5	6.0
L3 D50 5-6	D50	5-6	13.65	1.55	0.57	10.3	6.0
L3 D50 6-7	D50	6-7	14.30	1.70	0.54	9.8	7.0
L3 D50 7-8	D50	7-8	14.00	1.65	0.60	9.9	6.1
L3 D50 8-9	D50	8-9	14.10	1.60	0.69	10.3	5.1
L3 D50 9-10	D50	9-10	15.80	1.40	0.62	13.2	5.0
L3 D50 14-15	D50	14-15	14.00	1.30	0.55	12.6	5.3
L3 D50 19-20	D50	19-20	14.75	1.45	0.68	11.9	4.7
L3 D50 24-25	D50	24-25	15.45	1.60	0.57	11.3	6.2
L3 D50 29-30	D50	29-30	14.15	1.35	0.61	12.2	4.9
L3 D50 34-35	D50	34-35	14.10	1.40	0.66	11.8	4.7
L3 D50 35-36	D50	35-36	12.55	1.45	0.68	10.1	4.7
L3 D50 40-41	D50	40-41	13.70	1.25	0.69	12.8	4.0
	Mean		14.34	1.58	0.63	10.78	5.69
	SD		0.99	0.28	0.08	1.55	1.31
L3 D65 0-1	D65	0-1	15.15	1.65	0.84	10.7	4.3
L3 D65 2-3	D65	2-3	15.15	1.65	0.69	10.7	5.3
L3 D65 3-4	D65	3-4	13.75	1.50	0.57	10.7	5.8
L3 D65 4-5	D65	4-5	15.40	1.55	0.80	11.6	4.3
L3 D65 5-6	D65	5-6	13.65	1.50	0.68	10.6	4.9
L3 D65 7-8	D65	7-8	14.20	1.50	0.63	11.0	5.3
L3 D65 8-9	D65	8-9	14.70	1.65	0.77	10.4	4.7
L3 D65 9-10	D65	9-10	15.75	1.80	0.73	10.2	5.4
L3 D65 14-15	D65	14-15	15.70	1.55	0.69	11.8	4.9
L3 D65 19-20	D65	19-20	15.25	1.35	0.69	13.2	4.3
L3 D65 24-25	D65	24-25	14.80	1.55	0.62	11.1	5.5
	Mean		14.86	1.57	0.70	11.10	4.98
	SD		0.73	0.12	0.08	0.84	0.53

Table 1.2. Concentrations of total carbon (C), nitrogen (N), and phosphorus (P) at respective depths of cores sampled in the Louisiana Bight.

Sample ID	Station	Depth (cm)	Total C mg/gdm	Total N mg/gdm	Total P mg/gdm	C:N atomic	N:P atomic
L3 D80 1-2	D80	1-2	15.95	2.20	0.80	8.5	6.1
L3 D80 2-3	D80	2-3	15.80	2.40	0.82	7.7	6.5
L3 D80 3-4	D80	3-4	13.95	1.50	0.71	10.9	4.7
L3 D80 4-5	D80	4-5	14.15	1.35	0.73	12.2	4.1
L3 D80 5-6	D80	5-6	14.40	1.60	0.83	10.5	4.3
L3 D80 6-7	D80	6-7	15.75	2.25	0.73	8.2	6.8
L3 D80 7-8	D80	7-8	15.00	1.55	0.94	11.3	3.7
L3 D80 8-9	D80	8-9	14.35	1.50	0.89	11.2	3.7
L3 D80 9-10	D80	9-10	15.00	2.20	0.64	8.0	7.7
L3 D80 14-15	D80	14-15	15.25	1.85	0.67	9.6	6.1
L3 D80 19-20	D80	19-20	15.25	1.95	0.69	9.1	6.3
L3 D80 24-25	D80	24-25	15.05	1.95	0.60	9.0	7.2
L3 D80 29-30	D80	29-30	14.15	1.75	0.57	9.4	6.8
	Mean		14.93	1.85	0.74	9.65	5.68
	SD		0.68	0.34	0.11	1.44	1.40
L3 D110 0-1	D110	0-1	14.45	2.40	0.56	7.0	9.4
L3 D110 1-2	D110	1-2	12.40	1.10	0.62	13.2	3.9
L3 D110 2-3	D110	2-3	14.15	1.65	0.55	10.0	6.7
L3 D110 4-5	D110	4-5	13.30	1.70	0.48	9.1	7.9
L3 D110 5-6	D110	5-6	13.40	1.45	0.67	10.8	4.8
L3 D110 6-7	D110	6-7	14.65	1.55	0.56	11.0	6.2
L3 D110 8-9	D110	8-9	12.45	1.50	0.78	9.7	4.3
L3 D110 9-10	D110	9-10	12.75	1.25	0.51	11.9	5.4
L3 D110 14-15	D110	14-15	10.10	1.30	0.94	9.1	3.1
L3 D110 19-20	D110	19-20	11.55	1.55	0.52	8.7	6.6
L3 D110 24-25	D110	24-25	10.60	1.20	0.67	10.3	4.0
L3 D110 29-30	D110	29-30	19.15	2.35	0.49	9.5	10.7
L3 D110 32-33	D110	32-33	58.45	1.40	0.50	48.7	6.2
	Mean		16.72	1.57	0.60	13.00	6.08
	SD		12.74	0.40	0.13	10.84	2.24

Table 1.2. Concentrations of total carbon (C), nitrogen (N), and phosphorus (P) at respective depths of cores sampled in the Louisiana Bight.

Sample ID	Station	Depth (cm)	Total C mg/gdm	Total N mg/gdm	Total P mg/gdm	C:N atomic	N:P atomic
L3 E10 0-1	E10	0-1	12.25	1.55	0.57	9.2	6.0
L3 E10 1-2	E10	1-2	10.00	1.20	0.72	9.7	3.7
L3 E10 2-3	E10	2-3	8.10	1.05	0.68	9.0	3.4
L3 E10 3-4	E10	3-4	8.75	1.00	0.48	10.2	4.7
L3 E10 4-5	E10	4-5	9.45	1.20	0.45	9.2	6.0
L3 E10 11-12	E10	11-12	9.95	1.15	0.50	10.1	5.1
L3 E10 20-21	E10	20-21	15.65	1.05	0.67	17.4	3.5
	Mean		10.59	1.17	0.58	10.69	4.62
	SD		2.58	0.18	0.11	2.99	1.11
L3 E20 0-1	E20	0-1	17.35	2.70	0.64	7.5	9.3
L3 E20 1-2	E20	1-2	13.65	1.95	0.83	8.2	5.2
L3 E20 2-3	E20	2-3	14.00	1.95	0.74	8.4	5.8
L3 E20 3-4	E20	3-4	15.10	2.25	0.53	7.8	9.4
L3 E20 4-5	E20	4-5	13.20	1.85	0.81	8.3	5.1
L3 E20 5-6	E20	5-6	13.35	1.65	0.60	9.4	6.1
L3 E20 6-7	E20	6-7	15.10	1.90	0.60	9.3	7.0
L3 E20 7-8	E20	7-8	13.40	1.55	0.69	10.1	5.0
L3 E20 8-9	E20	8-9	14.65	1.90	0.54	9.0	7.7
L3 E20 14-15	E20	14-15	11.25	1.45	0.48	9.1	6.7
L3 E20 19-20	E20	19-20	10.20	1.35	0.53	8.8	5.7
L3 E20 24-25	E20	24-25	10.25	1.45	0.46	8.2	6.9
	Mean		13.46	1.83	0.62	8.68	6.66
	SD		2.09	0.38	0.12	0.74	1.52
L3 E30 0-1	E30	0-1	14.95	1.80	0.84	9.7	4.7
L3 E30 2-3	E30	2-3	16.95	2.10	0.69	9.4	6.7
L3 E30 3-4	E30	3-4	15.75	2.15	0.73	8.5	6.6
L3 E30 4-5	E30	4-5	17.55	1.85	0.79	11.1	5.2
L3 E30 7-8	E30	7-8	15.60	1.90	0.74	9.6	5.7
L3 E30 9-10	E30	9-10	15.25	2.05	0.66	8.7	6.8
L3 E30 14-15	E30	14-15	14.40	1.80	0.80	9.3	5.0
L3 E30 19-20	E30	19-20	13.50	1.55	0.77	10.2	4.5
L3 E30 24-25	E30	24-25	13.10	1.45	0.69	10.5	4.6
L3 E30 29-30	E30	29-30	12.20	1.35	0.70	10.5	4.3
L3 E30 34-35	E30	34-35	12.30	1.30	0.69	11.0	4.2
	Mean		14.69	1.75	0.74	9.87	5.29
	SD		1.78	0.30	0.06	0.87	0.99

Table 1.2. Concentrations of total carbon (C), nitrogen (N), and phosphorus (P) at respective depths of cores sampled in the Louisiana Bight.

Sample ID	Station	Depth (cm)	Total C mg/gdm	Total N mg/gdm	Total P mg/gdm	C:N atomic	N:P atomic
L3 E50 1-2	E50	1-2	13.15	1.85	0.68	8.3	6.0
L3 E50 2-3	E50	2-3	14.95	1.80	0.79	9.7	5.0
L3 E50 3-4	E50	3-4	14.85	1.70	0.85	10.2	4.4
L3 E50 4-5	E50	4-5	14.50	1.80	0.47	9.4	8.4
L3 E50 7-8	E50	7-8	14.55	2.05	0.83	8.3	5.5
L3 E50 9-10	E50	9-10	14.75	1.75	0.74	9.8	5.2
L3 E50 14-15	E50	14-15	12.70	2.00	0.89	7.4	5.0
L3 E50 19-20	E50	19-20	13.80	1.60	0.77	10.1	4.6
L3 E50 24-25	E50	24-25	13.80	1.65	1.02	9.8	3.6
L3 E50 29-30	E50	29-30	13.00	1.45	0.77	10.5	4.2
L3 E50 34-35	E50	34-35	12.40	1.45	0.72	10.0	4.4
	Mean		13.86	1.74	0.78	9.40	5.12
	SD		0.93	0.20	0.14	0.97	1.27
L3 E60 0-1	E60	0-1	14.45	1.90	0.88	8.9	4.8
L3 E60 2-3	E60	2-3	13.40	1.85	0.65	8.5	6.3
L3 E60 4-5	E60	4-5	12.75	1.55	0.82	9.6	4.2
L3 E60 6-7	E60	6-7	12.80	1.90	0.80	7.9	5.3
L3 E60 8-9	E60	8-9	12.90	2.05	0.57	7.3	7.9
L3 E60 9-10	E60	9-10	14.30	2.20	1.02	7.6	4.8
L3 E60 14-15	E60	14-15	13.50	2.15	0.68	7.3	7.0
L3 E60 19-20	E60	19-20	13.80	2.05	0.41	7.9	11.1
L3 E60 24-25	E60	24-25	12.85	1.80	0.63	8.3	6.3
L3 E60 29-30	E60	29-30	12.15	1.50	0.73	9.5	4.6
L3 E60 32-33	E60	32-33	11.75	1.65	0.24	8.3	15.2
	Mean		13.15	1.87	0.67	8.27	7.05
	SD		0.84	0.23	0.22	0.78	3.36
L3 E80 0-1	E80	0-1	12.90	1.35	0.51	11.1	5.9
L3 E80 0-1	E80	2-3	14.05	1.65	0.53	9.9	6.9
L3 E80 0-1	E80	3-4	14.55	1.45	0.56	11.7	5.7
L3 E80 0-1	E80	5-6	14.00	1.85	0.57	8.8	7.2
L3 E80 0-1	E80	7-8	14.00	1.65	0.59	9.9	6.2
L3 E80 0-1	E80	9-10	14.15	1.55	0.58	10.7	5.9
L3 E80 0-1	E80	14-15	13.15	1.35	0.57	11.4	5.2
L3 E80 0-1	E80	19-20	12.10	1.10	0.52	12.8	4.7
L3 E80 0-1	E80	24-25	12.00	0.95	0.55	14.7	3.8
	Mean		12.17	1.31	0.52	10.19	5.49
	SD		4.08	0.46	0.11	3.70	1.24

Table 1.2. Concentrations of total carbon (C), nitrogen (N), and phosphorus (P) at respective depths of cores sampled in the Louisiana Bight.

Sample ID	Station	Depth (cm)	Total C mg/gdm	Total N mg/gdm	Total P mg/gdm	C:N atomic	N:P atomic
L3 E110 0-1	E110	0-1	11.80	0.75	0.49	18.4	3.4
L3 E110 0-1	E110	2-3	13.25	0.95	0.58	16.3	3.6
L3 E110 0-1	E110	3-4	13.45	1.00	0.57	15.7	3.9
L3 E110 0-1	E110	5-6	13.75	0.80	0.56	20.1	3.2
L3 E110 0-1	E110	8-9	14.70	1.05	0.52	16.3	4.5
L3 E110 0-1	E110	9-10	15.15	0.55	0.51	32.1	2.4
L3 E110 0-1	E110	14-15	13.30	0.65	0.51	23.9	2.8
L3 E110 0-1	E110	19-20	11.80	0.30	0.49	45.9	1.4
L3 E110 0-1	E110	24-25	11.10	0.35	0.49	37.0	1.6
L3 E110 0-1	E110	29-30	11.70	0.75	0.46	18.2	3.6
	Mean		13.00	0.72	0.52	24.38	3.03
	SD		1.36	0.26	0.04	10.44	1.00
L3 F10	F10	0-1	13.20	0.40	0.69	38.5	1.3
L3 F10	F10	2-3	14.90	1.90	0.6	9.1	7.0
L3 F10	F10	3-4	13.85	1.45	0.59	11.1	5.4
L3 F10	F10	4-5	14.45	1.95	0.57	8.6	7.6
L3 F10	F10	15-16	13.00	1.50	0.55	10.1	6.0
L3 F10	F10	30-31	8.05	0.75	0.5	12.5	3.3
	Mean		12.91	1.33	0.58	15.01	5.11
	SD		2.49	0.63	0.06	11.59	2.39
L3 F20	F20	0-1	16.60	2.00	0.72	9.7	6.2
L3 F20	F20	2-3	16.40	1.95	0.63	9.8	6.9
L3 F20	F20	3-4	16.10	1.75	0.61	10.7	6.4
L3 F20	F20	4-5	15.80	1.85	0.59	10.0	6.9
L3 F20	F20	15-16	11.10	1.00	0.54	13.0	4.1
L3 F20	F20	26-27	10.30	0.95	0.51	12.6	4.1
	Mean		14.38	1.58	0.60	10.97	5.75
	SD		2.88	0.48	0.07	1.47	1.31

Table 1.2. Concentrations of total carbon (C), nitrogen (N), and phosphorus (P) at respective depths of cores sampled in the Louisiana Bight.

Sample ID	Station	Depth (cm)	Total C mg/gdm	Total N mg/gdm	Total P mg/gdm	C:N atomic	N:P atomic
L3 F35	F35	0-1	16.35	1.55	0.64	12.3	5.4
L3 F35	F35	2-3	14.75	1.65	0.5	10.4	7.3
L3 F35	F35	3-4	15.00	1.45	0.54	12.1	5.9
L3 F35	F35	4-5	14.35	1.40	0.52	12.0	6.0
L3 F35	F35	7-8	15.30	1.65	0.57	10.8	6.4
L3 F35	F35	9-10	15.45	1.80	0.56	10.0	7.1
L3 F35	F35	14-15	14.30	1.50	0.52	11.1	6.4
L3 F35	F35	19-20	13.20	1.15	0.54	13.4	4.7
L3 F35	F35	24-25	13.05	1.15	0.55	13.2	4.6
L3 F35	F35	29-30	13.35	1.20	0.52	13.0	5.1
L3 F35	F35	32-33	12.45	1.05	0.63	13.8	3.7
	Mean		14.32	1.41	0.55	12.01	5.69
	SD		1.20	0.25	0.05	1.28	1.11
L3 F50	F50	0-1	12.50	1.05	0.59	13.9	3.9
L3 F50	F50	2-3	13.70	1.50	0.57	10.7	5.8
L3 F50	F50	4-5	12.65	1.40	0.56	10.5	5.5
L3 F50	F50	6-7	14.40	1.85	0.6	9.1	6.8
L3 F50	F50	9-10	14.50	1.90	0.59	8.9	7.1
L3 F50	F50	14-15	12.45	1.45	0.51	10.0	6.3
L3 F50	F50	19-20	11.85	1.45	0.53	9.5	6.1
L3 F50	F50	24-25	10.60	0.95	0.51	13.0	4.1
L3 F50	F50	29-30	10.30	0.85	0.51	14.1	3.7
L3 F50	F50	34-35	10.20	1.00	0.52	11.9	4.3
	Mean		12.32	1.34	0.55	11.17	5.37
	SD		1.59	0.37	0.04	1.95	1.27
L3 F60	F60	0-1	12.40	1.30	0.54	11.1	5.3
L3 F60	F60	2-3	12.40	1.45	0.55	10.0	5.8
L3 F60	F60	4-5	12.65	1.50	0.58	9.8	5.7
L3 F60	F60	7-8	12.85	1.50	0.54	10.0	6.2
L3 F60	F60	9-10	13.65	1.85	0.57	8.6	7.2
L3 F60	F60	14-15	11.65	1.65	0.52	8.2	7.0
L3 F60	F60	24-25	11.05	1.55	0.55	8.3	6.2
L3 F60	F60	29-30	9.70	1.35	0.58	8.4	5.2
	Mean		12.04	1.52	0.55	9.31	6.08
	SD		1.22	0.17	0.02	1.07	0.73

Table 1.2. Concentrations of total carbon (C), nitrogen (N), and phosphorus (P) at respective depths of cores sampled in the Louisiana Bight.

Sample ID	Station	Depth (cm)	Total C mg/gdm	Total N mg/gdm	Total P mg/gdm	C:N atomic	N:P atomic
L3 F80	F80	0-1	11.70	1.55	0.51	8.8	6.7
L3 F80	F80	2-3	12.10	1.55		9.1	
L3 F80	F80	5-6	12.20	1.60	0.57	8.9	6.2
L3 F80	F80	7-8	13.00	1.55	0.57	9.8	6.0
L3 F80	F80	9-10	12.40	1.50	0.56	9.6	5.9
L3 F80	F80	14-15	13.25	1.70	0.56	9.1	6.7
L3 F80	F80	19-20	12.45	1.65	0.52	8.8	7.0
L3 F80	F80	24-25	11.00	1.40	0.55	9.2	5.6
L3 F80	F80	29-30	10.15	1.40	0.55	8.5	5.6
	Mean		12.03	1.54	0.55	9.08	6.24
	SD		0.97	0.10	0.02	0.42	0.53
L3 G10	G10	0-1	8.95	0.75	0.65	13.9	2.6
L3 G10	G10	2-3	6.00	0.70	0.56	10.0	2.8
L3 G10	G10	4-5	6.90	0.90	0.56	8.9	3.6
L3 G10	G10	11-12	9.70	1.30	0.5	8.7	5.8
L3 G10	G10	22-23	9.95	0.95	0.54	12.2	3.9
	Mean		8.30	0.92	0.56	10.76	3.71
	SD		1.76	0.24	0.05	2.25	1.27
L3 G20	G20	0-1	13.75	1.75	0.67	9.2	5.8
L3 G20	G20	2-3	11.35	1.40	0.6	9.5	5.2
L3 G20	G20	4-5	9.10	1.30	0.56	8.2	5.1
L3 G20	G20	7-8	11.25	1.35	0.58	9.7	5.2
L3 G20	G20	9-10	10.55	1.35	0.51	9.1	5.9
L3 G20	G20	14-15	11.75	1.20	0.48	11.4	5.5
L3 G20	G20	19-20	12.30	0.95	0.48	15.1	4.4
L3 G20	G20	14-25	10.40	1.15	0.53	10.6	4.8
L3 G20	G20	29-30	9.50	1.00	0.53	11.1	4.2
	Mean		11.11	1.27	0.55	10.42	5.11
	SD		1.43	0.24	0.06	2.04	0.58

Table 1.2. Concentrations of total carbon (C), nitrogen (N), and phosphorus (P) at respective depths of cores sampled in the Louisiana Bight.

Sample ID	Station	Depth (cm)	Total C mg/gdm	Total N mg/gdm	Total P mg/gdm	C:N atomic	N:P atomic
L3 G27	G27	0-1	10.65	1.30	0.53	9.6	5.4
L3 G27	G27	3-4	11.70	1.35	0.54	10.1	5.5
L3 G27	G27	5-6	10.90	1.50	0.56	8.5	5.9
L3 G27	G27	7-8	10.95	1.35	0.54	9.5	5.5
L3 G27	G27	9-10	11.00	0.90	0.51	14.3	3.9
L3 G27	G27	14-15	9.55	1.00	0.48	11.1	4.6
L3 G27	G27	19-20	9.20	1.00	0.48	10.7	4.6
L3 G27	G27	24-25	7.60	0.60	0.53	14.8	2.5
L3 G27	G27	29-30	9.90	1.10	0.53	10.5	4.6
	Mean		10.16	1.12	0.52	11.00	4.74
	SD		1.25	0.28	0.03	2.15	1.05
L3 G40	G40	0-1	12.00	1.45	0.61	9.7	5.3
L3 G40	G40	2-3	11.55	1.10	0.56	12.3	4.3
L3 G40	G40	4-5	12.15	1.15	0.55	12.3	4.6
L3 G40	G40	7-8	11.70	1.25	0.54	10.9	5.1
L3 G40	G40	9-10					
L3 G40	G40	16-17	12.30	1.20	0.57	12.0	4.7
	Mean		11.94	1.23	0.57	11.42	4.81
	SD		0.31	0.14	0.03	1.14	0.38
L3 G50	G50	0-1	9.75	0.95	0.59	12.0	3.6
L3 G50	G50	2-3	10.15	1.05	0.61	11.3	3.8
L3 G50	G50	4-5	11.00	0.95	0.57	13.5	3.7
L3 G50	G50	7-8	10.60	1.00	0.53	12.4	4.2
L3 G50	G50	9-10	9.55	0.95	0.57	11.7	3.7
L3 G50	G50	14-15	10.45	1.00	0.55	12.2	4.0
	Mean		10.25	0.98	0.57	12.17	3.83
	SD		0.54	0.04	0.03	0.76	0.23
L3 H20	H20	6-7	10.85	0.85	0.52	14.9	3.6
L3 H20	H20	8-9	10.50	0.65	0.56	18.8	2.6
L3 H20	H20	11-12	11.90	0.75	0.58	18.5	2.9
L3 H20	H20	13-14	12.70	0.90	0.61	16.5	3.3
L3 H20	H20	15-16	10.95	0.55	0.58	23.2	2.1
L3 H20	H20	17-18	11.65	0.75	0.57	18.1	2.9
	Mean		11.43	0.74	0.57	18.34	2.89
	SD		0.81	0.13	0.03	2.82	0.53

Table 1.2. Concentrations of total carbon (C), nitrogen (N), and phosphorus (P) at respective depths of cores sampled in the Louisiana Bight.

Sample ID	Station	Depth (cm)	Total C mg/gdm	Total N mg/gdm	Total P mg/gdm	C:N atomic	N:P atomic
L3 H27	H27	6-7	9.50	0.40	0.55	27.7	1.6
L3 H27	H27	8-9	10.70	0.50	0.61	25.0	1.8
L3 H27	H27	11-12	9.50	0.75	0.51	14.8	3.3
L3 H27	H27	13-14	9.75	0.35	0.5	32.5	1.6
L3 H27	H27	15-16	10.70	0.50	0.52	25.0	2.1
L3 H27	H27	17-18	9.90	0.40	0.51	28.9	1.7
	Mean		10.01	0.48	0.53	25.63	2.02
	SD		0.56	0.14	0.04	6.01	0.64
L3 H32	H32	0-1	12.30	1.00	0.6	14.4	3.7
L3 H32	H32	2-3	11.35	1.00	0.56	13.2	4.0
L3 H32	H32	4-5	11.20	0.75	0.56	17.4	3.0
L3 H32	H32	7-8	10.60	0.90	0.53	13.7	3.8
L3 H32	H32	9-10	9.65	1.00	0.48	11.3	4.6
L3 H32	H32	14-15	11.70	0.85	0.93	16.1	2.0
L3 H32	H32	17-18	11.25	0.75	0.9	17.5	1.8
	Mean		11.15	0.89	0.65	14.80	3.26
	SD		0.84	0.11	0.18	2.31	1.03
L3 H50	H50	0-1	11.45	1.10	0.87	12.1	2.8
L3 H50	H50	2-3	11.85	0.95	0.89	14.6	2.4
L3 H50	H50	4-5	11.40	0.80	0.62	16.6	2.9
L3 H50	H50	7-8	10.75	0.95	0.54	13.2	3.9
L3 H50	H50	9-10	13.00	1.15	0.54	13.2	4.7
L3 H50	H50	14-15	10.70	0.95	0.56	13.1	3.8
L3 H50	H50	15-16	13.00	0.85	0.63	17.8	3.0
	Mean		11.74	0.96	0.66	14.39	3.34
	SD		0.85	0.13	0.17	1.58	0.88

Table 1.3. Nutrient concentrations and ratios for each survey station in the Louisiana Bight study area.

Station ID	Depth	Latitude	Longitude	Total C mg/gdm	Total N mg/gdm	Total P mg/gdm	C:N atomic	N:P atomic
B20	20	28.9267	89.4697	18.13	1.94	0.73	10.90	5.9
B50	50	28.8437	89.4843	14.48	1.63	0.72	10.36	5.0
C10	10	29.0000	89.4600	15.52	1.64	0.60	11.07	6.0
C20	20	28.9667	89.4800	16.29	2.02	0.73	9.42	6.1
C50	50	28.8750	89.5250	15.73	1.69	0.69	10.83	5.4
C80	80	28.8283	89.5417	15.63	1.53	0.65	11.95	5.2
D10	10	29.1137	89.5417	9.25	0.87	0.48	12.42	4.0
D20	20	29.0300	89.6100	8.45	0.69	0.45	14.24	3.4
D40	40	28.9800	89.6083	15.11	1.54	0.60	11.43	5.7
D50	50	28.9333	89.5933	14.34	1.58	0.63	10.59	5.6
D65	65	28.8783	89.6083	14.86	1.57	0.70	11.06	5.0
D80	80	28.8167	89.6200	14.93	1.85	0.74	9.41	5.5
D110	110	28.6617	89.6083	16.72	1.57	0.60	12.43	5.8
E10	10	29.2083	89.7250	10.59	1.17	0.58	10.55	4.5
E20	20	29.1207	89.7438	13.46	1.83	0.62	8.58	6.6
E30	30	29.0417	89.7250	14.69	1.75	0.74	9.77	5.3
E50	50	28.9458	89.7258	13.86	1.74	0.78	9.31	4.9
E60	60	28.8625	89.7250	13.15	1.87	0.67	8.19	6.2
E80	80	28.7750	89.7250	12.17	1.31	0.52	10.84	5.6
E110	110	28.6417	89.7250	13.00	0.72	0.52	21.06	3.1
F10	10	29.2150	89.8333	12.91	1.33	0.58	11.32	5.1
F20	20	29.1375	89.8333	14.38	1.58	0.60	10.62	5.8
F35	35	29.0083	89.8333	14.32	1.41	0.55	11.85	5.7
F50	50	28.8750	89.8333	12.32	1.34	0.55	10.73	5.4
F60	60	28.8100	89.8333	12.04	1.52	0.55	9.24	6.1
F80	80	28.7375	89.8333	12.03	1.54	0.55	9.11	6.2
G10	10	29.1567	90.0000	8.30	0.92	0.56	10.53	3.6
G20	20	29.0600	90.0000	11.11	1.27	0.55	10.21	5.1
G27	27	28.9583	90.0000	10.16	1.12	0.52	10.58	4.8
G40	40	28.8333	90.0000	11.94	1.23	0.57	11.33	4.8
G50	50	28.7175	90.0328	10.25	0.98	0.57	12.20	3.8
H10	10	29.0475	90.1847			0.58		
H20	20	28.9433	90.1667	11.43	0.74	0.57	18.02	2.9
H27	27	28.8608	90.1667	10.01	0.48	0.53	24.33	2.0
H32	32	28.7583	90.1667	11.15	0.89	0.65	14.62	3.0
H50	50	28.7167	90.1667	11.74	0.96	0.66	14.27	3.2

Table 1.4. Accretion, sedimentation and nutrient accumulation rates for each survey station in the Louisiana Bight study area.

Station ID	Depth	Latitude	Longitude	Accretion Rate	Sedimentation Rates			
					Sediments	Carbon	Nitrogen	Phosphate
				cm/yr	g/cm2 yr	g m-2 yr-1	g m-2 yr-1	g m-2 yr-1
B20	20	28.9267	89.4697	2.60	1.755	318.09	34.05	12.81
B50	50	28.8437	89.4843	2.20	1.485	215.03	24.21	10.69
C10	10	29.0000	89.4600	2.20	1.485	230.47	24.28	8.91
C20	20	28.9667	89.4800	2.60	1.755	285.91	35.42	12.81
C50	50	28.8750	89.5250	2.20	1.485	233.64	25.16	10.25
C80	80	28.8283	89.5417	1.40	0.945	147.66	14.41	6.14
D10	10	29.1137	89.5417					
D20	20	29.0300	89.6100	0.30	0.203	17.11	1.40	0.91
D40	40	28.9800	89.6083	0.80	0.540	81.62	8.33	3.24
D50	50	28.9333	89.5933	5.10	3.443	493.57	54.39	21.69
D65	65	28.8783	89.6083	3.70	2.498	371.22	39.17	17.48
D80	80	28.8167	89.6200	2.90	1.958	292.19	36.21	14.49
D110	110	28.6617	89.6083	0.30	0.203	33.86	3.18	1.22
E10	10	29.2083	89.7250	0.02	0.014	1.43	0.16	0.08
E20	20	29.1207	89.7438	0.07	0.047	6.36	0.86	0.29
E30	30	29.0417	89.7250	0.62	0.419	61.46	7.34	3.08
E50	50	28.9458	89.7258	0.75	0.506	70.16	8.79	3.93
E60	60	28.8625	89.7250	0.72	0.486	63.91	9.10	3.27
E80	80	28.7750	89.7250	0.60	0.405	49.29	5.31	2.11
E110	110	28.6417	89.7250	0.15	0.101	13.16	0.73	0.53
F10	10	29.2150	89.8333	0.31	0.209	27.01	2.78	1.21
F20	20	29.1375	89.8333	0.23	0.155	22.32	2.45	0.93
F35	35	29.0083	89.8333	0.76	0.513	73.46	7.23	2.82
F50	50	28.8750	89.8333	0.33	0.223	27.44	2.98	1.23
F60	60	28.8100	89.8333	0.45	0.304	36.57	4.62	1.67
F80	80	28.7375	89.8333	0.24	0.162	19.49	2.49	0.89
G10	10	29.1567	90.0000			0.00	0.00	0.00
G20	20	29.0600	90.0000	0.74	0.500	55.49	6.34	2.75
G27	27	28.9583	90.0000	0.10	0.068	6.86	0.76	0.35
G40	40	28.8333	90.0000	0.23	0.155	18.54	1.91	0.88
G50	50	28.7175	90.0328	0.25	0.169	17.30	1.65	0.96
H10	10	29.0475	90.1847	0.23	0.155	0.00	0.00	0.90
H20	20	28.9433	90.1667	0.16	0.108	12.34	0.80	0.62
H27	27	28.8608	90.1667	0.11	0.074	7.43	0.36	0.39
H32	32	28.7583	90.1667			0.00	0.00	0.00
H50	50	28.7167	90.1667	0.21	0.142	16.64	1.36	0.94

Table 1.5. Rates of sedimentation and nutrient accumulation for each of four regions of the Louisiana Bight based on area-weighted analysis.

Section	Study Area		Sediment Burial		Carbon Accumulation			
			Unit Area	Study Area	Range	Average	Area	Study Area
	(km2)	Percent	(t km-2 yr-1)	(t/yr)	(t km-2 yr-1)		(km2)	(t/yr)
A	326	6.00	21,700	7,074,200	>300	394	217	85,498
B	487	9.00	13,500	6,574,500	150-300	252	379	95,508
C	975	18.00	4,800	4,680,000	50-150	75	1300	97,500
D	1246	23.00	2,500	3,115,000	25-50	31	1192	36,952
E	2383	44.00	1,100	2,621,300	<25	13	2329	30,277
SUM	5,417	100		24,065,000			5417	345,735
Burial (g m-2 yr-1)				4,442				64

Table 1.5. Rates of sedimentation and nutrient accumulation for each of four regions of the Louisiana Bight based on area-weighted analysis.

Section	Nitrogen Accumulation				Phosphorus Accumulation			
	Range (t km-2 yr-1)	Average	Area (km2)	Study Area (t/yr)	Range (t km-2 yr-1)	Average	Area (km2)	Study Area (t/yr)
A	>30	42.5	217	9,223	>15	17.33	217	3,761
B	15-30	29.1	379	11,029	8-15	11.43	379	4,332
C	5-15	8.4	1300	10,920	4-8	3.42	1300	4,446
D	2-5	3.4	1192	4,053	1-4	1.33	1192	1,585
E	<2	1.2	2329	2,795	<1	0.65	2329	1,514
SUM			5417	38,019			5417	15,638
Burial (g m-2 yr-1)				7.02				2.89

Chapter 2

BURIAL AND REMINERALIZATION OF TERRIGENOUS ORGANIC CARBON IN DELTAIC-SHELF ENVIRONMENTS

2.1 Abstract

Marine sediments are the predominant long-term reservoir of carbon on earth, and as much as 80% of modern carbon burial has been attributed to deltaic-shelf environments (Berner 1982, Romankevich 1984). However, little is known about the fate of particulate organic carbon supplied by rivers, and the relative contribution of this terrigenous input to carbon burial on continental shelves (Deuser 1988, Berner 1989, Smith and Hollibaugh 1993). Here we report seasonal and decadal rates of organic carbon storage in Mississippi delta-shelf sediments, and calculate the proportion of this carbon sink that is of terrestrial origin. Results reveal that approximately 30% of the particulate organic carbon supplied by the Mississippi River to the adjacent shelf is remineralized within 4 months and an additional 40% is remineralized on a decadal time scale. Based on these results, combined with similar information from the Amazon, Changjiang and Huanghe Rivers, we conclude that only 30% of the particulate organic carbon supplied to the ocean by rivers is buried. Our area-weighted estimate of organic carbon burial in deltaic-shelf sediments is 75 gC m^{-2} yr^{-1} with less than 50% of the organic carbon buried being of terrestrial origin. The resulting global estimate for terrigenous POC burial is 0.05 PgC yr^{-1}, representing less than half the value currently used to constrain global CO_2 budgets (Sarmiento and Sundquist 1992).

2.2 Introduction

Global geochemical budgets of organic carbon are based on the steady-state assumption that the flux of CO_2 out of the ocean is equal to the net organic carbon flux into the oceans from rivers (terrigenous organic carbon input minus burial in marine sediments) (Berner 1989, Sarmiento and Sundquist 1992). Thus, the magnitude and nature of carbon storage in shelf sediments is an important constraint on the global CO_2 budget. In a study utilizing molecular assays, Ittekkot (1988) estimated that about 65% of riverine POC (0.15 PgC yr^{-1}) is refractory and therefore may potentially be buried in oceanic environments. Berner (1982) estimated that 0.10 ± 0.05 Pg yr^{-1} of organic carbon is buried in deltaic-shelf environments, assuming that 17.3 Pg of sediment with a mean organic carbon content of 0.75% is buried annually accompanied by a 20% loss due to decomposition subsequent to burial. Berner's estimate of bulk organic carbon burial is comparable to the value predicted by Ittekkot (1988) for refractory riverine POC components. However, studies using molecular or isotopic indicators report that the bulk of organic carbon in shelf sediments is autochthonous (*in situ* coastal production) in origin, even in the proximity of river deltas (Gearing et al. 1977, Hedges and Mann 1979). It therefore appears that previous studies have overestimated the preservation potential of allochthonous (riverine input) POC and/or underestimated the rate of total organic carbon burial (allochthonous plus autochthonous) in continental shelf environments. In this study, we utilize direct seabed measurements in deltaic-shelf environments to determine area-weighted organic carbon burial rates and to quantify the diagenetic loss of terrigenous organic carbon within the seabed on seasonal and decadal time scales.

2.3 Methods

In April 1989, we collected 37 undisturbed box cores from a 5400 km^2 shelf area adjacent to the Mississippi River (within 100 km of the river mouth). Subcores from each station were carefully extruded, subsampled at 1 cm intervals and analyzed for organic carbon and ^{210}Pb (to determine sediment burial rates). One site (B50) located approximately 5 km from the dominant river mouth, Southwest Pass (Figure 2.1), was reoccupied four times over a period of 30 months (April 1988, April 1989, April 1990, October 1990) to examine the seasonal fate of riverine material. Cores from B50 were subsampled and analyzed for organic carbon and ^{234}Th (to determine sediment deposition rates). Sediment deposition rates determined using ^{234}Th geochronologies integrate over the four-month period preceding core collection (Figure 2.2) (McKee et al. 1983, Dukat and Kuehl 1995). Organic carbon burial rates were derived by multiplying the dry bulk sediment accumulation rate (g m^{-2} yr^{-1}) at each of the 37 sites, determined using ^{210}Pb geochronologies by the mean percent organic carbon content (dry weight) of sediments in the zone of net accumulation within each core. Station B50 (site of the seasonal organic carbon storage study presented in Figure 2.2) is denoted by an asterisk in Figure 2.1. Rates of seasonal organic carbon storage were determined by multiplying the dry bulk sediment deposition rate for each study period, determined using ^{234}Th, by the mean percent (dry weight) organic carbon content of sediments in the zone of recent deposition within each core. The riverine organic carbon supplied to B50 during each time period was determined as the percent (dry weight) organic carbon content of suspended river material (as measured during each time period) multiplied by the mass dry bulk sediment deposited at B50 during the four months preceding core collection (as determined by ^{234}Th deposition rates). The percent loss of riverine organic carbon to remineralization (determined as the difference between organic supply and storage for each seasonal period) was 30, 31, 28, and 34% for January-April 1988, January-April 1989, January-April 1990, and July-October 1990, respectively.

2.4 Results and Discussion

During this study, sediment deposition rates at B50 were proportional to Mississippi River discharge, ranging from 69 to 436 g m^{-2} d^{-1}. The corresponding supply of terrestrial POC to this site during each sampling period ranged from 1.6 to 8.7 gC m^{-2} d^{-1}, based on sediment deposition rates and riverine POC contents (range: 1.97 to 2.41%; Figure 2.2). The organic carbon content of sediments stored seasonally at B50 (sediments residing in the seabed for less than four months based on excess ^{234}Th) ranged from 1.36 to 1.61% and the resulting organic carbon deposition rates (1.1 to 6.3 gC m^{-2} d^{-1}) were 28-34% less than the riverine carbon supply (Figure 2.2). Thus, approximately 30% of the terrigenous carbon was remineralized within four months, less than some estimates of carbon decomposition proximal to river mouths (Spitzy and Ittekkot 1991), but consistent with studies that have identified the labile fraction of riverine sediments based on molecular assays (Ittekkot 1988, Ittekkot et al. 1985).

The decadal geochronologies constructed using ^{210}Pb integrate over the 10-120 years prior to core collection, depending on core lengths (~50 cm) and sediment burial rates (McKee et al. 1983, DeMaster et al. 1985, Kuehl et al. 1986). Sediment burial rates decrease within 100 km of the river mouth, from 3.44 g cm^{-2} yr^{-1} (5.1 cm yr^{-1}) to 0.01 g cm^{-2} yr^{-1} (0.02 cm yr^{-1}). A total of 22 x 10^{12} grams of sediment accumulate annually in the study area, about 50% of the annual sediment discharge via Southwest Pass (45 x 10^{12} grams) (Milliman and Meade 1983). We use this determination of sediment burial to constrain our estimate of the terrigenous organic carbon flux (from the Mississippi River) reaching our study area. The

mean organic carbon content of buried sediments in the study area is 1.3% (range: 0.6 to 2.1%). We have divided the study area into 5 regions based on organic carbon burial (Table 2.1, Figure 2.1) with rates ranging from >300 gC m^{-2} yr^{-1} (maximum: 494 gC m^{-2} yr^{-1}) to <25 gC m^{-2} yr^{-1} (minimum: 1 gC m^{-2} yr^{-1}). The region with rates >300 gC m^{-2} yr^{-1} is restricted to <15 km from the mouth of Southwest Pass and makes up about 4% of the study area, compared to 43% of the shelf study area with rates <25 gC m^{-2} yr^{-1} (Table 2.1). Deltaic-shelf environments typically exhibit strong spatial gradients for organic carbon burial rates (Figure 2.2), making assessments of regional carbon burial difficult based on single measurements. Therefore, an area-weighted approach was used here (37 rate values from a 5400 km^2 area), resulting in an organic carbon burial rate of 64 gC m^{-2} yr^{-1} for the entire area.

A number of studies using ^{13}C and biomarkers have partitioned the carbon content of shelf sediments, between autochthonous and allochthonous origin, at locations throughout our study area (Gearing et al. 1977, Shultz and Calder 1976, Thayer et al. 1983, Eadie et al. 1994, Hedges and Parker 1976). We have estimated the percentage of the buried organic carbon that is of allochthonous origin within each of the 5 regions, based on these studies and a two component mixing model (Newman et al. 1973) (Table 2.1). Results from this model, using stable carbon isotopes, have been shown to agree well with organic biomarker analyses (lipids, syringyl and vanillyl compounds) from conjoint cores within the study area (Eadie et al. 1994). In the region of high carbon burial rates, an average of 70% of the POC is of terrestrial origin, in contrast to the region of minimum rates where only 5% of the POC is from the river. We estimate that only 40% of the total organic carbon preserved in the study area is allochthonous in origin, based on area-weighted estimates of percent terrigenous carbon and organic carbon burial rates. Thus burial of riverine POC in the study area is 26 gC m^{-2} yr^{-1}. If we assume that the 22 x 10^{12} g yr^{-1} of riverine sediment buries in the study area had an initial organic carbon content of 2 ± 0.2% (based on historical information, Trefry and Presley 1982, Malcolm and Durum 1976), then the river input of POC to the study area over the past century has been 4.4 x 10^{11} gC yr^{-1} or 81 gC m^{-2} yr^{-1}. Therefore, 67% of the terrigenous POC originally associated with the sediments buried in the study area has been remineralized over the past century, with the remaining 33% being buried.

Similarly, data from other major deltaic-shelf environments (sedimentation rate, ^{13}C and organic carbon content) can be used to estimate rates of organic carbon burial and the relative preservation of riverine carbon (Table 2.2). Together with the Mississippi, the Amazon, Changjiang and Huanghe Rivers account for 15% of global riverine POC supply and 20% of the bulk sediment supply to the oceans. The Amazon, Changjiang and Huanghe studies cited include examinations of both proximal and distal portions of river dispersal systems (DeMaster et al. 1985, Kuehl et al. 1986, Showers and Angle 1986, Alexander et al. 1991, Cauwet and Mackenzie 1993, Aller et al. 1985, Tan et al. 1991, Zhang et al. 1992, Niino and Emery 1961). In these environments, organic carbon burial rate is 75 gC m^{-2} yr^{-1} (range: 39 to 120 gC m^{-2} yr^{-1}) and the buried organic carbon composition is 54% autochthonous and 46% allochthonous (Table 2.2). Similar results were noted for shelf sediments adjacent to the Columbia River (burial rate: 36 gC m^{-2} yr^{-1}; ~50% allochthonous) (Carpenter 1987, Prahl and Carpenter 1984). Burial rates in these deltaic-shelf environments are considerably higher than those reports for non-deltaic shelves (5-7 gC m^{-2} yr^{-1}) (Christensen 1994, Wollast 1991, Anderson et al. 1994), for highly productive oceanic environments (0.3 gC m^{-2} yr^{-1}) (Berner 1982), and for the open ocean (0.06 gC m^{-2} yr^{-1}) (Stein 1991).

Bulk sediment accumulation in the four deltaic-shelf areas examined (0.1 Pg yr^{-1}; 9.5 x 10^{10} m^2) represents 7% of the global sediment discharge to the oceans. Based on this

percentage and a global continental shelf area of 30 x 10^6 km^2, the area of deltaic shelves influenced by terrigenous input is estimated to be 1.4 x 10^6 km^2. Using an average burial rate of 75 gC m^{-2} yr^{-1}, deltaic shelves are a global sink for an estimated 0.11 PgC yr^{-1} of organic carbon. This agrees well with Berner's estimate for deltaic shelves (Berner 1982, 1989). However, two assumptions have been implicit when applying Berner's shelf carbon burial estimate to global carbon budgets: (1) all the organic carbon buried in deltaic-shelf sediments is terrigenous; and (2) the bulk of organic carbon buried in continental shelves accumulate in deltaic-shelf environments. Our data indicate that only 0.05 PgC yr^{-1} (less than half) of the organic carbon buried in deltaic-shelf environments is of terrestrial origin, inconsistent with the first assumption. Furthermore, data from recent studies (Christensen 1994, Wollast 1991, Anderson et al. 1994) indicate significant burial of organic carbon in non-deltaic shelf environments. This is inconsistent with the second assumption and emphasizes the need for more global-scale information regarding carbon burial in non-deltaic shelf sediments.

Based on our data, autochthonous carbon burial rates average 39 gC m^{-2} yr^{-1} in deltaic-shelf environments, resulting in a global estimate of 0.06 PgC yr^{-1}. This represents about 20% of the average in situ production on continental shelves (200 gC m^{-2} yr^{-1}). Therefore, only 80% of in situ production is remineralized within deltaic-shelf systems, compared to 97-98% loss in shelf environments which are not influenced by rivers (Christensen 1994, Wollast 1991). The enhanced preservation potential of autochthonous POC in deltaic-shelf environments, relative to non-deltaic shelves, is consistent with previous observations of more efficient organic carbon burial in environments with higher rates of total sediment burial (Canfield 1989, Heinrichs and Reeburgh 1987). Some of the CO_2 released from terrigenous organic carbon remineralization in shelf environments may be fixed by in situ production in the water column and later buried in shelf sediments with an "autochthonous" carbon signal. Therefore, more information concerning carbon burial on continental shelves is needed, especially direct measurements of organic carbon content coupled with bulk sediment burial rates and multiple tracer techniques that utilize isotopes and molecular biomarkers (Berner 1989, Prahl et al. 1994).

The mean burial rate for terrigenous organic carbon in deltaic-shelf environments is 36 gC m^{-2} yr^{-1} or about 31% of allochthonous supply (Table 2.2). The high percentage of riverine organic material remineralized (~2 times higher than previous estimates) (Wollast 1991) may be due to a co-oxidation of refractory allochthonous organics with more labile autochthonous material, as has been hypothesized for the Amazon Shelf (Aller et al. in press), or a result of more efficient remineralization due to the dominant role of metal oxides as oxidants of organic matter in these environments.

Our revised estimate of terrigenous organic carbon burial can be used to help constrain oceanic CO_2 flux models. Sarmiento and Sundquist (1992) revised previous global carbon estimates (Houghton et al. 1990, Tans et al. 1990) by using the net oceanic flux of riverine organic carbon to constrain estimates of air-sea CO_2 exchange. Based on our analysis, the average burial rate of riverine organic carbon in deltaic-shelf sediments (0.05 PgC yr^{-1}) is less than half the value used by Sarmiento and Sundquist (1992) (citing ref. 1 and 2). The steady-state assumption of their model is that the net oceanic carbon flux from rivers (terrigenous input minus burial) is balanced by a flux of CO_2 out of the ocean. Our results indicate that this net oceanic flux of organic carbon from rivers is significantly larger than current estimates because terrestrial carbon is more poorly preserved (more completely remineralized) in shelf sediments than previously thought.

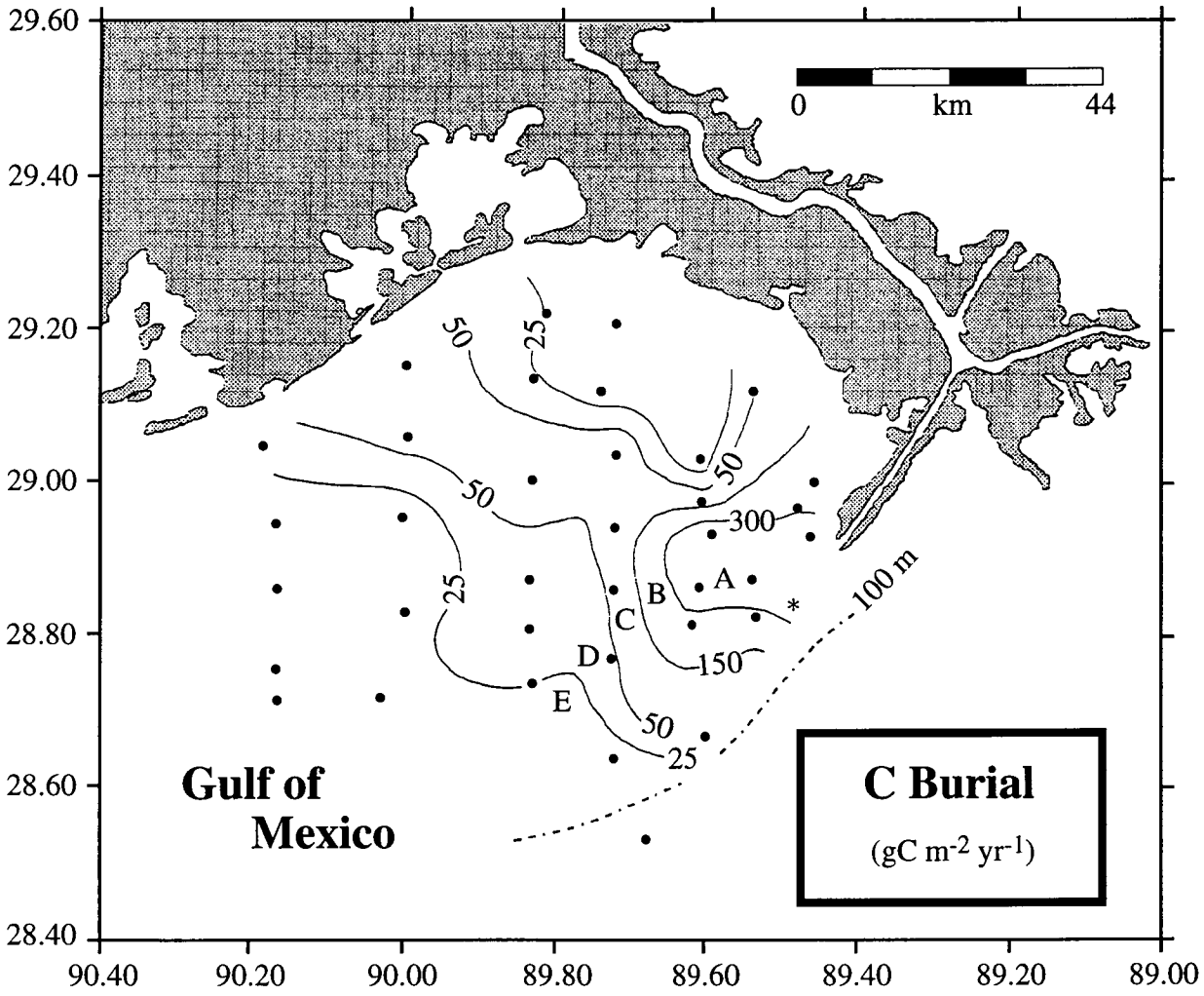

Figure 2.1. Spatial distribution of organic carbon burial rates (gC m^{-2} yr^{-1}) for the 5400 km^2 study site in the Mississippi deltaic-shelf environment.

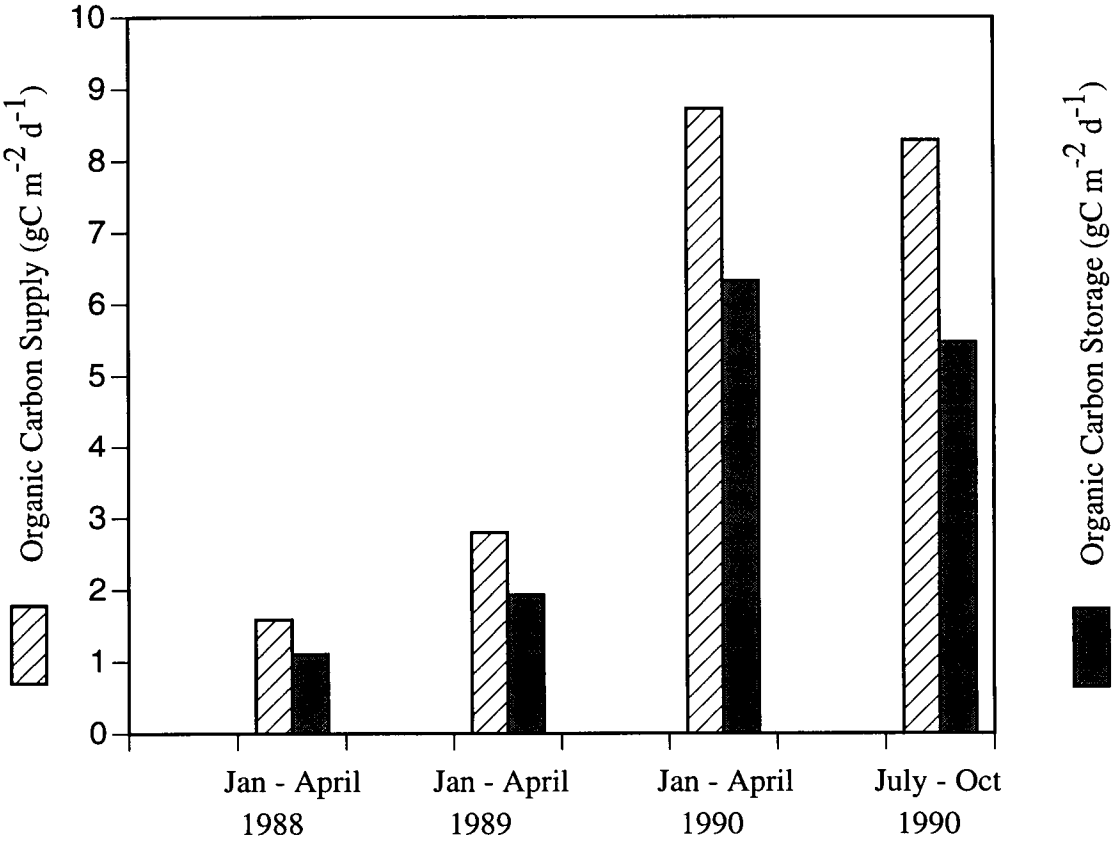

Figure 2.2. Temporal relationship between the organic carbon seasonally stored at station B50 (a site proximal to the mouth of the Mississippi River; see Figure 2.1 for location) and the particulate riverine organic carbon supplied during the same period.

Table 2.1. Organic carbon burial in the Mississippi deltaic-shelf environment.

Region	Boundaries (gC m^{-2} yr^{-1})	Mean Value (gC m^{-2} yr^{-1})	Area (km^2)	Carbon Burial (gC m^{-2} yr^{-1})	% tPOC*	Terrigenous Org. C Burial (gC yr^{-1} x 10^{10})	Terrigenous Org. C Burial (gC m^{-2} yr^{-1})
A	>300	394	217	8.5	70	6.0	276
B	150-300	252	379	9.5	50	4.8	127
C	50-150	75	1300	9.8	30	2.9	22
D	25-50	31	1192	3.7	10	0.4	3
E	<25	13	2329	3.1	5	0.2	1
Mean		64	5417	34.6	41	14.3	26

* Estimated percentage of organic carbon buried in each region that is of terrestrial origin, based on samples from the study area cited in the literature (Gearing et al. 1977, Shultz and Calder 1976, Thayer et al. 1983, Eadie et al. 1994, Hedges and Parker 1976, Newman et al. 1973).

Table 2.2. Organic carbon burial and remineralization in major river deltaic-shelf environments.

River	Riverine Supply ($gC\ m^{-2}\ yr^{-1}$)	Burial				Remineralization		References
		Total Burial ($gC\ m^{-2}\ yr^{-1}$)	% Alloch thonous	Alloch thonous ($gC\ m^{-2}\ yr^{-1}$)	Autoch thonous ($gC\ m^{-2}\ yr^{-1}$)	Alloch thonous ($gC\ m^{-2}\ yr^{-1}$)	% Alloch thonous	
Mississippi	81	64	40	26	38	55	68	This Study
Amazon	125	75	70	52	23	73	58	Kuehl et al. 1986 Aller et al. in press
Changjiang	202	120	45	54	66	148	73	DeMaster et al. 1985, Heinrichs and Reeburgh 1987 Canfield 1989, Prahl et al. 1994
Huanghe	49	39	30	12	27	37	76	Alexander et al. 1991, Heinrichs and Reeburgh 1987
Mean		75	46	36	39	78	69	

Chapter 3

INVENTORY OF BENTHIC FLUXES IN THE LOUISIANA BIGHT

3.1 Introduction

The coupling of benthic and pelagic processes apparently accounts for the elevated rates of primary productivity that are associated with land margin ecosystems. This is partially explained by the high rates of in situ nutrient remineralization that may be several orders of magnitude greater than allochthonous inputs. The annual contribution of nitrogen from sediments to primary production in shallow marine systems was from 28 to 35% in North Carolina (Fisher et al. 1982), from 15 to 27% during the summer in upper Chesapeake Bay (Boynton and Kemp 1985), 65% in the Patuxent River estuary (Boynton et al. 1980), 35% in the Potomac River estuary (Callender and Hammond 1982), and 25% in Narragansett Bay (Nixon 1981). Most conceptual models for shallow marine systems predict that seasonal deposition of organic matter during spring, in concert with high rates of both water column and benthic remineralization during summer months, provide the predominant mechanisms for sustaining peak rates of primary productivity during the summer in land margin ecosystems (Boynton et al. 1982).

The contribution of sediment remineralization in shelf ecosystems is less clear. In the North Sea, 75% of the nitrogen requirements are met by benthic regeneration (Billen 1978), and in the Kiel Bight this flux may provide 100% of the phytoplankton demand for nutrients (Zeitzschel 1980). Walsh et al. (1978) estimate that sediments contribute 38% of the total nitrogen regeneration in the Mid Atlantic Bight, equivalent to the regeneration by zooplankton in the water column. Rowe et al. (1975) originally suggested that sediments in shallow shelf ecosystems, such as in the New York Bight, may provide "more than the total required nitrogen" based on an ammonium flux of 144 μmol m^{-2} h^{-1}. In a later analysis, regenerated nitrogen in the Mid Atlantic Bight during the summer of 1980 provided 50-80 % of nitrogen productivity, yet the contribution by sediments was only 7 % of the total nitrogen regeneration (Harrison et al. 1983). This lower estimate of benthic regeneration was based on an ammonium flux of only 15.4 ug at m^{-2} h^{-1}, although rates of benthic regeneration in Table VI in that article average 75 μmol m^{-2} h^{-1}. Other direct measurements of benthic ammonium flux in Christiansen Basin, and stations in the New Jersey and Long Island shelf regions average 71 and 105 μmol m^{-2} h^{-1}, respectively (Rowe 1978). Ammonium flux from sediments in the shelf off the mouth of the Changjiang River, East China Sea, ranged from 108 to 142 μmol m^{-2} h^{-1} (negative indicates uptake by sediments), with an average of only 29 μmol m^{-2} h^{-1} (Aller et al. 1985). The variation observed in rates of benthic nitrogen regeneration in shelf ecosystems depends on the further oxidation of ammonium to nitrate. It appears that benthic regeneration of nitrogen in most shelf ecosystems is about half that amount observed in shallow land margin systems such as estuaries.

The LASER and COMUS cruises provided several opportunities to study benthic fluxes in the plume region of the Louisiana Bight (Figure 1.2). Chapter 3 provides an inventory of all these flux studies with information on logistics and ambient sediment and bottom water conditions. This information should provide necessary information on sediment boundary conditions for modelling efforts of this region of the Louisiana-Texas continental shelf. In addition, this chapter describes the spatial patterns of benthic fluxes as described from the first three LASER cruises. This spatial coverage is more thoroughly described

relative to specific sediment characteristics in Chapter 5. The temporal pattern of benthic fluxes at selected stations in the study area is described in Chapter 4. The hypothesis of these studies is that benthic nutrient regeneration in river-dominated continental shelf is spatially and temporally controlled by input of terrigenous materials. The quantity of materials deposited to the seabed is specifically linked to discharge and loading rates of sediments and nutrients through Southwest Pass to the Louisiana Bight. The quality of material is a function of the transformation of these materials to primary productivity and chlorophyll biomass that is eventually delivered to the seabed, at a different spatial and temporal pattern as to bulk deposition. How these allochthonous and autochthonous materials control the patterns of benthic nutrient regeneration is the focus of studies described in Chapters 3, 4, and 5.

3.2 Methods

3.2.1 Benthic Fluxes

Intact sediment cores from stations in the shelf were incubated aboard ship under near ambient conditions to determine the exchange of inorganic nitrogen (ammonium, nitrate, nitrite), phosphate, silicate and dissolved oxygen across the sediment-water interface. Intact sediment cores were used to measure ambient rates of nutrient fluxes and sediment oxygen demand which are dependent on the chemical and physical properties of the intact sediment structure. Undisturbed sediment cores were subsampled from a box core with 9 cm diameter, 20 cm long acrylic tubes. The bottom of the core was sealed with a rubber stopper, and the upper end was sealed with gaskets and plexiglass plates (6 mm thick). The ambient overlying water was removed via siphon and replaced with filtered (GFF,1.1 um pore size) ambient bottom water to represent ambient conditions.

Problems associated with substrate and dissolved oxygen depletion in batch core experiments are remedied by a flow-through design in which an autoanalyzer pump (Cole Palmer) delivers the experimental solutions from reservoirs at controlled flow rates (typically 4 mL/min) through influent and effluent lines connected to the cores (Koike and Hattori 1978, Miller-Way and Twilley 1996). Miniature immersible water pumps (0.47 L/min capacity at 0.3 m head, Edmund Scientific) with variable transformer control were used to mix the overlying water within the cores without resuspending sediment. Reservoirs of the respective filtered water and sediment cores were incubated at ambient seawater temperatures onboard ship. The influent and effluent solutions were sampled at approximate 1.5 h intervals for 8 h for analyses of dissolved oxygen and inorganic nutrients (PO_4, NO_3, NH_4, NO_2, SiO_4). Rates of nutrient flux were calculated using influent (I) and effluent (E) concentrations of the respective nutrient by the following equation: $(I-E)V/A$ = Flux (μmol m^{-2} h^{-1}); where V is the flow rate (L/h), and A is the surface area of the core.

3.2.2 Sediments Analyses

Flux cores at each station were subsampled with a 2.5 cm^2 acrylic core to a depth of 10 cm and analyzed for total carbon, nitrogen and phosphorus. Similar subsamples were centrifuged at 2000 rpm for 20 min and the supernatant (pore-waters) filtered (GFF glass fiber) and assayed for dissolved inorganic nitrogen and phosphorus using standard colorimetric techniques (Strickland and Parsons 1972). Sample preparation and reagent additions were made in anaerobic environments using nitrogen filled glove bags to prevent precipitation of inorganic P in pore-waters. The top 2 cm of each core was homogenized and analyzed for size, water content, and bulk density by drying 3 cm^3 fresh sediment at 85°C to constant weight. These dried samples were ground, and subsamples ashed at 450°C for 3 h. Other

subsamples were assayed for total carbon and nitrogen with a LECO Elemental Analyzer. Total phosphorus was determined by dissolving the ashed samples with HCl and determining PO_4 concentrations. Surface sediment chlorophyll was extracted from 1 cm^3 samples with DMSO for 1 h and assayed on a Turner fluorometer.

3.3 Results and Discussion

3.3.1 Benthic Flux Inventory

A complete inventory of benthic nutrient fluxes and sediment oxygen demand of all the LASER and COMUS cruises is given in Table 3.2. There were no sediment respiration estimates during the COMUS cruises. This composite of benthic fluxes includes a wide spatial array of the study area (Figure 1.2) and for some stations a temporal measure of processes for all 8 cruises (such as C-50). The spatial trends in benthic fluxes is described below (Section 3.3.2) and temporal variatio in Chapter 4. The COMUS results are analyzed in Chapter 5.

3.3.2 Spatial Fluxes (LASER 1 - LASER 3)

The ambient conditions of bottom waters at stations where benthic fluxes were measured are based on CTD casts prior to each experiment (Table 3.1). These waters are usually approximately 1 m above the sediment-water interface. Ambient temperatures of bottom waters ranged from 14.9°C at C-80 during LASER 2 to about 27°C that was recorded at all of the 20 m stations during LASER 1 (Table 3.1). The lowest dissolved oxygen concentration of bottom waters during the first three LASER cruises was 0.25 mg/L and occurred at E-20 during the August 1987 cruise. Concentrations of DO <3.0 mg/L occurred at only two other occassions during these three cruises; one of these was again at the E-20 station during April 1989 and the other at D-50 also during the April 1989 cruise (Table 3.1).

Concentrations of nitrate recorded during LASER 1-3 ranged from 1.3 to 60.1 µmol/L at E-50 and E-20, respectively; and E-20 also had the high concentrations of nitrite at 3.2 µmol/L (Table 3.1). Peak concentrations of ammonium (7.7 µmol/L, at B-20), phosphate (4.2 µmol/L, at E-20), and silicate (46.7 µmol/L, at B-20). Thus the shallow water stations generally had the higher concentrations of nutrients, either at the near- or far -field locations relative to the mouth of Southwest Pass. Lowest concentrations of phosphate and silicate occurred at the E-80 station.

Pore-water and sediment characteristics of the cores used in estimates of benthic ffluxes during LASER 1-3 cruises are given in Table 3.3.

Rates of sediment oxygen demand (SOD) are sensitive to temperature control and the high rates at C-80, E-80 during LASER 1 and E-20 during LASER 3 (Figure 3.2) are associated with a 5°C higher water temperatures in the flux cores compared to ambient temperatures from CTD casts at each respective station (Table 3.1). All the other SOD rates for LASER 1-3 (Figure 3.2) were determined under conditions of water temperature that are within 2°C of ambient conditions. SOD rates along the 50-m contour decrease with distance from Southwest Pass during LASER 1 and 3 from 3 to about 1.8 g m^{-2} d^{-1} (Figure 3.2). Rates along the 80 m contour are generally lower than the more shallow stations (ignoring the LASER 1 rates) with no clear pattern relative to distance from Southwest Pass. With the exception of LASER 1, there is also a spatial pattern of SOD rates among the stations along the 20 m contour, with slightly lower rates at increase distance from Southwest Pass.

There was generally a release of phosphate during LASER 1 and 3 at all stations measured, whereas phosphate fluxes were negligible at these stations during LASER 2. There was no clear spatial pattern in phosphate fluxes relative to either depth or distance from Southwest Pass (Figure 3.3). Highest rates of phosphate release from sediment to the water column ranged from 40-50 μmol m^{-2} h^{-1}, particularly during LASER 3. Highest uptake of phosphate was -10 μmol m^{-2} h^{-1}, measured at E-20 during LASER 1.

Rates of silicate release from sediments were higher during LASER 1 and 3 compared to lower rates during LASER 2 (Figure 3.4). Flux rates >450 μmol m^{-2} h^{-1} were observed at D-20 and C-80 during LASER 1 and C-50 and E-80 during LASER 3; thus no clear spatial pattern in peak rates among the cruises. During LASER 2, silicate flux was similar among all the stations ranging from 100-200 μmol m^{-2} h^{-1}. One of the lowest rates of silicate flux, at 50 μmol m^{-2} h^{-1}, was observed at D-50 next to one of the highest rates of benthic silicate flux during LASER 3 (Figure 3.4).

Benthic fluxes of ammonium ranged from uptake of -10 μmol m^{-2} h^{-1} to release of 550 μmol m^{-2} h^{-1} during LASER 1 to 3 (Figure 3.5). Rates were generally lower during LASER 1 and II and higher during LASER 3. There was a general spatial trend of higher ammonium flux at stations nearer to Southwest Pass and decreasing with distance to the west, particularly along the 50-m contour for all three LASER cruises. This spatial gradient in ammonium flux was particularly evident at this depth during LASER 3. Lowest rates of ammonium regeneration from sediments were consistently observed at the E station at each of the three depths.

There was generally a release of nitrite from sediments to overlying water during LASER 1 and III, whereas there was an uptake of nitrite during LASER 2 (Figure 3.6). Highest rates of release ranged from 20-40 μmol m^{-2} h^{-1}, particularly at 50-m transect during LASER 1 and 3.

Nitrate uptake occurred across the sediment-water interface was observed at most of the stations during LASER 1, 2, and 3 (Figure 3.7). There were some notable exceptions that included rates of nitrate release of >75 μmol m^{-2} h^{-1} at stations B-20 during LASER 3, and E-80 during LASER 2. Nitrate release also occurred at most of the 20-m stations during LASER 2. Benthic nitrate uptake was up to 50 μmol m^{-2} h^{-1} during LASER 1 and 2; but during LASER 3 there was an uptake rate of -150 μmol m^{-2} h^{-1} at B-50. The other sites where nitrate uptake occurred during LASER 3 also had rates of about 50 μmol m^{-2} h^{-1} (Figure 3.7). For all three LASER cruises, 7 stations had nitrate release, 6 had nitrate uptake, and 2 stations had negligible rates of nitrate exchange.

Fluxes of nutrients and dissolved oxygen across the sediment water interface of the Louisiana shelf ecosystem are within the upper range of rates for most shelf ecosystems (Figure 3.8). These remineralization rates are based on measurements at 9 stations in the shelf region near the vicinity of the Mississippi River plume, during August 1987, April 1988 and 1989. Mean shelf rates of ammonium regeneration ranged from 75 to 200 μmol m^{-2} h^{-1}. Lohrenz et al. (1990) have estimated phytoplankton demand for nitrogen (2.0 x 10^7 g N d^{-1}) based on models of primary productivity in a 1700 km^2 region of the Louisiana shelf in April 1988. Using a mean flux of 200 μmol m^{-2} h^{-1} of ammonium from sediments during this period, we calculate that benthic remineralization could contribute about 40% (0.8 x 10^7 g N d^{-1}) of the phytoplankton demand for nitrogen in this ecosystem. The contribution of sediments

may be even higher in summer when river nutrient input is lower and benthic remineralization rates are higher. Thus in the Louisiana Bight, sediments may be significant in sustaining high rates of primary productivity during trhe summer when allochthonous input is low.

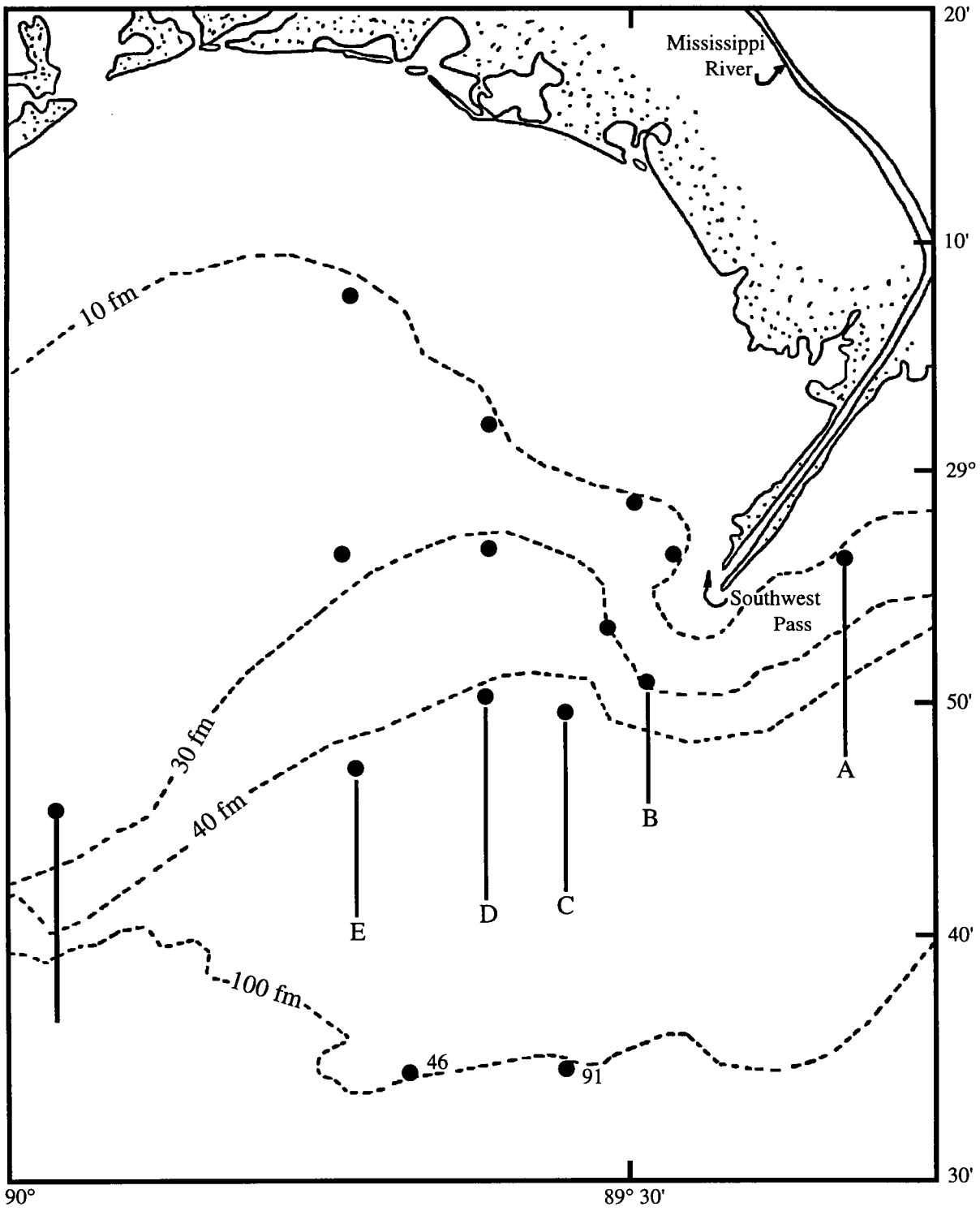

Figure 3.1. Location of sampling stations at three depths and four different transects each at increasing distance from mouth of Southwest Pass.

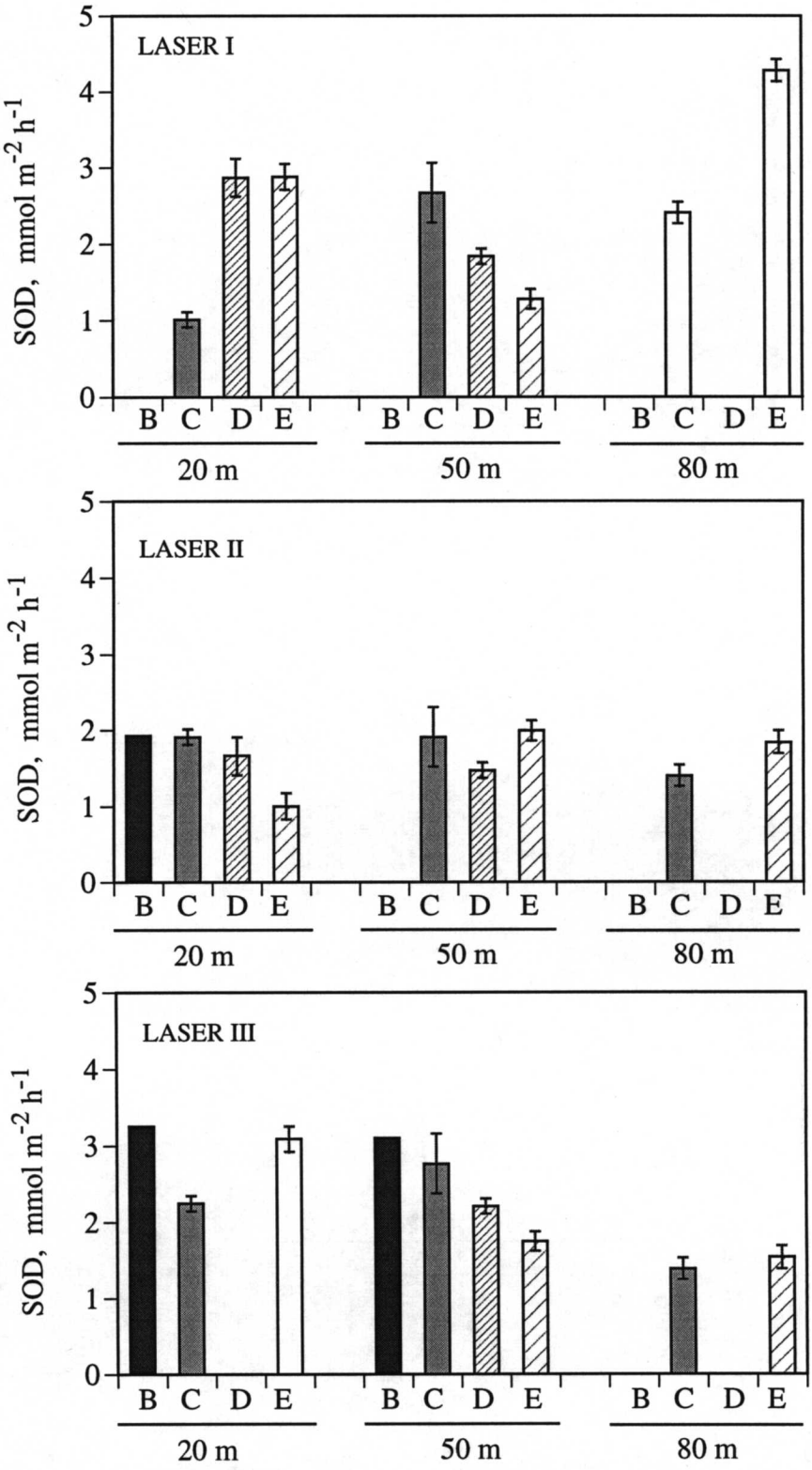

Figure 3.2. Sediment oxygen demand at three depths along transects at increasing distance from the mouth of Southwest Pass.

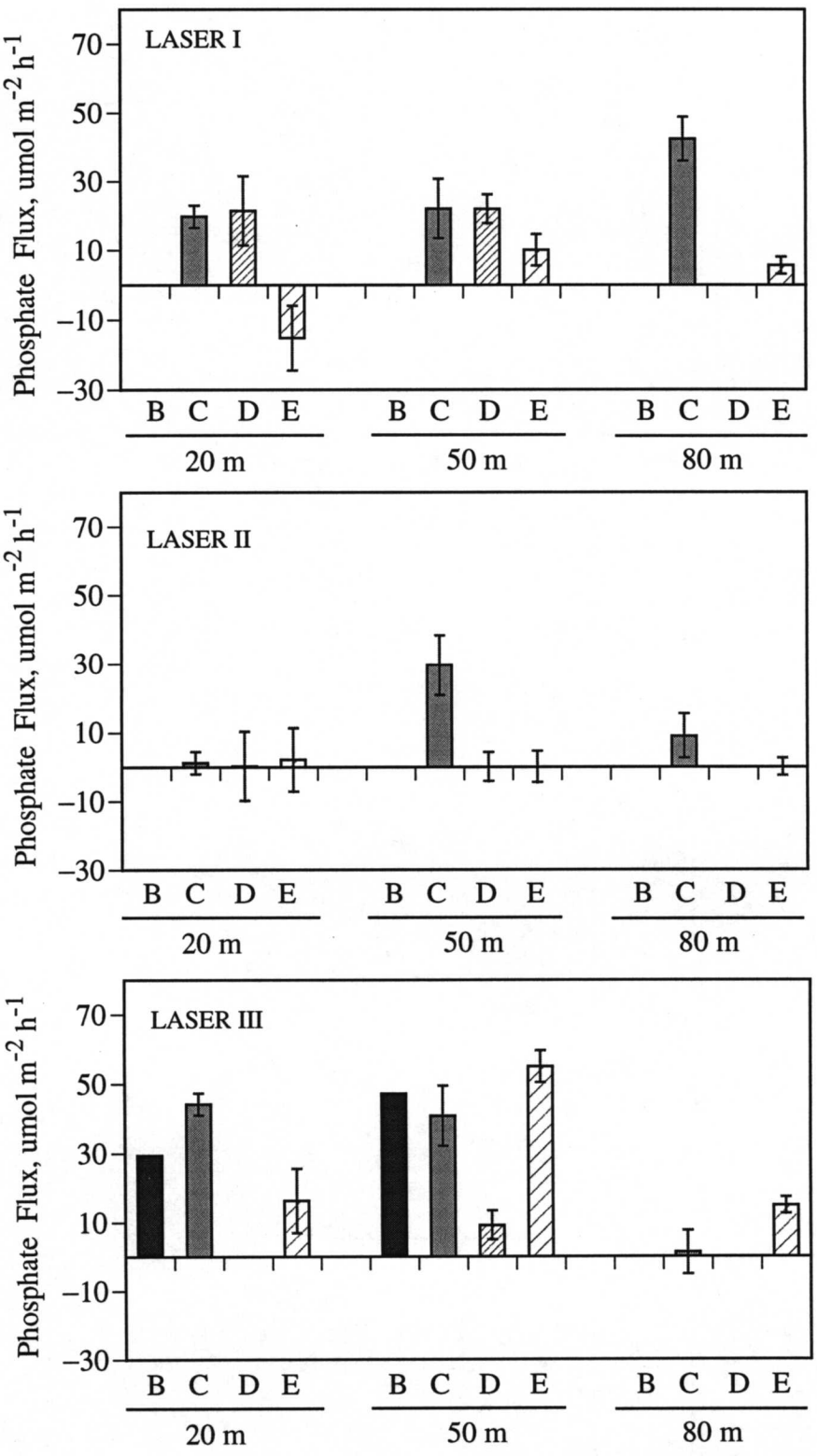

Figure 3.3. Benthic fluxes of phosphate at three depths along transects at increasing distance from the mouth of Southwest Pass.

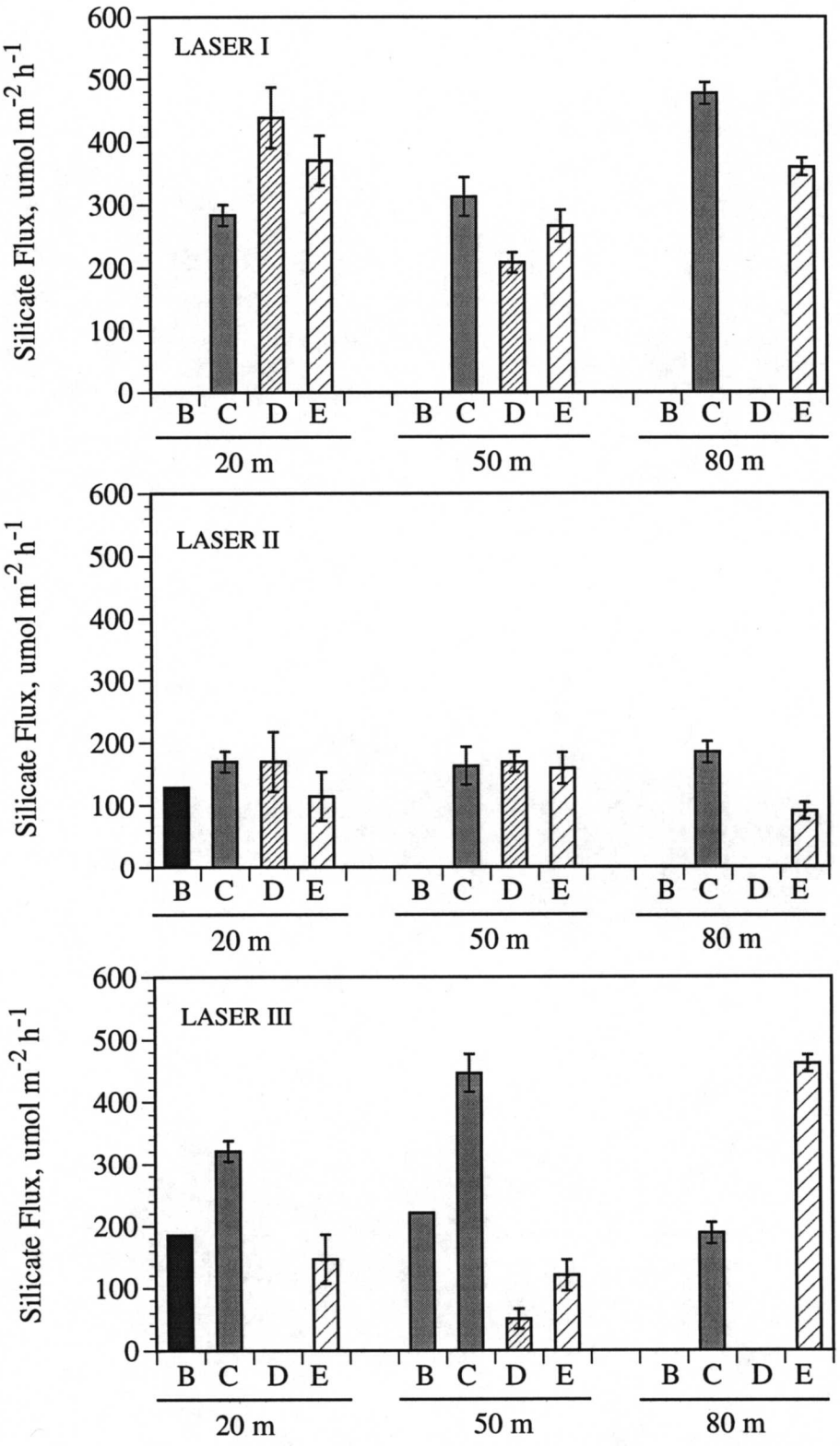

Figure 3.4. Benthic fluxes of silicate at three depths along transects at increasing distance from the mouth of Southwest Pass.

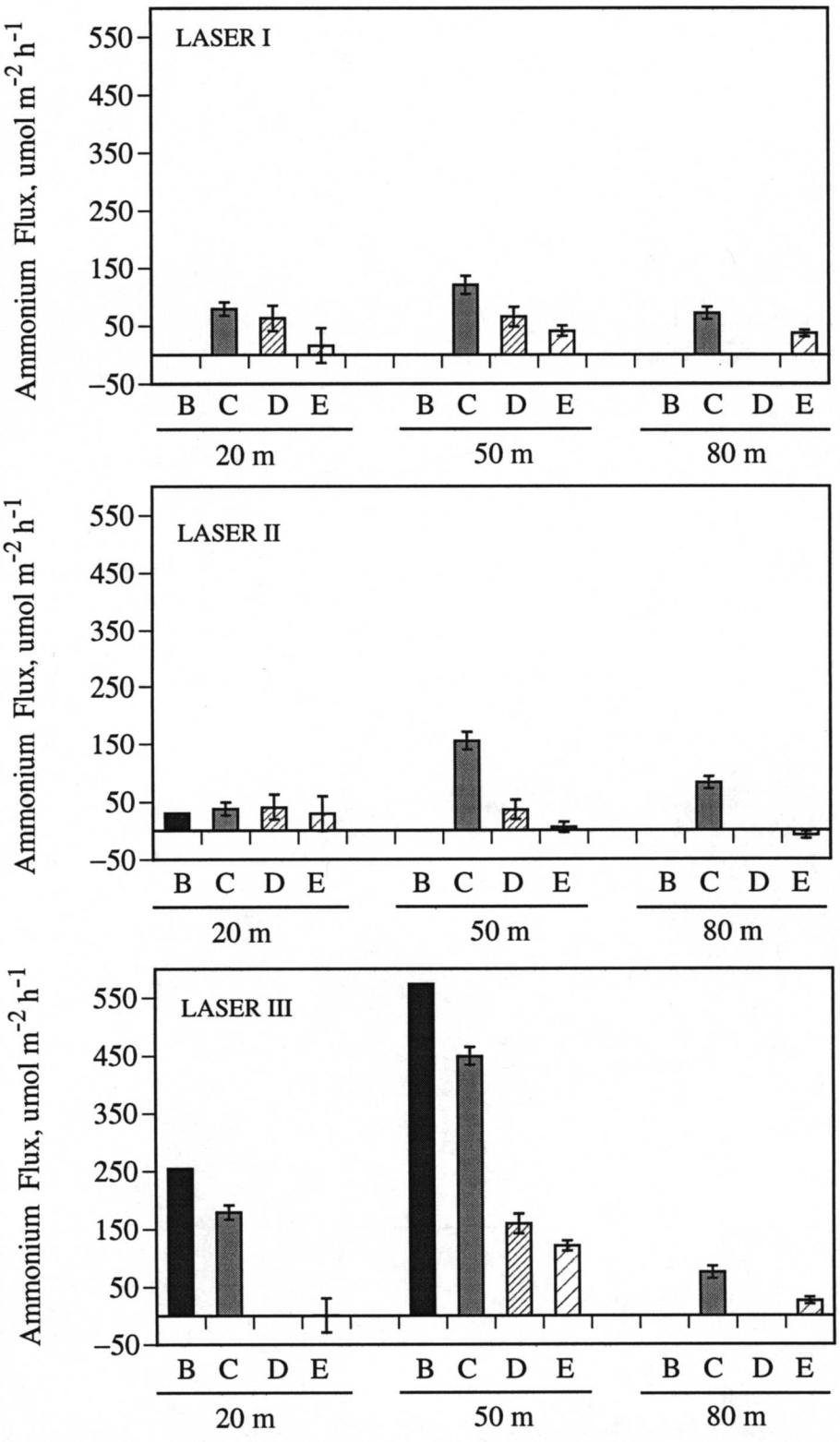

Figure 3.5. Benthic fluxes of ammonium at three depths along transects at increasing distance from the mouth of Southwest Pass.

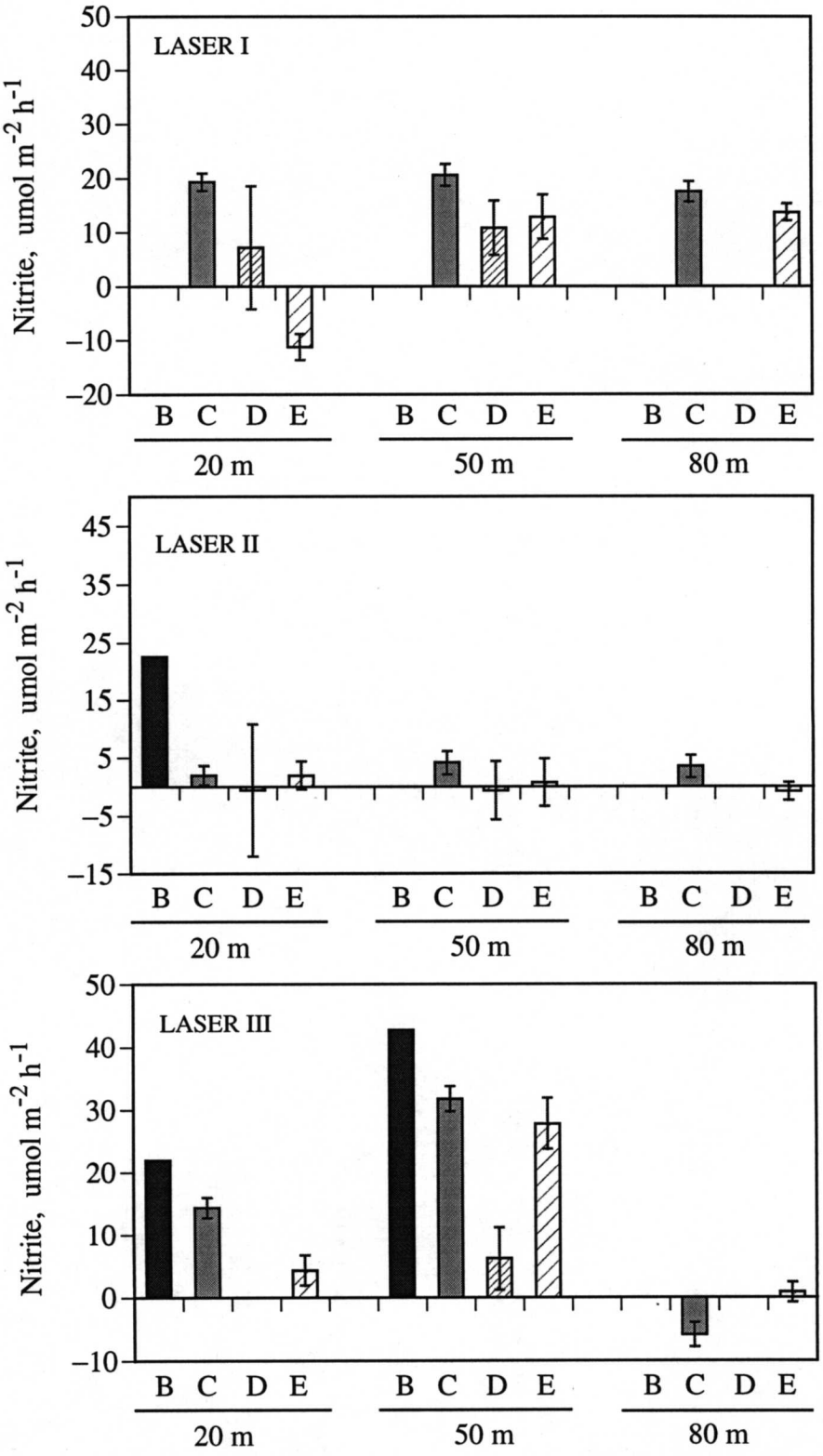

Figure 3.6. Benthic flux of nitrite at three depths along transects at increasing distance from the mouth of Southwest Pass.

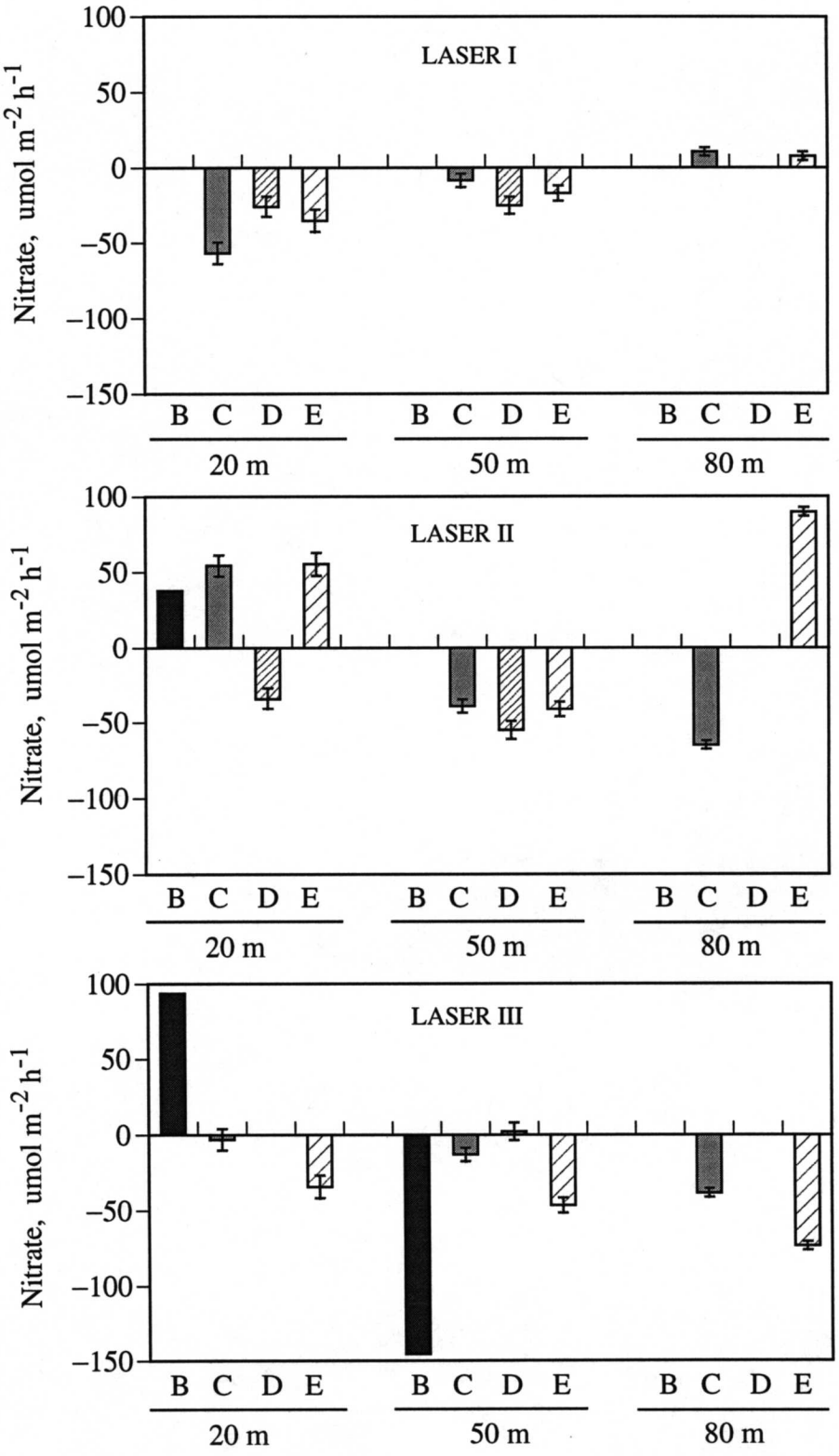

Figure 3.7. Benthic flux of nitrate at three depths along transects at increasing distance from the mouth of Southwest Pass.

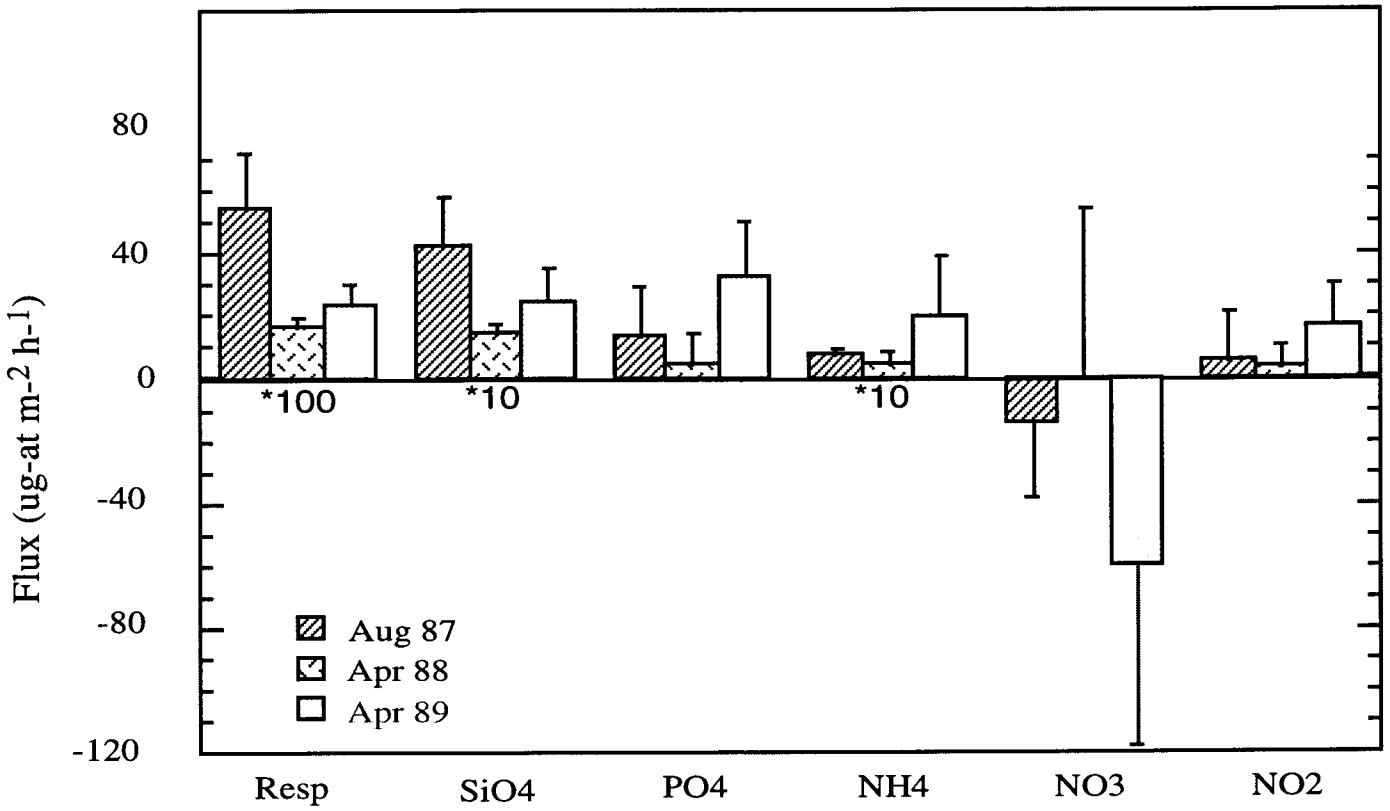

Figure 3.8. Rates of exchange of dissolved oxygen, silicate, phosphate, ammonium, nitrate and nitrite across the sediment-water interface in a Louisiana shelf ecosystem.

Table 3.1. Description of bottom waters at each of the benthic flux stations during LASER and COMUS cruises.

Station ID	Cruise	CTD Station	Latitude	Longitude	Date	Time	Station Bottom Water							
							Salinity (psu)	Temp (C)	DO (mg/L)	NO3 (umol/L)	NO2 (umol/L)	NH4 (umol/L)	PO4 (umol/L)	SIO4 (umol/L)
B-20	L2	2062	28 55.60	89 28.18	4/22/88	1900	33.39	19.62	5.86	4.13	0.42	3.20		46.65
B-20	L3	3035	28 55.53	89 28.18	4/16/89	0701	31.15	20.80	3.17	11.38	1.17	7.68	0.80	6.76
B-50	L3	3036	28 50.63	89 29.02	4/16/89	1351	36.39	19.92	3.14	14.81	1.08	4.11	1.18	7.10
B-50	L4	4023	28 50.43	89 29.50	9/23/89	0121	36.32	25.08	4.82					
B-50	L5	5007	28 50.82	89 29.22	4/23/90	2100	35.66	20.93	5.95					
B-50	L6													
B-50	C1		25 50.47	89 29.07			36.49	20.00	2.90					
B-50	C3		28 50.48	89 29.19			36.25	19.80	5.34					
C-20	L1	1104	28 58.00	89 28.50	7/31/87	0230	34.84	27.27	1.21	11.78	1.45	0.61	2.10	19.95
C-20	L2	2032	28 58.00	89 28.61	4/19/88	1717	35.71	18.87	3.22	15.56	1.18	5.44	0.71	12.67
C-20	L3	3037	28 57.97	89 28.59	4/17/89	0720	33.71	20.87	2.69	11.67	1.28	0.99	0.58	5.60
C-50	L1	1075	28 52.50	89 31.50	7/23/87	2025				5.76	0.93	2.21	ns	11.68
C-50	L2	2006	28 52.46	89 31.34	4/16/88	2155	36.28	18.20	4.31	17.28	0.06	0.10	1.19	7.47
C-50	L3	3038	28 52.43	89 31.77	4/17/89	1146	36.45	20.20	3.19	12.74	0.66	1.99	0.79	13.07
C-50	L5	5022	28 52.48	89 31.67	4/25/90	1515	36.04	21.35	5.89					
C-50	L6	6034	28 52.42	89 31.09										
C-50	C1		28 25.48	89 31.68			36.75	20.00	3.00					
C-50	C3		28 52.51	89 31.52			36.15	20.50	6.10					
C-80	L1	1028	28 49.70	89 32.50	7/23/87	1528	36.24	21.91	3.46	3.39	0.50	1.78	0.62	6.29
C-80	L2	2013	28 49.70	89 32.59	4/17/88	2025	35.91	14.94	3.61	25.94	0.11	1.56	1.50	9.71

Table 3.1. Description of bottom waters at each of the benthic flux stations during LASER and COMUS cruises.

Station ID	Cruise	CTD Station	Latitude	Longitude	Date	Time	Station Bottom Water							
							Salinity (psu)	Temp (C)	DO (mg/L)	NO3 (umol/L)	NO2 (umol/L)	NH4 (umol/L)	PO4 (umol/L)	SIO4 (umol/L)
C-80	L3	3041	28 49.70	89 32.86	4/18/89	1140	36.40	19.69	2.99	6.39	1.05	0.52	0.68	23.38
D-20	L1	1074	29 01.80	89 36.60	7/28/87	2357	35.37	26.72	4.94	2.97	2.98	2.74	ns	15.87
D-20	L2	2023	29 01.71	89 36.69	4/18/88	1905	33.74	19.50	6.79					
D-50	L1	1066	28 56.00	89 35.60	7/27/87	2139	36.25	21.10	4.17	5.73	1.01	1.74	0.83	12.44
D-50	L2	2044	28 56.02	89 35.63	4/20/88	2344	36.16	17.57	3.63	20.04	0.67	1.24		11.20
D-50	L3	3043	28 55.88	89 35.66	4/19/89	0704	36.41	19.71	2.29	13.28	0.34	1.74	2.01	15.66
D-50	L4	4036	28 56.02	89 35.50	9/26/89	1831	33.76	28.01	5.42					
D-50	L5	5023	28 55.82	89 35.82	4/25/90	1852	36.00	21.47	6.05					
D-50	L6													
D-50	C1		28 56.03	89 35.58			nd	20.00	4.00					
D-50	C3		28 56.01	89 35.60			35.98	18.75	3.86					
E-20	L1	1001	29 08.45	89 43.26	7/21/87	1026	34.37	27.42	0.25	60.12	3.17	2.96	4.15	42.26
E-20	L2	2033	29 08.41	89 43.40	4/19/88	2200	33.82	19.60	8.70	5.00	0.88	3.80	0.65	7.78
E-20	L3	3047	29 07.24	89 44.63	4/19/89	1139	35.93	20.60	2.40	3.28	1.39	1.16	1.31	7.22
E-20	L6	6032	29 07.25	88 44.52										
E-20	C3		29 07.25	89 44.56			35.84	21.99	2.21					
E-30	C1		29 02.44	89 43.60			34.20	26.00	3.50					
E-50	L1	1051	28 56.74	89 43.55	7/26/87	2310	36.20	22.38	3.57	5.41	1.35	2.33	0.93	11.76
E-50	L2	2043	28 56.83	89 43.60	4/20/88	1955	36.20	17.88	3.59	16.40	0.55	1.28		12.25
E-50	L3	3048	28 56.75	89 43.55	4/20/89	1220	36.44	20.18	3.49	1.29	0.71	0.58	0.42	7.91

Table 3.1. Description of bottom waters at each of the benthic flux stations during LASER and COMUS cruises.

Station ID	Cruise	CTD Station	Latitude	Longitude	Date	Time	Station Bottom Water							
							Salinity (psu)	Temp (C)	DO (mg/L)	NO3 (umol/L)	NO2 (umol/L)	NH4 (umol/L)	PO4 (umol/L)	SIO4 (umol/L)
E-50	L5	5042	28 56.73	89 43.50	4/27/90	1936	35.33	21.00	5.61					
E-50	L6	6033	28 56.73	89 43.62										
E-50	C1		28 56.88	89 43.53			34.40	20.00	4.00					
E-50	C3		28 56.69	89 43.54			30.70	20.00	5.20					
E-60	C1		28 51.65	89 43.52			nd	20.35	4.35					
E-80	L1	1039	28 46.50	89 43.50	7/24/87	2250	36.27	20.91	3.34	3.13	0.50	0.88	0.51	7.63
E-80	L2	2052	28 46.66	89 43.60	4/21/88	1940	36.46	18.31	4.90	9.57	0.12	2.15		3.51
E-80	L3	3040	28 46.49	89 43.53	4/18/89	0710	36.43	19.50	4.55	2.56	0.31	0.52	0.20	4.13
F-20	C1		29 08.26	89 50.03			32.53	26.80	2.59					
F-50	C1		28 52.51	89 50.08			nd	21.00	4.00					
F-50	C3		28 52.49	89 50.03			34.70	19.27	3.10					
G-50	C1		28 43.19	90 01.97			35.18	24.50	5.92					
G-50	C3		28 42.79	90 02.00			nd	20.40	6.50					
H-50	C1		28 42.97	90 10.08			33.46	25.00	5.34					
H-50	C3		28 42.80	90 10.22			nd	20.80	5.80					
SP	C3		29 00.36	89 09.28			0.00	24.90	5.20					

Table 3.2. Summary statistics for benthic fluxes at stations on the Louisiana Bight during LASER and COMUS cruises.

Station ID	CRUISE	CTD Station	Latitude	Longitude	Date	Respiration X (g m-2 d-1)	Respiration SE (g m-2 d-1)	PO4 FLUX X (ug-at m-2 h-1)	PO4 FLUX SE (ug-at m-2 h-1)	SiO4 FLUX X (ug-at m-2 h-1)	SiO4 FLUX SE (ug-at m-2 h-1)
B-20	L2	2062	28 55.60	89 28.18	4/22/88	0.74	0.03			127.9	13.2
B-20	L3	3035	28 55.53	89 28.18	4/16/89	1.25	0.03	29.4	10.2	185.2	20.5
B-50	L3	3036	28 50.63	89 29.02	4/16/89	1.19	0.04	47.2	13.2	221.1	18.7
B-50	L4	4023	28 50.43	89 29.50	9/23/89			19.1	18.6		
B-50	L5	5007	28 50.82	89 29.22	4/23/90	0.69	0.22	-24.9	42.4	259.4	175.4
B-50	L6					0.89	0.22	18.3	10.9	189.6	52.1
B-50	C1		25 50.47	89 29.07				39.4	4.5	291.4	29.6
B-50	C3		28 50.48	89 29.19				40.7	3.0	506.3	61.6
C-20	L1	1104	28 58.00	89 28.50	7/31/87	0.39	0.04	19.8	3.2	283.5	16.8
C-20	L2	2032	28 58.00	89 28.61	4/19/88	0.73	0.04	1.2	0.8	168.9	17.4
C-20	L3	3037	28 57.97	89 28.59	4/17/89	0.86	0.04	44.2	10.8	320.9	34.5
C-50	L1	1075	28 52.50	89 31.50	7/23/87	1.03	0.15	22.1	8.7	312.8	30.6
C-50	L2	2006	28 52.46	89 31.34	4/16/88	0.73	0.04	29.6	8.2	162.0	19.5
C-50	L3	3038	28 52.43	89 31.77	4/17/89	1.07	0.07	40.8	29.0	446.5	32.2
C-50	L5	5022	28 52.48	89 31.67	4/25/90	1.33	0.22	6.5	5.2	570.8	168.0
C-50	L6	6034	28 52.42	89 31.09				33.1	24.8	298.4	71.6
C-50	C1		28 25.48	89 31.68				41.3	8.4	313.5	45.9
C-50	C3		28 52.51	89 31.52				22.3	2.7	461.9	41.8
C-80	L1	1028	28 49.70	89 32.50	7/23/87	0.93	0.05	42.4	6.4	476.5	17.3
C-80	L2	2013	28 49.70	89 32.59	4/17/88	0.54	0.02	8.9	1.3	183.6	12.3
C-80	L3	3041	28 49.70	89 32.86	4/18/89	0.54	0.05	1.3	17.1	188.3	47.8
D-20	L1	1074	29 01.80	89 36.60	7/28/87	1.10	0.10	21.5	10.1	438.3	48.2
D-20	L2	2023	29 01.71	89 36.69	4/18/88	0.64	0.04	0.2	1.2	168.9	15.3

Table 3.2. Summary statistics for benthic fluxes at stations on the Louisiana Bight during LASER and COMUS cruises.

Station ID	CRUISE	CTD Station	Latitude	Longitude	Date	Respiration X (g m-2 d-1)	Respiration SE (g m-2 d-1)	PO4 FLUX X (ug-at m-2 h-1)	PO4 FLUX SE (ug-at m-2 h-1)	SiO4 FLUX X (ug-at m-2 h-1)	SiO4 FLUX SE (ug-at m-2 h-1)
D-50	L1	1066	28 56.00	89 35.60	7/27/87	0.71	0.04	22.0	4.2	207.8	15.9
D-50	L2	2044	28 56.02	89 35.63	4/20/88	0.57	0.03			168.1	10.4
D-50	L3	3043	28 55.88	89 35.66	4/19/89	0.85	0.04	9.2	3.3	50.5	65.7
D-50	L4	4036	28 56.02	89 35.50	9/26/89			10.9	20.8	280.3	150.5
D-50	L5	5023	28 55.82	89 35.82	4/25/90	1.03	0.28	24.9	23.3	595.4	197.2
D-50	L6					0.71	0.18	9.3	9.2	229.9	46.6
D-50	C1		28 56.03	89 35.58				43.4	5.3	339.2	58.3
D-50	C3		28 56.01	89 35.60				16.6	2.4	481.7	20.6
E-20	L1	1001	29 08.45	89 43.26	7/21/87	1.11	0.06	-15.2	9.3	370.1	39.2
E-20	L2	2033	29 08.41	89 43.40	4/19/88	0.38	0.02	2.0	0.7	113.2	7.0
E-20	L3	3047	29 07.24	89 44.63	4/19/89	1.19	0.07	16.3	4.9	146.8	16.6
E-20	L6	6032	29 07.25	88 44.52		0.73	0.11	4.7	5.6	242.1	45.5
E-20	C3		29 07.25	89 44.56				2.6	2.5	195.6	32.4
E-30	C1		29 02.44	89 43.60				23.5	4.8	483.7	48.0
E-50	L1	1051	28 56.74	89 43.55	7/26/87	0.49	0.05	10.1	4.5	266.4	25.2
E-50	L2	2043	28 56.83	89 43.60	4/20/88	0.77	0.04			158.1	8.7
E-50	L3	3048	28 56.75	89 43.55	4/20/89	0.67	0.13	55.0	15.3	120.6	7.8
E-50	L5	5042	28 56.73	89 43.50	4/27/90	1.14	0.34	36.7	40.8	747.9	217.4
E-50	L6	6033	28 56.73	89 43.62		1.02	0.35	-8.4	16.6	206.8	127.0
E-50	C1		28 56.88	89 43.53				58.8	4.9	516.9	28.3
E-50	C3		28 56.69	89 43.54				14.7	2.0	441.5	16.3
E-60	C1		28 51.65	89 43.52				11.6	2.0	314.4	17.6

Table 3.2. Summary statistics for benthic fluxes at stations on the Louisiana Bight during LASER and COMUS cruises.

Station ID	CRUISE	CTD Station	Latitude	Longitude	Date	Respiration X (g m-2 d-1)	Respiration SE (g m-2 d-1)	PO4 FLUX X (ug-at m-2 h-1)	PO4 FLUX SE (ug-at m-2 h-1)	SiO4 FLUX X (ug-at m-2 h-1)	SiO4 FLUX SE (ug-at m-2 h-1)
E-80	L1	1039	28 46.50	89 43.50	7/24/87	1.64	0.06	5.6	2.4	359.7	13.7
E-80	L2	2052	28 46.66	89 43.60	4/21/88	0.71	0.03			88.9	23.0
E-80	L3	3040	28 46.49	89 43.53	4/18/89	0.59	0.08	14.9	9.6	461.5	64.8
F-20	C1		29 08.26	89 50.03				12.9	3.9	479.6	61.3
F-50	C1		28 52.51	89 50.08				11.0	1.7	276.3	29.2
F-50	C3		28 52.49	89 50.03				-0.1	2.5	229.2	19.1
G-50	C1		28 43.19	90 01.97				8.3	0.8	189.7	15.2
G-50	C3		28 42.79	90 02.00				1.2	1.0	101.0	7.6
H-50	C1		28 42.97	90 10.08				11.0	1.6	190.8	28.2
H-50	C3		28 42.80	90 10.22				4.1	1.2	135.2	19.1
SP	C3		29 00.36	89 09.28				-19.9	5.1	-246.4	233.8

Table 3.2. Summary statistics for benthic fluxes at stations on the Louisiana Bight during LASER and COMUS cruises.

Station ID	CRUISE	CTD Station	Latitude	Longitude	Date	NH4 FLUX X (ug-at m-2 h-1)	NH4 FLUX SE	NO2 FLUX X (ug-at m-2 h-1)	NO2 FLUX SE	NO3 FLUX X (ug-at m-2 h-1)	NO3 FLUX SE
B-20	L2	2062	28 55.60	89 28.18	4/22/88	30.2	8.7	22.6	1.6	37.7	3.1
B-20	L3	3035	28 55.53	89 28.18	4/16/89	253.8	26.8	21.9	4.2	93.6	72.3
B-50	L3	3036	28 50.63	89 29.02	4/16/89	573.6	40.1	42.7	18.5	-145.7	26.4
B-50	L4	4023	28 50.43	89 29.50	9/23/89	22.4	46.4				
B-50	L5	5007	28 50.82	89 29.22	4/23/90	287.8	124.4	-0.8	6.4	-14.0	19.1
B-50	L6					108.1	99.1	10.2	4.5	-17.9	9.6
B-50	C1		25 50.47	89 29.07		210.0	43.7	7.8	0.7	-3.9	7.7
B-50	C3		28 50.48	89 29.19		550.5	48.6	3.8	0.7	-33.4	3.8
C-20	L1	1104	28 58.00	89 28.50	7/31/87	79.5	11.8	19.3	1.6	-56.9	7.0
C-20	L2	2032	28 58.00	89 28.61	4/19/88	37.6	10.6	2.0	0.8	54.1	32.2
C-20	L3	3037	28 57.97	89 28.59	4/17/89	179.3	20.4	14.3	4.9	-3.2	7.6
C-50	L1	1075	28 52.50	89 31.50	7/23/87	120.4	15.7	20.6	2.0	-8.4	4.5
C-50	L2	2006	28 52.46	89 31.34	4/16/88	154.9	17.8	4.1	0.4	-39.2	9.5
C-50	L3	3038	28 52.43	89 31.77	4/17/89	449.0	38.4	31.8	13.4	-13.0	39.2
C-50	L5	5022	28 52.48	89 31.67	4/25/90	408.0	114.0	8.8	4.4	88.7	64.6
C-50	L6	6034	28 52.42	89 31.09		50.2	264.9	-2.5	6.7	-15.0	5.6
C-50	C1		28 25.48	89 31.68		165.4	46.7	5.2	0.5	-12.2	5.1
C-50	C3		28 52.51	89 31.52		381.4	32.5	3.2	2.7	-32.0	12.5
C-80	L1	1028	28 49.70	89 32.50	7/23/87	71.7	10.9	17.5	1.9	10.4	2.9
C-80	L2	2013	28 49.70	89 32.59	4/17/88	82.0	12.9	3.4	0.0	-64.9	14.5
C-80	L3	3041	28 49.70	89 32.86	4/18/89	75.4	14.1	-5.9	4.4	-38.5	22.1
D-20	L1	1074	29 01.80	89 36.60	7/28/87	63.1	21.8	7.2	11.4	-25.8	6.7
D-20	L2	2023	29 01.71	89 36.69	4/18/88	40.4	18.7	-0.6	0.1	-34.2	13.8

Table 3.2. Summary statistics for benthic fluxes at stations on the Louisiana Bight during LASER and COMUS cruises.

Station ID	CRUISE	CTD Station	Latitude	Longitude	Date	NH4 FLUX X (ug-at m-2 h-1)	NH4 FLUX SE (ug-at m-2 h-1)	NO2 FLUX X (ug-at m-2 h-1)	NO2 FLUX SE (ug-at m-2 h-1)	NO3 FLUX X (ug-at m-2 h-1)	NO3 FLUX SE (ug-at m-2 h-1)
D-50	L1	1066	28 56.00	89 35.60	7/27/87	65.5	17.0	10.8	5.0	-25.1	5.7
D-50	L2	2044	28 56.02	89 35.63	4/20/88	35.8	5.1	-0.7	0.7	-55.1	11.8
D-50	L3	3043	28 55.88	89 35.66	4/19/89	159.6	13.5	6.2	2.0	2.2	6.8
D-50	L4	4036	28 56.02	89 35.50	9/26/89	3.1	49.5	-5.1	2.4	-3.5	18.4
D-50	L5	5023	28 55.82	89 35.82	4/25/90	168.8	143.2	17.4	10.5	30.7	33.2
D-50	L6					73.3	159.1	10.8	9.8	-17.9	9.0
D-50	C1		28 56.03	89 35.58		175.3	49.3	2.4	0.3	-24.1	12.7
D-50	C3		28 56.01	89 35.60		153.7	13.1	4.3	1.2	-87.2	48.9
E-20	L1	1001	29 08.45	89 43.26	7/21/87	15.8	30.0	-11.3	2.4	-35.3	7.5
E-20	L2	2033	29 08.41	89 43.40	4/19/88	29.3	9.5	1.9	0.7	55.1	19.3
E-20	L3	3047	29 07.24	89 44.63	4/19/89	0.9	16.0	4.3	2.0	-34.4	7.2
E-20	L6	6032	29 07.25	88 44.52		77.4	101.2	-5.8	3.9	-2.2	9.8
E-20	C3		29 07.25	89 44.56		29.8	8.4	1.1	1.7	-9.7	12.5
E-30	C1		29 02.44	89 43.60		100.2	10.9	0.6	1.6	1.6	3.2
E-50	L1	1051	28 56.74	89 43.55	7/26/87	40.7	8.9	12.8	4.1	-17.1	5.1
E-50	L2	2043	28 56.83	89 43.60	4/20/88	5.1	3.0	0.7	0.7	-41.3	19.2
E-50	L3	3048	28 56.75	89 43.55	4/20/89	121.4	20.7	27.8	8.3	-46.6	7.4
E-50	L5	5042	28 56.73	89 43.50	4/27/90	240.7	162.9	7.4	5.1	27.6	14.5
E-50	L6	6033	28 56.73	89 43.62		157.5	149.4	4.0	5.3	-49.7	32.7
E-50	C1		28 56.88	89 43.53		194.8	17.2	3.2	2.4	27.4	8.8
E-50	C3		28 56.69	89 43.54		76.7	23.2	9.0	4.4	-43.3	19.1
E-60	C1		28 51.65	89 43.52		100.0	27.5	2.7	1.4	-5.6	7.5

Table 3.2. Summary statistics for benthic fluxes at stations on the Louisiana Bight during LASER and COMUS cruises.

Station ID	CRUISE	CTD Station	Latitude	Longitude	Date	NH4 FLUX X (ug-at m-2 h-1)	NH4 FLUX SE (ug-at m-2 h-1)	NO2 FLUX X (ug-at m-2 h-1)	NO2 FLUX SE (ug-at m-2 h-1)	NO3 FLUX X (ug-at m-2 h-1)	NO3 FLUX SE (ug-at m-2 h-1)
E-80	L1	1039	28 46.50	89 43.50	7/24/87	36.9	6.0	13.8	1.6	7.5	2.8
E-80	L2	2052	28 46.66	89 43.60	4/21/88	-8.3	7.8	-0.9	0.4	89.6	35.4
E-80	L3	3040	28 46.49	89 43.53	4/18/89	26.1	17.2	0.8	5.0	-73.5	38.4
F-20	C1		29 08.26	89 50.03		243.6	37.7	-1.2	0.6	-33.6	3.0
F-50	C1		28 52.51	89 50.08		197.4	23.0	0.7	0.4	-4.7	8.4
F-50	C3		28 52.49	89 50.03		31.0	9.8	2.5	2.4	-42.4	29.1
G-50	C1		28 43.19	90 01.97		37.4	14.2	-3.0	1.0	10.8	3.1
G-50	C3		28 42.79	90 02.00		-0.9	8.0	-0.4	0.8	-24.5	1.8
H-50	C1		28 42.97	90 10.08		66.8	14.0	-5.1	2.6	-2.6	6.1
H-50	C3		28 42.80	90 10.22		47.2	13.2	-1.9	3.7	-8.4	3.0
SP	C3		29 00.36	89 09.28		1461.8	286.6	29.1	4.7	-454.3	276.2

Table 3.3. Sediment charactertistics of the benthic stations during the LASER and COMUS cruises.

Station ID	CRUISE	CTD Station	Latitude	Longitude	Date	Sediment Chlorophyll (ug/cm3)	POREWATER NH4 (umol/L)	POREWATER SIO4 (umol/L)	POREWATER PO4 (umol/L)	TOTAL SEDIMENT Carbon (mg/gdm)	TOTAL SEDIMENT Nitrogen (mg/gdm)	C:N Ratio
B-20	L2	2062	28 55.60	89 28.18	4/22/88						2.5	
B-20	L3	3035	28 55.53	89 28.18	4/16/89	0.40				17.4	2.3	9.0
B-50	L3	3036	28 50.63	89 29.02	4/16/89	0.56				14.0	1.9	8.6
B-50	L4	4023	28 50.43	89 29.50	9/23/89	0.54	166	194	19.1			
B-50	L5	5007	28 50.82	89 29.22	4/23/90	0.46						
B-50	L6					0.87	1065	200	5.4			
B-50	C1		25 50.47	89 29.07		0.44	100	97	7.7	19.5	2.4	9.7
B-50	C3		28 50.48	89 29.19		0.30	182	26	5.1	16.2	1.6	12.2
C-20	L1	1104	28 58.00	89 28.50	7/31/87		96	254	53.0	17.5	2.5	8.2
C-20	L2	2032	28 58.00	89 28.61	4/19/88	0.40				19.0	2.7	8.2
C-20	L3	3037	28 57.97	89 28.59	4/17/89	0.34	215	691	17.0	16.3	1.5	12.7
C-50	L1	1075	28 52.50	89 31.50	7/23/87		337	1491	43.0	17.8	1.8	11.5
C-50	L2	2006	28 52.46	89 31.34	4/16/88	0.48				17.1	2.3	8.7
C-50	L3	3038	28 52.43	89 31.77	4/17/89	0.87	488	502	71.0	15.8	1.8	10.2
C-50	L5	5022	28 52.48	89 31.67	4/25/90	0.42						
C-50	L6	6034	28 52.42	89 31.09								
C-50	C1		28 25.48	89 31.68		0.40	105	102	6.3	17.8	2.2	9.7
C-50	C3		28 52.51	89 31.52		0.50	231	30	9.5	17.2	1.9	10.5
C-80	L1	1028	28 49.70	89 32.50	7/23/87					16.0	2.0	9.3
C-80	L2	2013	28 49.70	89 32.59	4/17/88	0.30				16.5	2.4	8.0
C-80	L3	3041	28 49.70	89 32.86	4/18/89	0.63	5	105	12.0	15.5	1.4	12.9

Table 3.3. Sediment charactertistics of the benthic stations during the LASER and COMUS cruises.

Station ID	CRUISE	CTD Station	Latitude	Longitude	Date	Sediment Chlorophyll (ug/cm3)	POREWATER NH4 (umol/L)	POREWATER SIO4 (umol/L)	POREWATER PO4 (umol/L)	TOTAL SEDIMENT Carbon (mg/gdm)	TOTAL SEDIMENT Nitrogen (mg/gdm)	C:N Ratio
D-20	L1	1074	29 01.80	89 36.60	7/28/87		159	426	17.0	8.3	1.2	8.1
D-20	L2	2023	29 01.71	89 36.69	4/18/88	0.25				7.5	0.9	9.7
D-50	L1	1066	28 56.00	89 35.60	7/27/87		285	1151	21.0	16.6	2.2	8.8
D-50	L2	2044	28 56.02	89 35.63	4/20/88	0.32				16.9	2.6	7.6
D-50	L3	3043	28 55.88	89 35.66	4/19/89	0.33	64	74	55.0	13.2	1.8	8.5
D-50	L4	4036	28 56.02	89 35.50	9/26/89	0.11	241	227	26.2			
D-50	L5	5023	28 55.82	89 35.82	4/25/90	0.33						
D-50	L6					0.98	657	184	4.9			
D-50	C1		28 56.03	89 35.58		0.44	78	75	11.1	19.2	2.5	9.0
D-50	C3		28 56.01	89 35.60		0.30	76	29	6.1	16.9	2.2	9.0
E-20	L1	1001	29 08.45	89 43.26	7/21/87		442	587	13.0	13.5	1.3	12.1
E-20	L2	2033	29 08.41	89 43.40	4/19/88	0.26				13.1	2.0	7.6
E-20	L3	3047	29 07.24	89 44.63	4/19/89	0.28	99	72		15.2	2.1	8.4
E-20	L6	6032	29 07.25	88 44.52		0.51	1018	272	21.7			
E-20	C3		29 07.25	89 44.56		0.17	39	28	7.3	14.9	1.7	10.5
E-30	C1		29 02.44	89 43.60		0.30	113	110	18.5	20.0	2.9	8.2
E-50	L1	1051	28 56.74	89 43.55	7/26/87		225	1068	26.0	16.9	2.2	9.0
E-50	L2	2043	28 56.83	89 43.60	4/20/88	0.28				17.5	2.9	7.0
E-50	L3	3048	28 56.75	89 43.55	4/20/89	0.31	24	66		17.0	3.2	6.2
E-50	L5	5042	28 56.73	89 43.50	4/27/90							
E-50	L6	6033	28 56.73	89 43.62								

Table 3.3. Sediment charactertistics of the benthic stations during the LASER and COMUS cruises.

Station ID	CRUISE	CTD Station	Latitude	Longitude	Date	Sediment Chlorophyll (ug/cm3)	POREWATER NH4 (umol/L)	POREWATER SIO4 (umol/L)	POREWATER PO4 (umol/L)	TOTAL SEDIMENT Carbon (mg/gdm)	TOTAL SEDIMENT Nitrogen (mg/gdm)	C:N Ratio
E-50	C1		28 56.88	89 43.53		1.08	127	124	32.8	20.0	3.3	7.1
E-50	C3		28 56.69	89 43.54		0.30	94	52	16.5	17.9	2.5	8.5
E-60	C1		28 51.65	89 43.52		0.40	90	87	1.6	18.0	2.4	8.8
E-80	L1	1039	28 46.50	89 43.50	7/24/87		34	897	16.0	14.7	1.4	12.3
E-80	L2	2052	28 46.66	89 43.60	4/21/88	0.11				15.9	2.5	7.4
E-80	L3	3040	28 46.49	89 43.53	4/18/89	0.04	12	40	19.0	15.3	2.8	6.4
F-20	C1		29 08.26	89 50.03		0.48	119	115	14.5	18.5	2.4	9.0
F-50	C1		28 52.51	89 50.08		0.27	215	212	13.2	17.1	2.2	9.0
F-50	C3		28 52.49	89 50.03		0.30	52	34	6.8	16.8	2.2	8.9
G-50	C1		28 43.19	90 01.97		0.47	51	48	1.3	11.6	1.2	11.7
G-50	C3		28 42.79	90 02.00		0.30	28	22	2.8	10.7	1.0	12.4
H-50	C1		28 42.97	90 10.08		0.34	65	62	0.7	13.6	1.1	14.4
H-50	C3		28 42.80	90 10.22		0.23	38	23	2.8	11.4	1.0	13.9
SP	C3		29 00.36	89 09.28		0.80	328	34	0.3	18.8	2.2	9.9

Chapter 4

SEASONAL INVESTIGATIONS OF BENTHIC FLUXES WITHIN THE LOUISIANA BIGHT

4.1 Introduction

The rate and efficiency of material cycling through both benthic and water-column communities are central to the ultimate fate of inorganic nutrients and organic matter within the Louisiana Bight region, and land-margin ecosystems in general. Of particular importance to understanding ecosystem response to nutrient enhancement is an understanding of those processes directly concerned with the input, remineralization, and loss of nutrients. The coupling of these processes is central to understanding the linkages of nutrient enrichment to the development of hypoxia in this region of the Louisiana shelf ecosystem. Previous studies of deposition suggest that the proximal region of the Mississippi River plume is a zone of extreme input of allochthonous particulate material to the seabed. Much of this material appears to be remineralized or transported out of the region. An important focus of this report is to determine the relative contributions of deposition and regeneration (redistribution) to the fate of sediments and nutrients in the Louisiana shelf ecosystem.

The plume region of river-dominated land margin ecosystems are sites of high sedimentation of allochthonous carbon, nitrogen and phosphorus. However, nutrient retention may vary within the plume region, particularly during high flow, depending on differences in depth and circulation. A common observation in river-dominated environments is that most of the sediment discharge is initially deposited near the river mouth; sedimentation rates decrease with increasing distance from the river (DeMaster et al. 1985; Nittrouer et al. 1987). Chapters 1, 2, and 3 show distinct spatial patterns in sedimentation, nutrient accumulation and benthic nutrient regeneration in the plume region of the Louisiana Bight. The spatial pattern in benthic nutrient regeneration is a combination of both the delivery of allochthonous materials to the seabed, with particularly high rates near Southwest Pass. There are also regions of nutrient regeneration in sediments that are not directly related to zones of terrigenous sedimentation, but may be more influenced by deposition of organic matter produced in the water column. Specific temporal patterns of benthic fluxes in response to river flow and water column processes should give more insights as to the coupling of benthic and pelagic processes in the plume region of the Louisiana Bight. This chapter describes patterns of deposition and benthic nutrient regeneration at selected stations along a 50-m contour west of Southwest Pass during times of high and low river discharge. These repeated measures of deposition and fluxes are compiled from LASER and COMUS cruises since 1987 (Figure 4.1).

4.2 Methods

The temporal sequence of benthic flux measurements in the Louisiana Bight relative to discharge of Mississippi River are shown in Figure 4.1. The LASER (L1-L6) and COMUS (C1 and C3) cruises are discussed in this chapter since they focus on the temporal benthic fluxes along the 50-m contour of the Louisiana Bight study area (Figure 2.1). The NECOP (N1-N2) cruises focussed on the study of the effects of hypoxia on benthic fluxes at selected sites, and are not included in this report. Cruises during high flow regimes include L2, L3, L5, compared to cruises during low discharge that included L1, L4, and L6. Both the C1 and C3 cruises occurred at the end of a high flow period.

4.2.1 Deposition

Box core samples were collected from stations in Louisiana Bight study area along the 50-m contour at transects B, C, D, and E during LASER and COMUS cruises periodically from 1987 to 1994 (Figure 4.1). Cores were subsampled from box cores within this grid after high and low river discharge periods for measurements of ^{234}Th, which is a naturally occurring (^{234}Th) radionuclide used to determine rates of deposition. These radionuclides are very particle-reactive (i.e., rapidly sorbed onto particle surfaces) and have proven to be very useful as particle tracers (Broecker et al. 1973; Santschi et al. 1980). Because of natural radioactive decay, this radionuclide is particularly useful in examining rates of sedimentary processes at time scales of days to months (e.g., sediment deposition related to flood and storm events).

Large diameter (16.5 cm) subcores were taken from box cores at each sampling station. Each core was carefully extruded and simultaneously subsectioned at precise 0.5-1.0 cm intervals. Yield tracers ($^{232}U/^{228}Th$) were added to the dried core samples, then leached with a combination HNO_3, HCl and $HClO_4$ solution. Thorium and uranium are isolated and purified via ion exchange methods, plated onto stainless steel planchets and counted on a low-background beta detection system (McKee et al. 1986). The deposition of materials in bottom sediments was calculated from the following equation (Hatton et al. 1983): A = Cd x R x D x 104 (g m^{-2} yr^{-1}); where A is the rate of nutrient deposition, Cd is the dry mass nutrient concentration, D is bulk density, and R is the deposition rate (determined by ^{234}Th).

4.2.2 Benthic Regeneration

Cores were subsampled from each of the box cores at stations along the 50-m contour in the study area to measure rates of benthic nutrient regeneration. Estimates of benthic flux followed the procedures of Miller-Way and Twilley (1996) as described in Section 3.2.1 (also see Chapter 5, Figure 5.4). Sediment analyses associated with these cores were as described in section 3.2.2.

4.3 Results and Discussion

Deposition rates calculated from samples collected in April of three consecutive years range from 69 to 436 gdw m^{-2} d^{-1} near the mouth (station B50) of southwest pass. This interannual variation reflects differences in cumulative discharge during the 3-4 months prior to sampling. Rates of deposition for similar discharge periods were generally less at downfield stations. During the low flow period, river discharge decreases by about 85%, resulting in reduced riverine input to the shelf.

Deposition rates (100-day time scale) within the plume region of the Mississippi River (Figure 1) are 5-10 times greater than the sediment accumulation rates (100-year time scale) determined using ^{210}Pb. The contrast in fate of materials deposited to the seabed based on relative rates of deposition and burial indicate that a substantial portion of these materials may be redistributed. Redistribution may occur from the shelf to shelf slope, or to more distal parts of the dispersal system along the shelf. Redistribution of materials delivered during high river flow leads to a more uniform distribution of particulates throughout the dispersal system.

The effect of high and low river discharge on the delivery of sediment to the Louisiana Bight study area, as measured by ^{234}Th deposition, for the 8 cruises are depicted in Figure

4.2. There are no data for L1 and L4 The most complete temporal data set of deposition exists for the B-50 and C-50 stations. Highest input rates of the 6 events measured at B-50 was LASER 5 during April 1990 at 3.8 cm/mo and the lowest was during LASER 2 in April 1988 at 0.2 cm/mo (Figure 4.2). At C-50 the April 1990 event is not as high as measured at B-50, with a rate of 2.5 cm/mo, nearly a cm/mo less than B-50. Generally rates of deposition during each cruise was higher at B-50 than C-50, except for April 1988 and April 1989 (Figure 4.2).

The best record for sediment chlorophyll is at B-50 and D-50 that depict the temporal quality of material in the top 1 cm depth of sediment (Figure 4.3). The highest chl-a concentration at D-50 and B-50 occurred in October 1990 at about 1 ug/cm^3 (for dates that measurements exists). The lowest concentration at D-50 occurred in September 1989, whereas at B-50 the lowest concentration was in June 1994. The low concentration at D-50 was about 0.1 ug/cm^3. The high concentrations of sediment chl-a (Figure 4.3) did not occur during events of highest deposition (Figure 4.3). There was not particular spatial pattern relative to distance from Southwest Pass as indicated by value of nearly 1 ug/cm^3 also measured at E-50 during November 1993.

Generally there was a release of phosphate among the stations for most of the cruises (Figure 4.4). Rates >50 μmol m^{-2} h^{-1} occurred at E-50 during two cruises including April 1989 and November 1993. These two dates were also the highest rates of phosphate release for the other stations along the 50-m contour, with the exceptio of D-50 during the April 1989 cruise. Phosphate uptake was recorded only once at B-50 during the April 1990 cruise. However, negligible benthic exchange of phosphate was observed on three occasions at D-50, twice at E-50 and once at C-50. Rates of phosphate flux were generally lower at D-50 during the cruises.

There was always a release of silicate from sediments at all stations along the 50-m contour for all cruises (Figure 4.5). Benthic fluxes of silicate >575 μmol m^{-2} h^{-1} occurred during April 1990 at C-50, D-50, and E-50; and these rates represented peak fluxes at these three locations. During the same cruise, silicate flux at B-50 was one of the lowest rates measured during this study. The temporal trend in benthic silicate fluxes at stations D-50 and E-50 were very similar among the 8 cruises (fluxes in September 1989 were not measured at E-50).

There was always a release of ammonium from sediments at the stations along the 50-m contour for the times measured during this study (Figure 4.6). Rates were generally higher at B-50 and C-50 compared to D-50 and E-50. At B-50 and C-50 peak rates of ammonium flux were 400-600 μmol m^{-2} h^{-1} and occurred in April 1989, April 1990, and June 1994 at both sites. In fact, the temporal trend in benthic ammonium fluxes among the 8 cruises was similar for these two stations. Temporal trends at D-50 and E-50 are similar with highest rates in April 1990 and November 1993. These peak rates are only about 200 μmol m^{-2} h^{-1}, much lower than the peak rates at B-50 and C-50.

In most experiments there was a release of nitrite from sediments along the 50-m contour of the study area (Figure 4.7). Highest rates of nitrite release ranged from 30 to 40 μmol m^{-2} h^{-1} at B, C, and E stations during the April 1989 cruise. Nitrite release at D-50 during this cruise was much lower at about 8 μmol m^{-2} h^{-1}. Nitrite uptake was only measured in 4 out of 27 experiments and all rates were < -7 μmol m^{-2} h^{-1}.

There was generally a pattern of nitrate uptake at stations along the 50-m contour (Figure 4.8). Nitrate release was observed during only 4 of the 27 measurements and rates in 3 of these observations were <25 μmol m^{-2} h^{-1}; an exception was the measurement at C-50 during April 1990 with a release rate of 75 μmol m^{-2} h^{-1}. The peak nitrate uptake rate was measured at B-50 during the April 1989 and was 145 μmol m^{-2} h^{-1}. The bottom water nitrate concentration at this station was only 14.8 μmol/L (Table 3.1). There were 9 observations where nitrate uptake rates ranged from 25 to 50 μmol m^{-2} h^{-1}; and several times the flux of nitrate was measured as negligible.

The relation of benthic fluxes with rates of sediment deposition (measured as an accretion rate) for just the stations along the 50-m contour of the Louisiana Bight study area is shown in Figure 4.9. Ammonium and phosphate fluxes are not particularly correlated to rates of deposition. Benthic fluxes of silicate shows some evidence of an increase in flux with deposition rate up to 2.5 cm/mo; above that rate of deposition the flux of silicate is lower. This metric of deposition is based on quantity of material added; there also needs to be an evaluation of the quality of that material.

Figure 4.10 includes deposition and benthic fluxes for all of the stations in the study area of the Louisiana Bight, covering several effects of distance from Southwest Pass and water depth. Again, ammonium and phosphate fluxes show no trend with deposition. And silicate again shows some evidence of silicate flux increasing with deposition up to 2-2.5 cm/mo; above which there is a decrease in flux.

Seasonal deposition of allochthonous organic matter during spring provides the predominant mechanism for sustaining peak rates of benthic regeneration in the plume region of the shelf. During April, ammonium regeneration in the plume region (station B-50 and C-50) may exceed 500 μmol m^{-2} h^{-1}, compared to fluxes of less than 200 μmol m^{-2} h^{-1} during low river discharge in September and October. Further downfield (stations D-50 and E-50), ammonium regeneration is generally less than 200 μmol m^{-2} h^{-1}. Seasonal differences in benthic regeneration are most evident nearest the mouth of the Mississippi River, while rates are more constant both temporally and spatially in more distant regions. The link between sediment deposition and benthic nutrient regeneration is clearly demonstrated in results of silicate flux at near and far-field stations on the Louisiana shelf. Fluxes of silicate across the sediment-water interface to the water column increase linearly with deposition rates from 0.3 to 2.5 cm/mo, reaching maximum silicate flux rates of 550 μmol m^{-2} h^{-1}. Above a deposition rate of 2.5 cm/mo, silicate flux was lower at less than half the maximum rates. However, this may be a station effect; there was a strong regression between deposition and silicate regeneration for station C-50, but silicate fluxes at B-50 were similar disregardless of the sediment deposition rate (Figure 4.2). Thus, the response of benthic fluxes to temporal variation of particulate input may vary spatially in the Louisiana shelf.

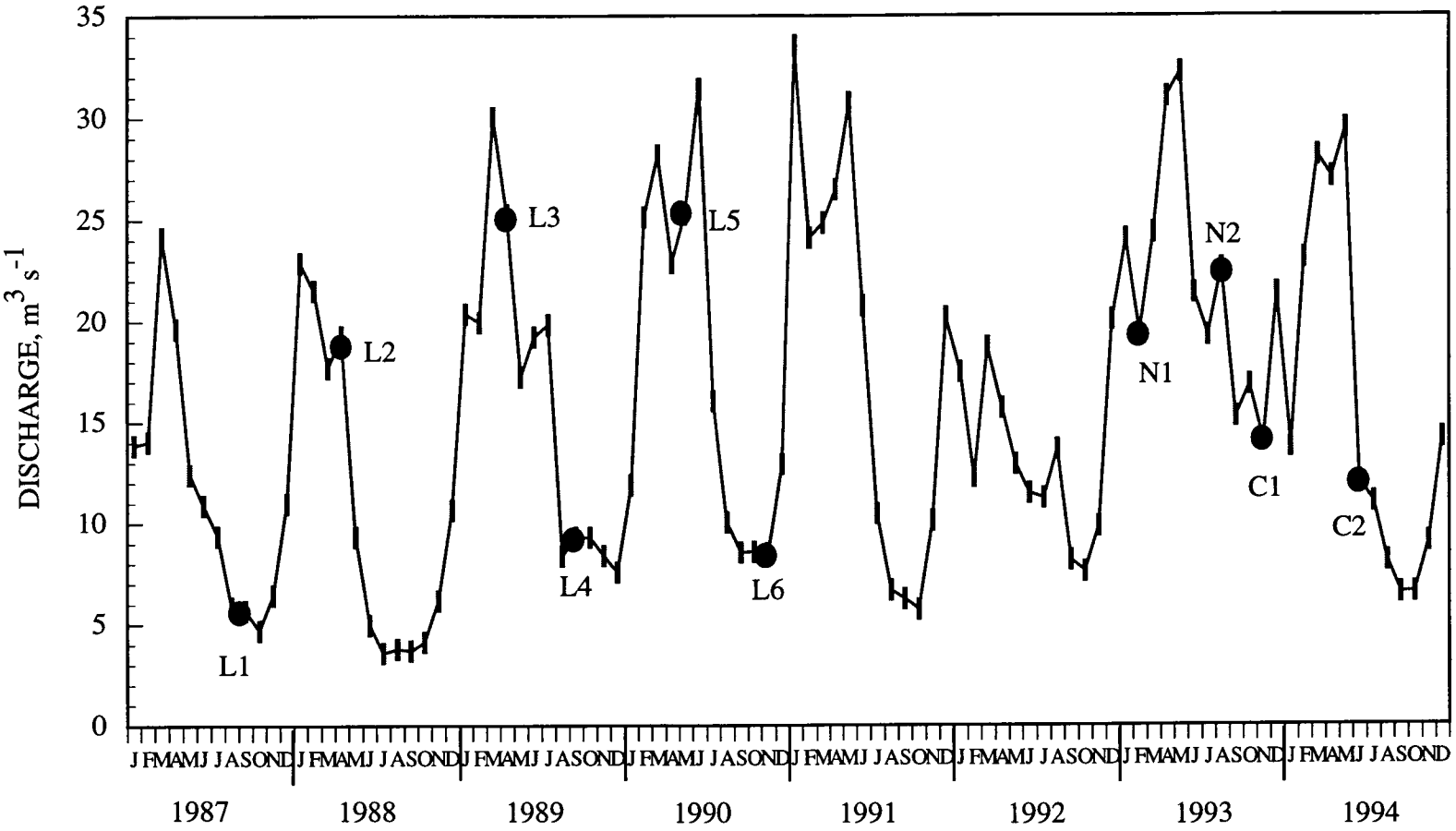

Figure 4.1. The timing of measuring benthic fluxes in the Louisiana Bight relative to the seasonal discharge of the Mississippi River.

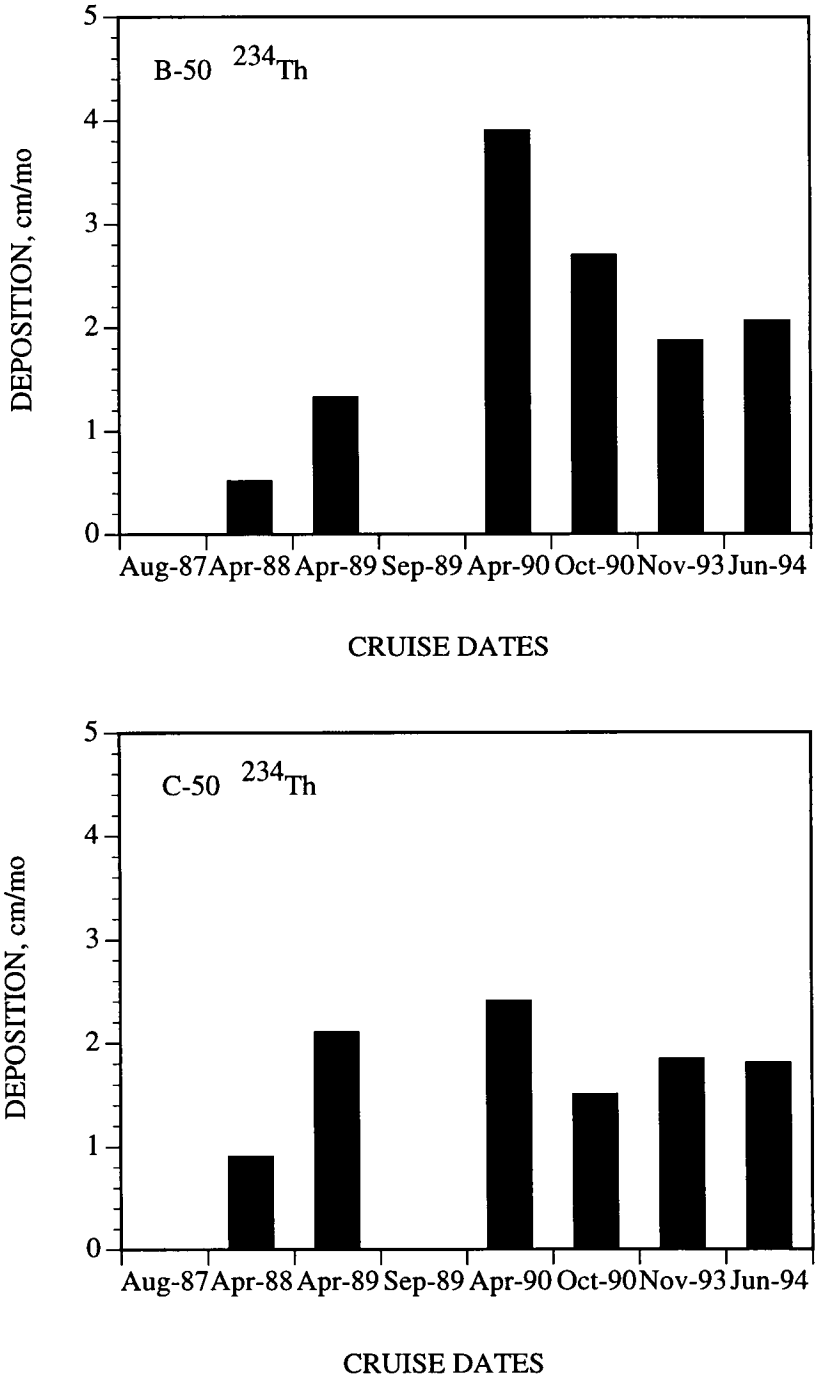

Figure 4.2. Rates of deposition based on accretion of thorium-234 at stations B-50 and C-50 during different LASER and COMUS cruises.

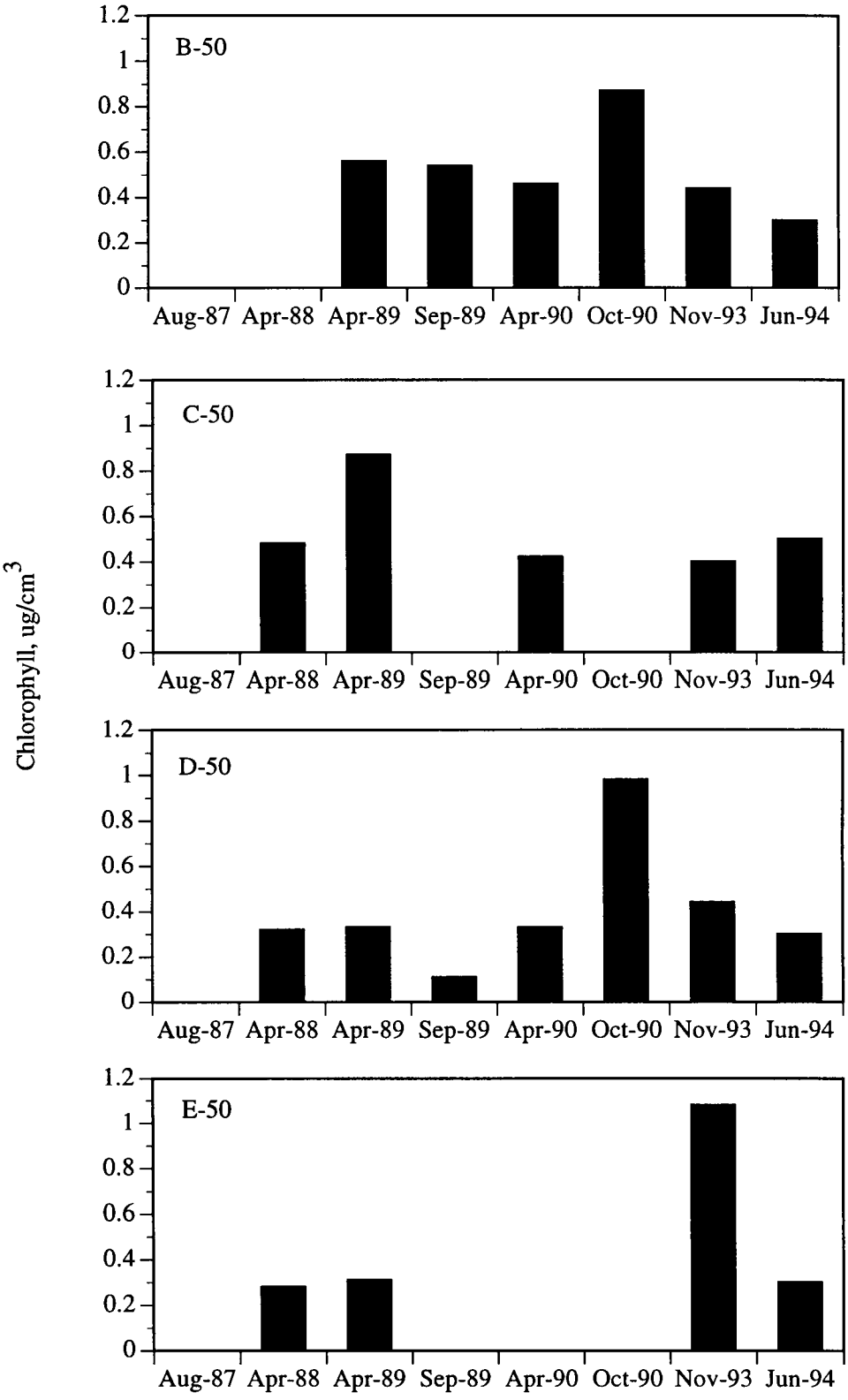

Figure 4.3. Concentrations of benthic chlorophyll along the 50-m contour of the Louisiana Bight at different distances from the mouth of Southwest Pass.

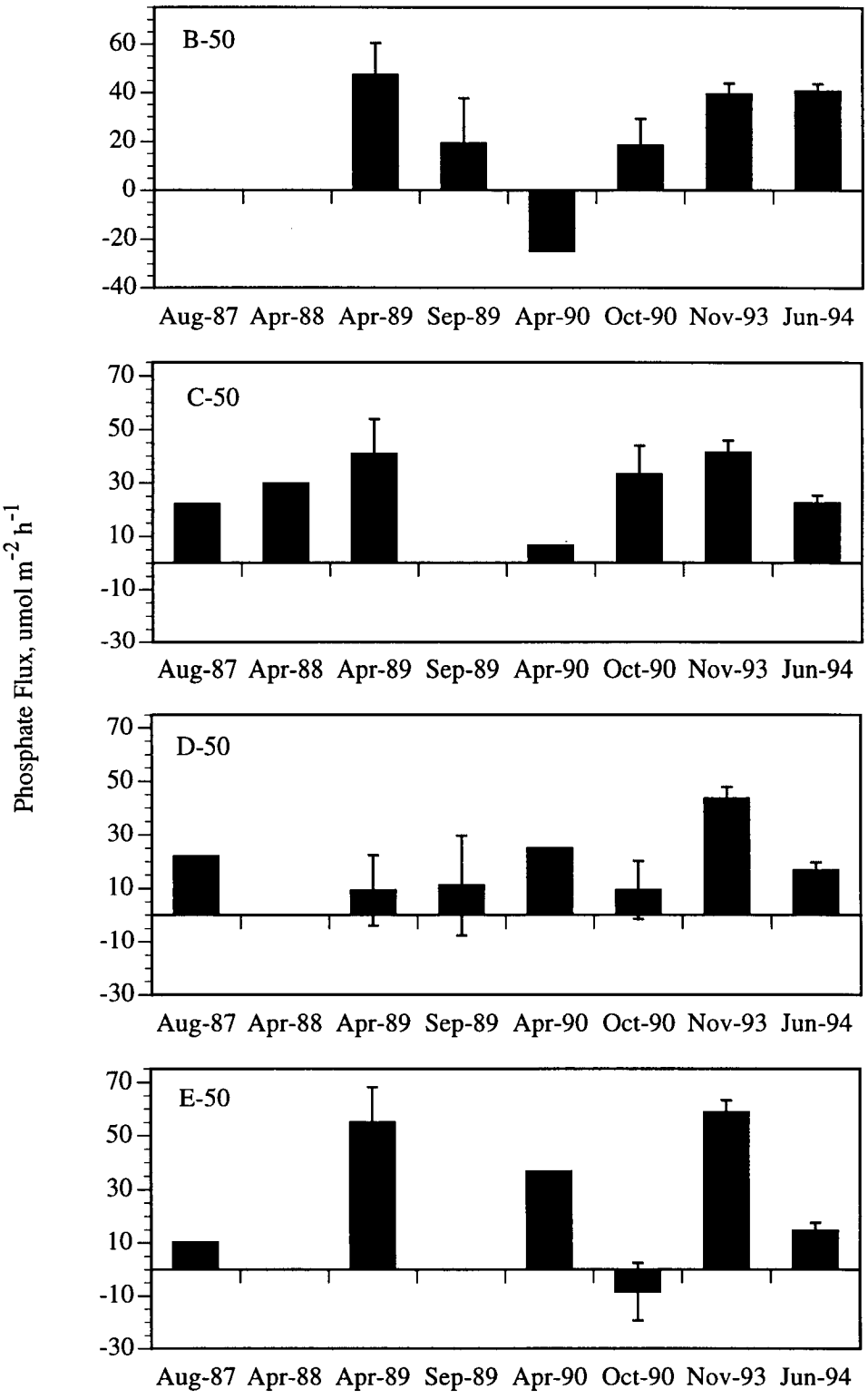

Figure 4.4. Benthic fluxes of phosphate along the 50-m contour of the Louisiana Bight at different distances from the mouth of Southwest Pass.

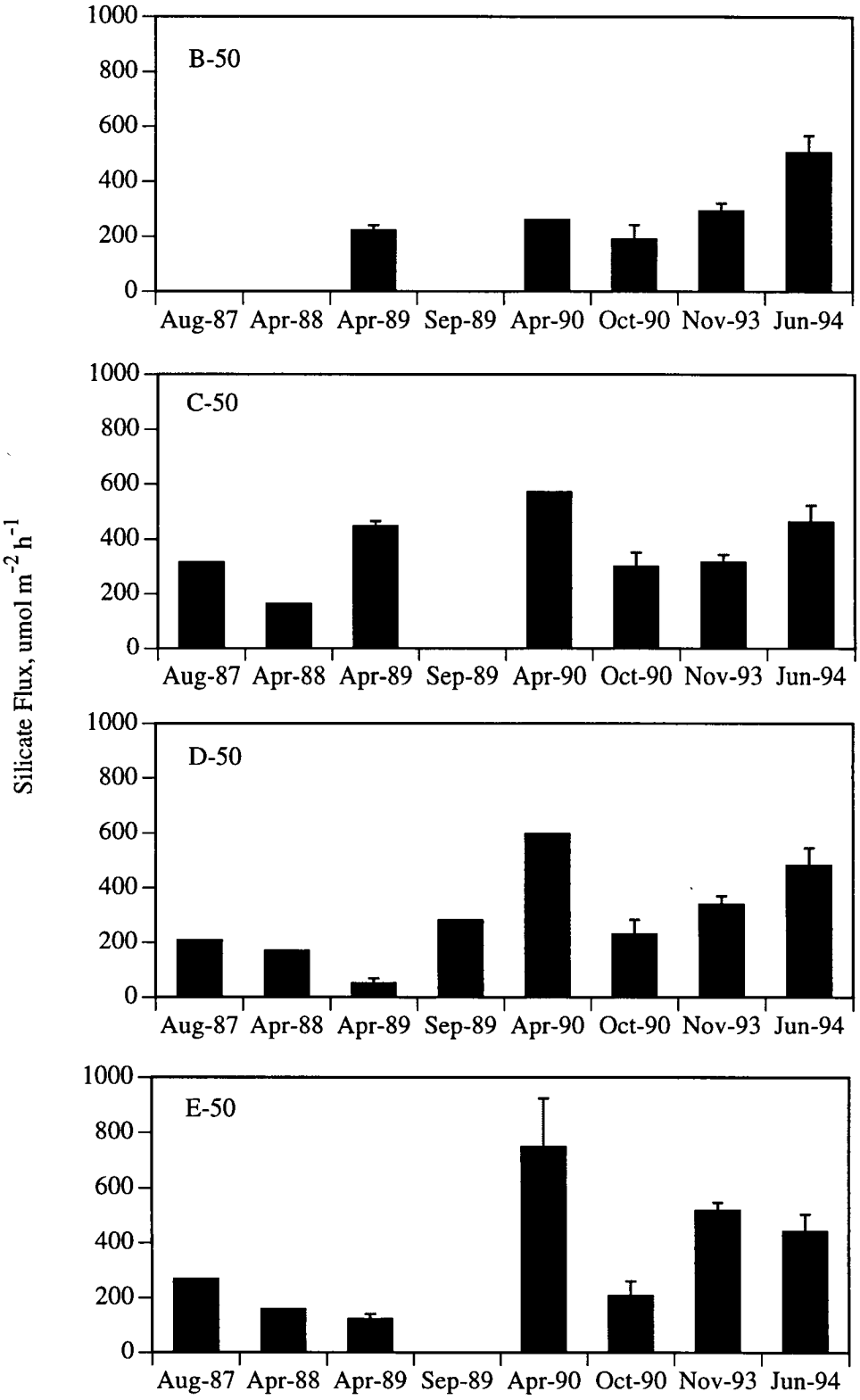

Figure 4.5. Benthic fluxes of silicate along the 50-m contour of the Louisiana Bight at different distances from the mouth of Southwest Pass.

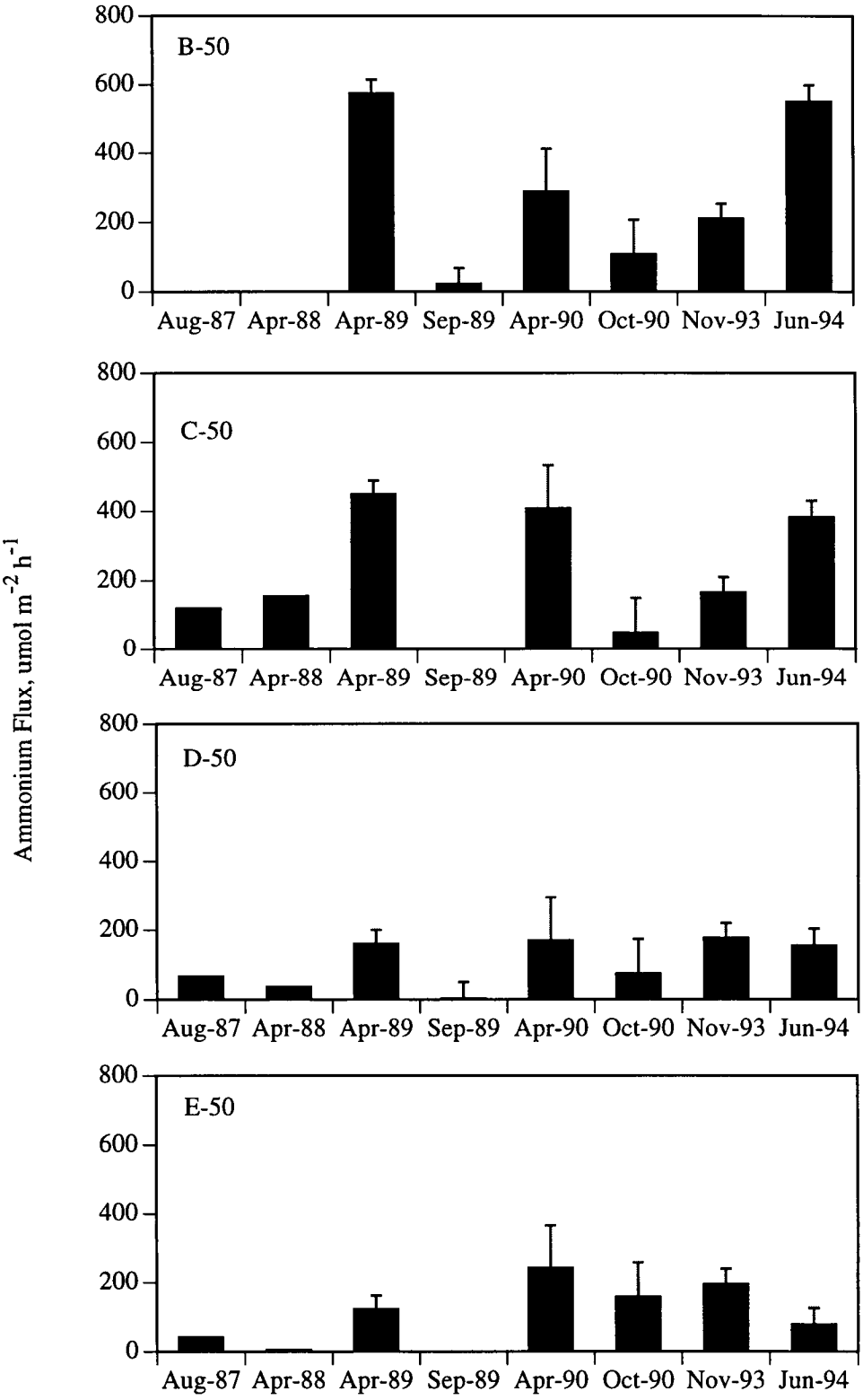

Figure 4.6. Benthic fluxes of ammonium along the 50-m contour of the Louisiana Bight at different distances from the mouth of Southwest Pass.

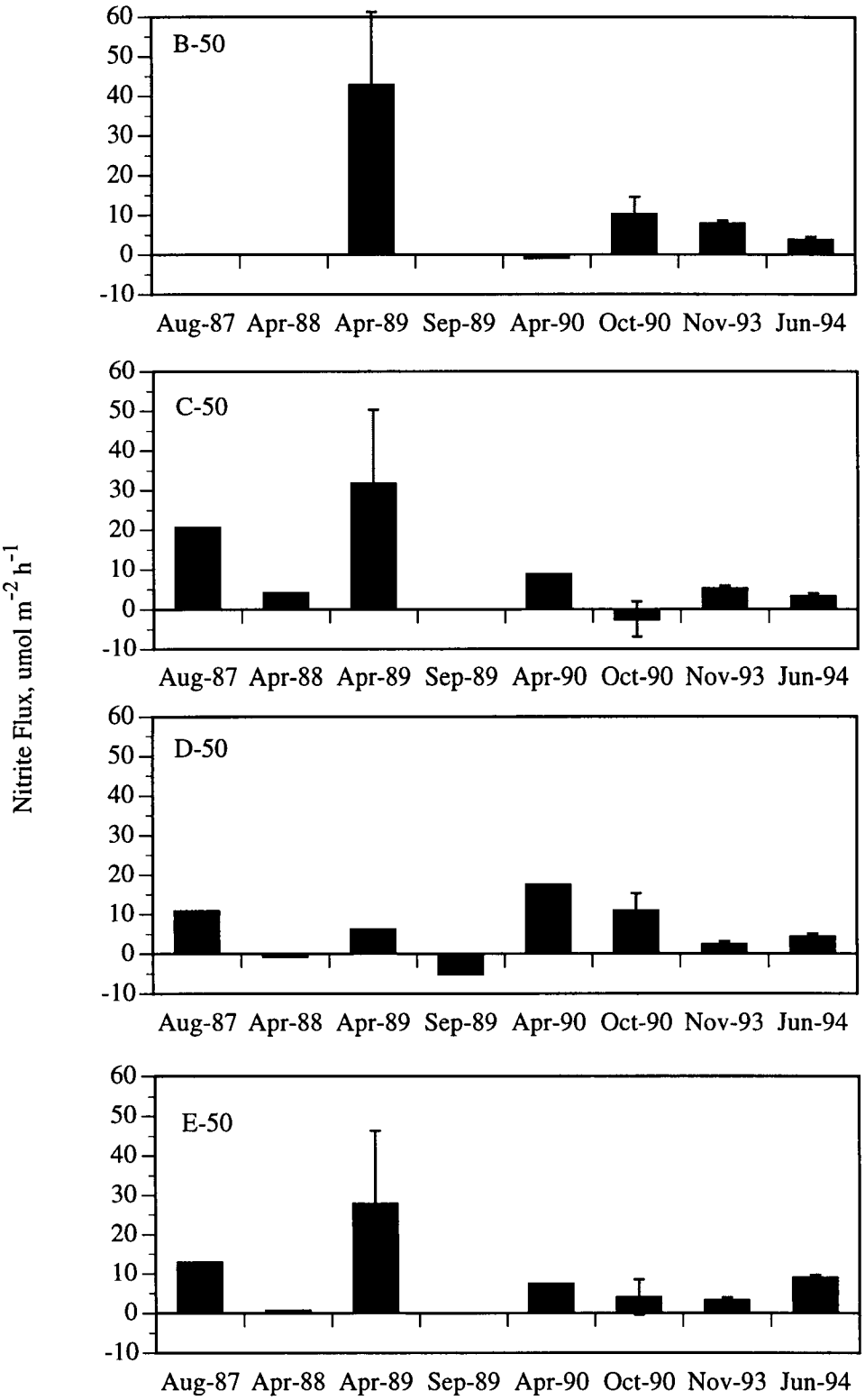

Figure 4.7. Benthic fluxes of nitrite along the 50-m contour of the Louisiana Bight at different distances from the mouth of Southwest Pass.

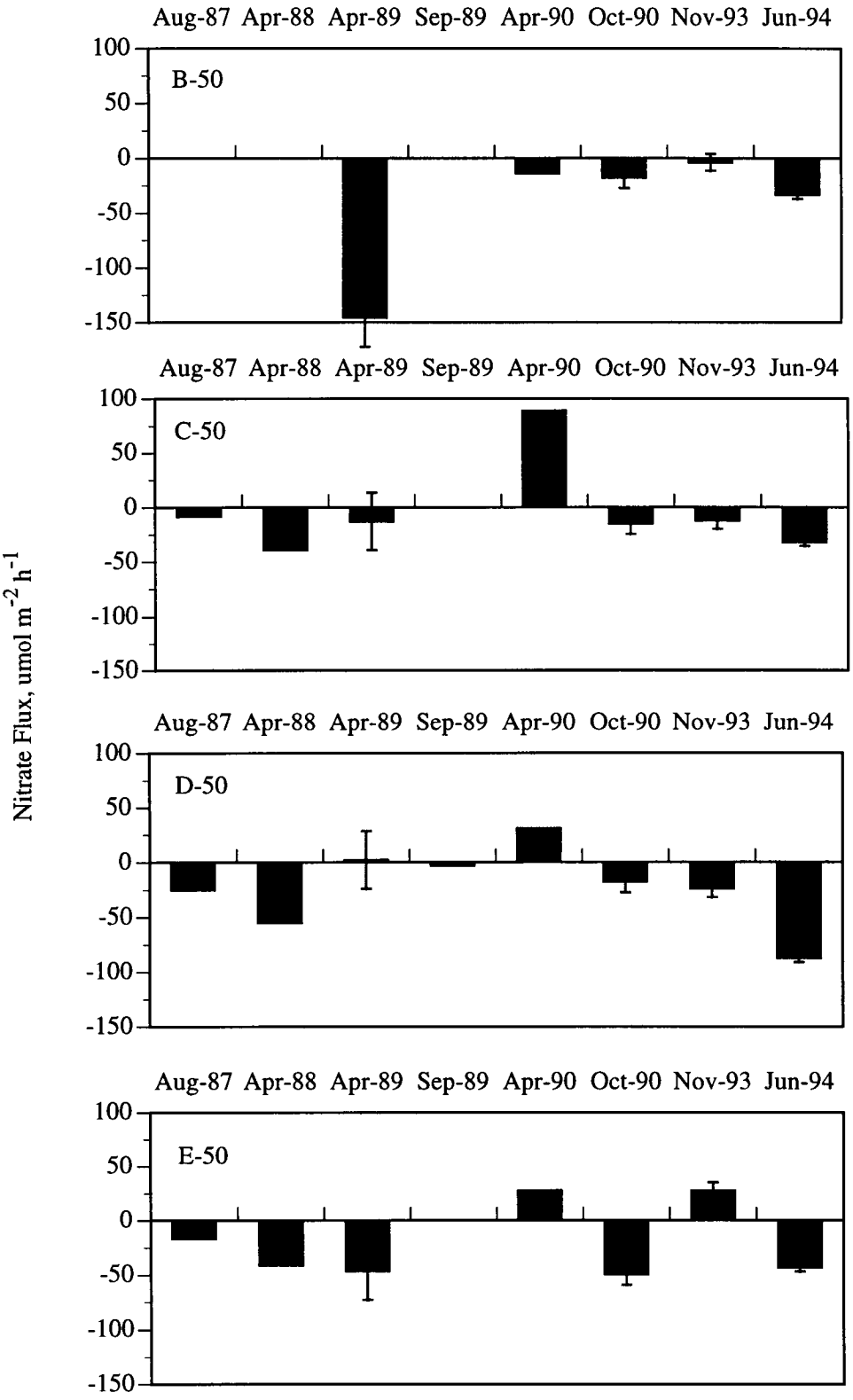

Figure 4.8. Benthic fluxes of nitrate along the 50-m contour of the Louisiana Bight at different distances from the mouth of Southwest Pass.

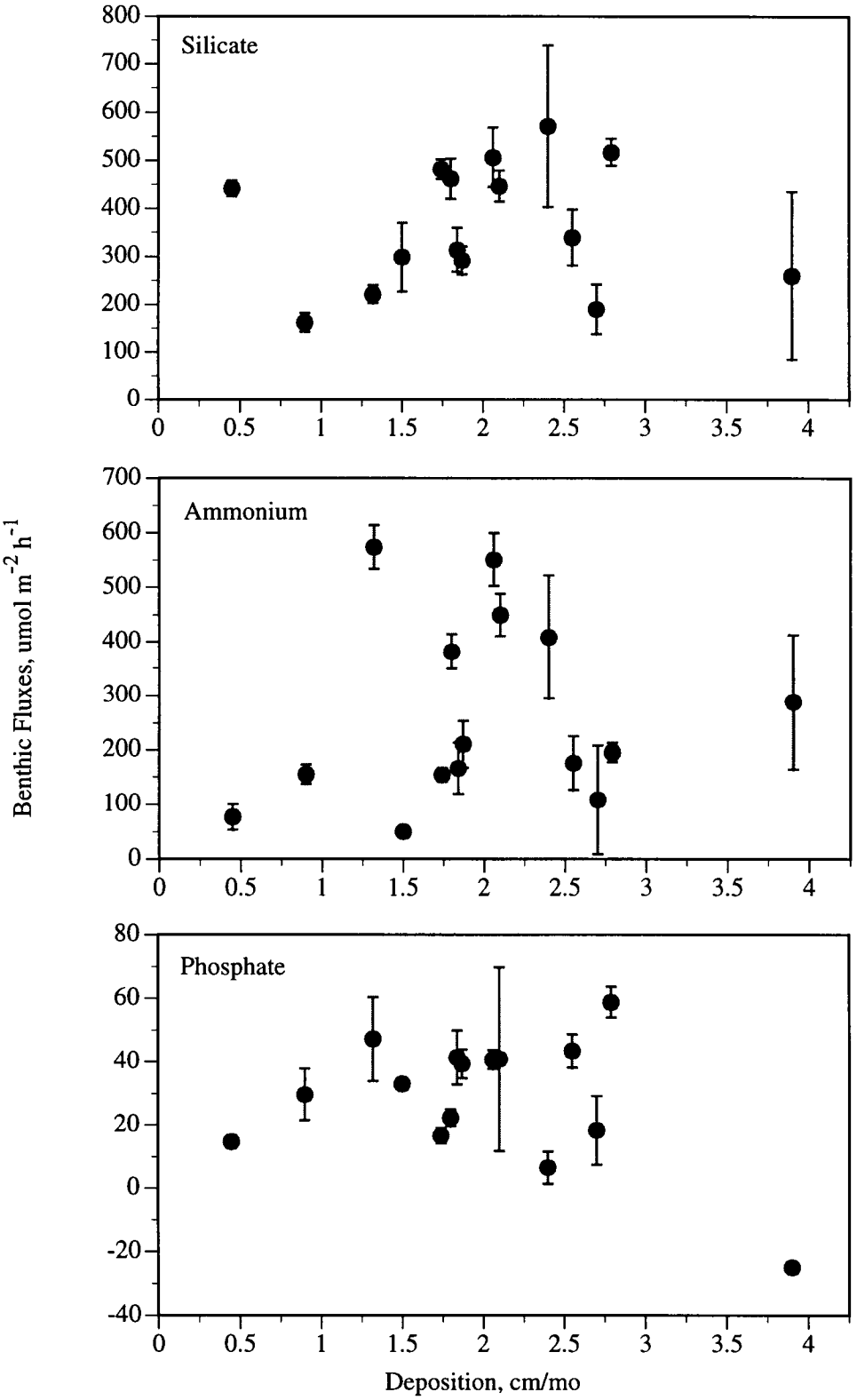

Figure 4.9. Benthic fluxes of silicate, ammonium, and phosphate relative to the measurement of deposition at stations along the 50-m contour.

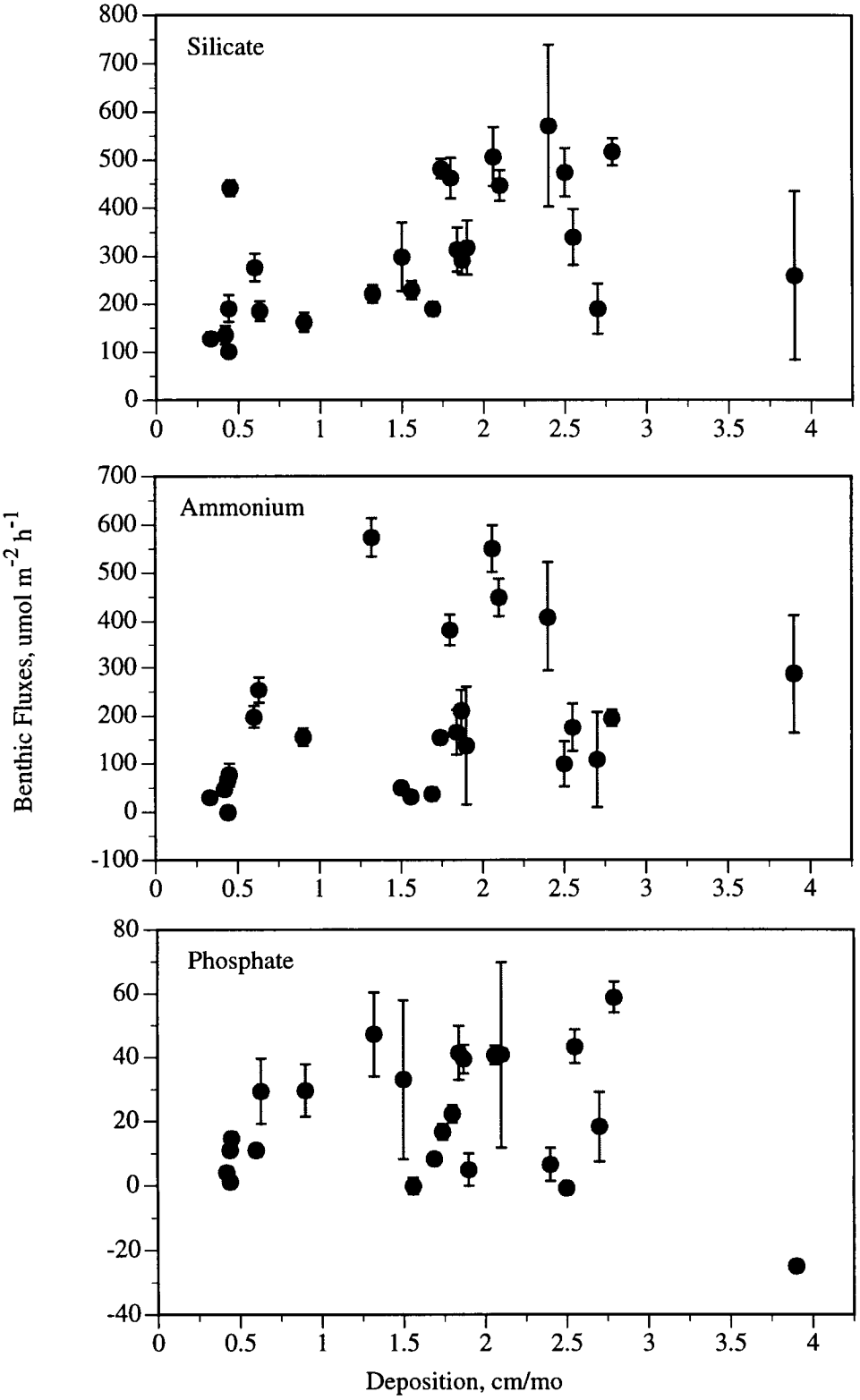

Figure 4.10. Benthic fluxes of silicate, ammonium, and phosphate relative to the measurement of deposition at all stations in the Louisiana Bight.

Chapter 5

SPATIAL PATTERNS OF BENTHIC NUTRIENT REGENERATION AND SEDIMENT CHARACTERISTICS ON THE LOUISIANA CONTINENTAL SHELF

(This Chapter is a revision of a Master of Science thesis by John Bourgeois)

5.1 Abstract

The Mississippi River exhibits influences on the coastal processes that are important not only to the productivity of the region, but also to the global carbon and nitrogen cycles. Rates of benthic nutrient regeneration were measured on the Louisiana continental shelf at a total of nineteen stations over two cruises. Ten stations were sampled on the first cruise (COMUS 1, November 1993), while nine stations were sampled on the second cruise (COMUS 3, June 1994). Rates of benthic regeneration were determined by a flow through core chemostat system for NO_3, NO_2, NH_4, PO_4, and SiO_4. At each site, samples from the incubated cores were also taken for redox, pore-water concentrations, sediment composition (carbon, nitrogen, phosphorus, and chlorophyll a), and macroinfauna, as well as coordinate measures of ^{234}thorium for deposition analysis. Rates of benthic nutrient flux tended to decrease with distance from the riverine source, with a significant difference between the two cruises only for NO_3 and PO_4. Modeling nutrient fluxes from pore-water gradients showed little correlation to the actual measured nutrient flux. The sediment characteristics provided some insight for outliers in the analysis. Benthic fluxes always showed a higher correlation to some qualitative index (input of carbon, nitrogen, phosphorus, or chlorophyll a) of deposition to the benthos than to the quantitative input of sediment.

5.2 Introduction

The Mississippi River is one of 20 rivers worldwide that, in total, are responsible for almost 50% of the terrigenous materials being transported to coastal oceans. The Mississippi River ranks third in the world in drainage basin area, sixth in water discharge, and seventh in sediment load (Milliman and Meade 1983; Milliman 1991). The riverine influence on the coastal processes is not only important in the global cycling of carbon and nitrogen, but is also responsible for the high productivity found in these coastal regions. The low energy Louisiana continental shelf is therefore the site of high allochthonous nutrient deposition.

The cycling of material in this land margin ecosystem is dependent on the coupling of benthic and water column processes (Figure 5.1, in Twilley et al. 1994). The linkage of these ecological processes is important in determining the productivity of the coastal zone, as nutrient regeneration (the release of inorganic nutrients into the water column) rates relative to allochthonous input determine the amount of material available to primary producers. If rates of input are higher than regeneration, the result is nutrient burial and therefore reduced availability of those nutrients to the water column.

As outlined in Figure 5.1, understanding the fate of materials is linked to the various ecological and physical processes that are spatially distributed relative to the river plume. The high concentrations of materials introduced by the river corresponds to high rates of deposition. These deposition rates are proportional to benthic nutrient regeneration rates with

respect to proximity to the river mouth. Primary production in this zone is largely inhibited by water column turbidity.

However, in more distal regions of the plume, particulate matter settles out from the water column, but dissolved nutrients remain, allowing high rates of autotrophic production. Benthic regeneration rates are hypothesized to be high in this zone due to the combination of relatively high quantity of deposition to the seabed (although not as high as the "Turbid Zone"), in combination with a higher quality (material of marine origin) of this deposited material. Continuing along this longitudinal axis away from the plume, primary production becomes more dependent on remineralization, particularly in the water column, as allochthonous input is now minimal. Benthic regeneration rates in this zone should prove efficient largely because of the high quality of material being deposited. Although rates of benthic regeneration are low, this zone is receiving little input to the sediments. This zone may also be subject to hypoxia resulting from lateral redistribution of benthic sediments into this area. This distal zone receives a majority of its sediments via this lateral movement of materials rather than deposition from the water column.

Benthic nutrient regeneration is important in determining the fate of organic matter in the Louisiana shelf, and therefore the amount of nutrients available for production. Benthic nutrient regeneration has been estimated to supply anywhere from 15% to 65% of the phytoplankton demand for reduced nitrogen (Boynton et al. 1980; Fisher et al. 1982). Previous studies have been performed on the effects of the quantity and quality of materials being deposited, and deposition was found to influence benthic remineralization (Hargrave 1973). Müller and Suess (1979) found that sedimentation rates are directly related to amounts of organic material produced by autotrophs and deposited to the benthos. This implies that benthic regeneration is directly proportional to sedimentation (Billen et al. 1991).

The reactivity of the sediments being deposited is also important in determining benthic nutrient regeneration (Canfield 1989). Studies on the quality of material in relation to benthic nutrient regeneration have shown that organic material of marine origin (plankton-derived) is about 5 times as reactive as material of terrestrial origin (Hedges et al. 1988). The research in this thesis analyzes the influence of both the quantity and quality of deposited material on the patterns of benthic nutrient regeneration on the Louisiana continental shelf.

The primary objective of this study was to determine the spatial and temporal patterns of benthic nutrient regeneration as controlled by the benthic boundary layer characteristics; particularly the relationship between pore-water nutrient concentrations and sediment deposition to benthic nutrient regeneration. This analysis allowed an evaluation of the benthic nutrient regeneration trends in the plume region of the continental shelf, and consequently elucidated the significance of this source of nutrients to primary productivity. Benthic nutrient fluxes were compared to biological as well as geophysical and chemical characteristics at the sediment-water interface. Nutrient exchange was also evaluated in terms of the quantity and quality of deposited material. The factors compared to nutrient flux for this study were chosen *a priori* based on two criteria; first, those factors which were thought to influence nutrient flux based on previous investigations (Dagg et al. 1991; Dr. R.R. Twilley, personal communication), and secondly, those factors that we had the means to analyze. Quantity of input was evaluated by thorium-234 radiochemical techniques. Quality of input was analyzed in terms of chlorophyll a sediment concentration, as well as concentrations of carbon, nitrogen, and phosphorus in the sediment, and carbon to nitrogen ratios, to distinguish material of marine (high quality) versus terrestrial (low quality) origin.

Benthic nutrient regeneration has been hypothesized to make a significant contribution to primary production. The quantification of the effects of the proposed factors on benthic nutrient fluxes can further our basic ecological understanding of shelf processes. This new understanding can potentially be used in conjunction with ecosystem modeling to help project the response of this system to changes in riverine input. The objectives of this study are listed below with the statistical approach used to evaluate the factors that control spatial and temporal patterns of benthic nutrient regeneration on the Louisiana shelf.

Objective 1: To assess the temporal pattern in benthic nutrient regeneration rates using two cruises on the Louisiana continental shelf. This objective was evaluated by compiling benthic nutrient regeneration rates for each nutrient by cruise, only for those stations that were sampled on both cruises. The values were then subjected to a t-test to determine significant differences between cruises for each of the five nutrients.

Objective 2: To examine spatial trends in benthic nutrient regeneration rates on the Louisiana continental shelf. Regeneration rates at all stations from both cruises were combined and subjected to cluster analysis. Major divisions were mapped, and the average flux rate for each grouping was calculated and included on a map (one for each nutrient). These maps were then interpreted based on their degree of agreement with the conceptual model (Figure 5.1) and other relevant factors (e.g. macroinfauna).

Objective 3: Determine the importance of pore-water concentration gradients to rates of benthic nutrient regeneration in conjunction with other physical, chemical, and biological characteristics. Regressions of benthic nutrient flux with the respective pore-water nutrient gradient were plotted. Any points not agreeing with the linear curve fit were identified by cruise and station and were examined for any anomalous characteristics that may account for the variability. A stepwise regression on all sediment characteristics was used as a basis for the examination of those characteristics which most influence the nutrient fluxes.

Objective 4: Examine the relative influence of quantity versus quality of depositional flux to benthic nutrient regeneration rates. A stepwise regression analysis of deposition rates versus regeneration rates was employed, comparing the input of material to benthic fluxes. Quantity of deposition was quantified in terms of sediment fluxes to the benthos derived from thorium-234 analysis. Quality of deposition was determined by taking sediment deposition rates and multiplying them by the concentration of carbon, nitrogen, phosphorus, and chlorophyll a.

5.3 Site Description

Sampling for this research took place on the Louisiana continental shelf, in the dispersal area of the Mississippi River's Southwest Pass. The research was accomplished during two cruises aboard the R/V Pelican (LUMCON (Louisiana Universities Marine Consortium), Cocodrie, LA). The cruises were named COMUS 1 and COMUS 3; an acronym based on the title of a companion NSF project (Coastal Ocean Margin Uranium Study, Dr. B.A. McKee, Principal Investigator). COMUS 1 took place from 1 to 12 November 1993, during a typical low flow period for the Mississippi River. The mean flow of the river during the cruise was 10,157 $m^3 s^{-1}$, ranging initially from 12,712 $m^3 s^{-1}$ and decreased to 9,884 $m^3 s^{-1}$ by the end of the cruise (Figure 5.2). The lowest discharge level of 1993 was two days later, 14 November, at 9,604 $m^3 s^{-1}$. COMUS 3 took place from 1 to 10 June 1994, during typically high river flow, with an average flow of 13,098 $m^3 s^{-1}$ for this time period. Initial flow was 18,788 $m^3 s^{-1}$ and decreased to 11,480 $m^3 s^{-1}$ by the end of the cruise (Figure 5.2). About

two weeks prior to COMUS 3, on 11 May 1994, the river was at its peak discharge for the year at 32,592 $m^3 s^{-1}$. All river discharge numbers were taken at Tarbert Landing, Louisiana by the U.S. Geological Survey (personal communication, Dr. B.A. McKee).

Nineteen benthic stations were established over the two cruises, seven of these stations were repeated during both cruises for a total of twelve independent sampling stations (Figure 5.3). These repeated stations were all along the 50 m contour. The station labels consisted of a letter (from B to H with increased distance from the mouth of Southwest Pass) followed by a number (which denotes station depth in m). The latitude and longitude of these stations were listed in Table 5.1. The one notable exception in the sampling stations was South Pass (SP) as it was the only station outside of the Southwest Pass dispersal system. The temperature, salinity and oxygen conditions for the bottom waters of the stations were outlined in Table 5.1. Conspicuously absent was any hypoxia during either cruise.

5.4 Methods

5.4.1 Field Sampling

The continuous flow or chemostat system for determining benthic nutrient flux as outlined by Miller-Way (1994) and Miller-Way and Twilley (1996) was employed. This microcosm system consisted primarily of a water reservoir, the sediment cores, and a peristaltic pump (Figure 5.4). The pump drew water from the reservoir into the cores, and from the cores into sampling vials. The system was plumbed with thick-walled (1.6 mm wall thickness) Tygon™ tubing (to reduce the slight reaeration found by Miller-Way and Twilley 1996) and polypropylene connectors at tubing junctions. Effluent tubing was routed through a series of three-way valves and allowed to flow into a common waste line when sampling was not occurring. During sampling, the effluent was directed into a series of vials via the appropriate three-way valve. Flow rate was controlled by the Ismatec™ multichannel cartridge pump which can maintain a maximum of 16 lines. The flow rate was set and monitored at a range of 6.5 to 7.0 ml/min, with residence times ranging from 260 to 280 min. Therefore, during a 9 h (540 min) incubation period, approximately two complete water volume turnovers should occur.

A sediment core was a Lexan™ tube 15 cm in diameter and 30 cm in height, which was sealed off at either end by Plexiglas disks. These disks were held tight by rubber caps on the bottom and rubber sleeves on the top, both fastened with screw clamps. The top Plexiglas disk had three holes which were sealed with rubber septa to serve as ports for inflow lines, outflow lines, and for direct sampling access. The influent and effluent ports consisted of stainless steel needles (which have Luer lock™ fittings) inserted through a rubber septum into the overlying water of the core, and attached to the appropriate lines with polypropylene connectors.

Field sampling consisted of subcoring box cores to a sediment depth of approximately 20 cm. Intact cores were capped with plexiglas disks and rubber caps for safe transport to the incubation chamber. Bottom water was collected at the site by the shipboard CTD system (which also recorded ambient temperature and dissolved oxygen). The water was filtered through a 0.45 μm nylon cartridge filter and a 0.20 μm Gelman™ capsule filter in series to remove most bacteria and suspended particulate matter. This filtration allowed the assumption that any changes in nutrient concentrations between influent and effluent lines can be attributed solely to processes at the sediment-water interface in the cores. The filtered water was then placed in the reservoirs (a 20 liter rectangular carboy) and the ambient dissolved oxygen

conditions were maintained by either increasing (an aquarium pump) or decreasing (nitrogen gas) oxygen concentrations.

Cores were placed in the incubation chamber, which consisted of a large Nalgene™ tub, with water at ambient temperature controlled by a Neslab™ CFT 25 heat circulator (and ice when necessary). One difference in the present system as compared to the system described by Nishio et al. (1982), was the presence of a control line which originated in the reservoir, bypassed the cores, and emptied directly into a sampling flask. This line served to correct for any tubing-induced changes in concentrations. Benthic flux rates were based on the change in concentration of each measured nutrient between the influent (control) and effluent lines. Flux rates were calculated according to the following equation:

$$(C_I - C_E) * \text{flow rate / core surface area} = \text{flux};$$

where C_I was the influent concentration (control line) of a nutrient, and C_E was its effluent concentration. Nutrient regeneration rates were expressed as $\mu mol\ m^{-2}\ h^{-1}$. Influent concentrations were measured by sampling a single control line for both of the cores from the corresponding station.

A homogeneous overlying water column in the core was maintained by an internally mounted Nalgene™ stir bar suspended from the top plexiglas disk. A variable speed stirrer (Cole-Parmer™ Micro-V model no. 4805-00) was placed upside down on the top of the core and adjusted so that the water is well mixed without disturbing the sediment-water interface. Small plexiglas squares were also internally mounted from the top plexiglas disk to prevent any possible vortexing that may have been caused by the stirring.

For each of the two research cruises, sampling consisted of 2 cores per station. Each pair of cores was incubated for 9 h, with sampling for ambient nutrient flux every 3 h, giving a total of 3 sampling intervals for each set of cores. After the incubation, breakdown of the sediment cores consisted of measuring different parameters on different cores, due to the destructive nature of some of the techniques (Figure 5.5). One core was sectioned at 1 cm intervals to a depth of 4 cm (in a hypoxic chamber (glove box) to prevent precipitation of Fe^{+3} and PO_4 in the pore-water). The four samples were then centrifuged and the pore-water decanted and filtered with GFF 25 mm filters (again in an hypoxic chamber) for nutrient analysis. In addition, the first core was used for a redox profile (prior to being cut). The second core was also used for a series of measurements, including a sediment plug for bulk density and concentration of carbon, nitrogen, and phosphorus, a smaller plug for chlorophyll analysis, and finally, the remaining sediment was sieved for macroinfauna.

^{234}Thorium profiles in the sediment were examined for excess ^{234}Th during both cruises, and deposition rates calculated according to McKee et al. (1983). Deposition refers to the "temporary emplacement of particles on the seabed," (McKee et al. 1983). ^{234}Thorium is rapidly adsorbed onto particles and deposited to the seabed with those particles, as the ^{234}thorium becomes buried and isolated from new atoms, the radioactive decay can be measured. A typical profile with depth shows a logarithmic decrease in radioactivity, and deposition can be estimated from the slope of that line (McKee et al. 1983). The ^{234}Th profile was from a third core taken at the stations and was done as a part of the COMUS project (Dr. B.A. McKee, Principal Investigator); only the seven stations along the 50 m contour are included in this analysis. This gave a representative seasonal rate of deposition, as the rate is integrated over a 100 day period due to the 24.1 day half-life of ^{234}Th.

5.4.2 Analytical Techniques

Depth profiles of temperature, salinity, and oxygen were made at each station with a SeaBird CTD, a Beckman RS-5 salinometer, and an Orbisphere oxygen meter. Nutrient regeneration rates were determined for inorganic nitrogen (ammonium, nitrate, and nitrite), phosphate, and silicate. Samples for ambient flux and pore-waters were stored in 4 ml sample cups, capped, and frozen until analysis on an Alpkem RFA/2 autoanalyzer at the University of Southwestern Louisiana following the procedures of Strickland and Parsons (1972), with the exception of ammonium, which was determined after Parsons et al. (1984).

Redox measurements (Whitfield 1969) were made in the first core at 1 cm intervals to a depth of 4 cm, including measurements of the overlying water and at the sediment-water interface, using a platinum electrode mounted on a modified micrometer for precise control of depth. Bulk density was determined by cutting the point off of a 50 ml syringe and inserting it into the core to a depth of 2 cm. The sediment plugs were placed in pre-weighed 250 ml bottles and frozen. The samples were later thawed, weighed for wet weight, dried at 60°C for 72 h, and weighed again for dry weight. The dried plugs were ground and analyzed for total phosphorus by dissolving the ashed (480°C for 3 h) sediment in HCl and assaying for PO_4 concentrations (Parsons et al. 1984; Aspila et al. 1976). Total carbon and nitrogen were determined from the same ground sediment with a LECO Elemental Analyzer.

Chlorophyll concentrations in a 1 cm^3 sediment plug were measured by adding 5 ml of DMSO/acetone and incubating for 1 h in the dark. The mixture was centrifuged, the supernatant decanted and read on a Turner fluorometer (calibrated at K=237.8). Macroinfauna was extracted by first placing the entire core into a bucket and spraying the core thoroughly with sea water. Then, the contents of the bucket were passed through a 1 mm sieve. Once the core was sieved, any retained organisms on the sieve were transferred to a 125 ml bottle with 10% formalin and Rose Bengal, and then frozen. Upon return to the laboratory, the organisms were thawed and identified to general taxonomic group, counted for density, dried for 72 h at 60°C, and weighed. They were then ashed at 500°C for 6 h and re-weighed.

5.4.3 Statistical Analyses

The statistical methods employed included four models applied to four different objectives. The first of these objectives was to determine any temporal difference in nutrient flux. A t-test was used to evaluate any difference between the two cruises for each nutrient flux. Only the stations sampled during both cruises (i.e. the stations along the 50 m contour) were used in this analysis. A cluster analysis was performed to uncover any spatial patterns in nutrient flux. All nutrient flux data from both cruises were combined to determine the groupings of all the stations. These groupings were then mapped.

The significance of nutrient pore water concentrations in determining nutrient flux was analyzed by plotting the measured fluxes of NO_3, NH_4, PO_4, and SiO_4 against pore water concentration gradient with depth (from the overlying water to 1 cm). Expected fluxes were calculated according to Fick's first law (which is based on concentration gradients, Li and Gregory 1974), and the relationship of these calculated fluxes to actual observed fluxes was examined. A stepwise regression was run for each nutrient flux against all other factors measured. The results of the stepwise regressions were used to attempt to explain any outliers from the linear curve fit of observed flux to pore-water gradient.

The final objective was to ascertain the relative influence of the quantity versus quality of sedimentation on benthic nutrient regeneration. A stepwise regression was run for each nutrient flux against the quantitative flux of sediments to the benthos, as well as against the qualitative indices (carbon, nitrogen, phosphorus, and chlorophyll a deposition). Linear curve fitting was used on all analyses, non-linear methods were attempted, but never elucidated patterns in the data better than the linear model. All statistics were run on JMP 3.0.2 for Macintosh (Quadra 650).

5.5 Results

5.5.1 Benthic Fluxes

Benthic nutrient regeneration rates in μmol m^{-2} h^{-1} were calculated for each flux measurement, and the average rate (with standard error bars) for each station per cruise was plotted in Figure's 5.6a and 5.6b. The station at South Pass (SP) was removed in these Figure's due to differences in scale, but the values for this station can be found in each of the respective tables. Nitrate fluxes ranged from 54.9 to -255.9 μmol m^{-2} h^{-1}, NO_2 fluxes ranged from 30.5 to -9.7 μmol m^{-2} h^{-1}, NH_4 fluxes ranged from 686.1 to -22.4 μmol m^{-2} h^{-1}, PO_4 fluxes ranged from 77.2 to -9.0 μmol m^{-2} h^{-1}, and SiO_4 fluxes ranged from 794.3 to 69.9 μmol m^{-2} h^{-1} for the Southwest Pass dispersal system over both cruises.

Pore-water concentrations for NO_3 and NO_2 were all below 0.3 μmol L^{-1} at all depths, with the exception of the top cm at South Pass (COMUS 3), and thus were excluded from graphical analysis. The general trend for NH_4, PO_4, and SiO_4 was a general increase in concentration with depth (Figures. 5.7, 5.8, 5.9). Ammonium pore-water concentrations ranged from 328.2 to 28.0 μmol L^{-1} in the 0-1 cm section and from 527.9 to 40.3 μmol L^{-1} in the 3-4 cm section. Phosphate pore-water concentrations ranged from 32.8 to 0.3 μmol L^{-1} in the 0-1 cm section and from 53.7 to 1.0 μmol L^{-1} in the 3-4 cm section. Silicate pore-water concentrations ranged from 212.1 to 21.5 μmol L^{-1} in the 0-1 cm section and from 332.4 to 21.7 μmol L^{-1} in the 3-4 cm section. Phosphate and SiO_4 concentrations in the pore-waters both appeared to be lower during COMUS 3 for most stations.

5.5.2 Sediment Characteristics

Bulk density tended to decrease with distance from Southwest Pass until the region of maximum deposition (around D-50 and E-50), and then began to increase (Figure 5.10; values ranged from 0.26 to 0.79 g/cm^3. Chlorophyll a concentrations did not show a consistent trend. There was a sharp peak in November at station E50 (1.1 $\mu g/cm^3$), while the rest of the values ranged from 0.80 $\mu g/cm^3$ at SP (COMUS 3) to 0.17 $\mu g/cm^3$ at E-20 (COMUS 3) (Figure 5.11). There are spatial differences in total carbon, nitrogen, and phosphorus concentrations (% dry weight) in shelf sediments (Figure 5.12). Carbon values ranged from 2.02% to 1.04%, nitrogen values ranged from 0.34% to 0.09%, and phosphorus values ranged from 0.090% to 0.040%. Stations G-50 and H-50 were noticeably lower in total nitrogen for both cruises, but no other patterns were obvious.

The redox (Eh) profiles with depth, from the overlying water to 4 cm into the sediment, showed a rather consistent pattern during COMUS 1, with a sharp change in Eh from the surface to 1cm (Figure 5.13). The majority of Eh values in the sediment ranged from 100 to 200 mV. For COMUS 3, however, the profiles divided into two groups (neither of which

showed as sharp a change in Eh with depth). The first of these two groups, which was at a lower Eh (between 0 and -100 mV at 4 cm), consisted of the three stations closest to the river outlets: B-50, C-50, and SP. The remaining stations for COMUS 3 ranged in Eh values from 140 to 320 mV at 4 cm, and all were above 300 mV at the sediment surface.

Benthic macroinfauna was dominated by polychaete worms and some small crustaceans, while only one vertebrate, a four inch long worm eel, was found during either cruise (Figure 5.14). Macroinfaunal density and biomass showed no consistent pattern across the shelf; the largest number and biomass occurred at station B-50 during COMUS 3 and station F-20 during COMUS 1.

5.6 Discussion

5.6.1 Factors Controlling Nutrient Regeneration

Sediment Characteristics: Table 5.2 displays the results of stepwise regressions of each nutrient flux to the series of benthic core parameters. For all nutrients except for PO_4, pore-water gradients showed the highest correlation to benthic nutrient regeneration. Phosphate fluxes, however, showed the strongest correlation to a redox gradient. Nitrate fluxes showed the strongest correlation to a single parameter, which was the gradient in NO_3 concentration between the overlying water and pore-water at 4 cm depth. The r^2 value was 0.95, compared to only 0.61 for the next highest correlation between flux and first variable for the other nutrients. This high correlation reflects variation in the NO_3 concentration in the overlying water, since all NO_3 pore-water values at 4 cm depth were below accurate detection. Therefore, the only difference in the two pore-water gradients for NO_3 and NO_2 was the values in the 1 cm section for station SP. Macroinfaunal mass and density occurred in the regression analysis only for the fluxes of NH_4 and PO_4. They were not significant to the other fluxes (Table 5.2).

Deposition versus Regeneration: Analysis of deposition was performed for seven stations on the 50 m depth contour, which were sampled during both cruises. Table 5.3 displays the results of stepwise regressions of each nutrient flux in relation to the deposition of sediments and the relative deposition of carbon, nitrogen, phosphorus, and chlorophyll a. The first graph in each of the Figs. 5.15 through 5.19 is of the mean nutrient flux versus the flux of sediments to the benthos. The second graph in the series is between the nutrient flux and the depositional component with the highest correlation to the flux as determined by the stepwise regression analysis. Finally, the third graph shows the correlation of nutrient flux to the component which most logically would be related to nutrient flux. Since the relative magnitude of burial and regeneration of nutrients was determined somewhat by the quantity and quality of particulate matter being deposited, the indices graphed in Figs. 5.15 to 5.19 should reflect the differential effects of deposition to benthic nutrient regeneration (Zeitzschel 1980).

For four of the five nutrients, rates of benthic regeneration did not follow the pattern of sediment deposition to the seabed. The exception was PO_4 flux, which was correlated to deposition to the seabed. In Figures. 5.15 to 5.19, A) represents the correlation of the respective nutrient flux to sediment deposition. Both B) and C) represent two indices of quality, B) is the index that showed the highest correlation and C) is the index that was hypothesized *a priori* to show the highest correlation. In all cases, some index of quality of deposition had the highest correlation to nutrient flux (B), but never was that qualitative index the hypothesized index (C). For example, deposition of phosphorus explained SiO_4 flux better

than sediment inputs, but chlorophyll a inputs had a lower correlation with fluxes than sediment deposition (Figure 5.19). The above trend was found throughout the analysis, as chlorophyll a deposition best explained NO_3 flux, carbon deposition best explained NO_2 and PO_4 flux, and phosphorus deposition best explained NH_4 and SiO_4 flux. It is evident that the quality of deposited material, such as chlorophyll a or nutrient content, did not improve the correlations with benthic fluxes than the quantitative inputs.

Pore-Water Gradients versus Regeneration: A gradient (dC/dz) of nutrient concentrations between overlying waters and pore waters (to a depth of 1 cm) was calculated from the difference in these concentrations and dividing by two (2) cm. Values for overlying water were based on concentrations in the control line (C_I) of the chemostatic system. This pore-water gradient was compared to specific benthic fluxes for NO_3, NH_4, PO_4, and SiO_4, (Figure 5.20). Nitrate, and particularly NH_4 were the only two nutrients that showed a significant r^2 value in the correlations between fluxes and pore-water gradients. The difference in the r^2 value in Figure 5.20 to those in Table 5.2 (when pore-water gradient from OW to 1cm was the first step) can be attributed to the fact that station SP was included in the stepwise regression analysis, yet was removed for Figure 5.20. For NO_3 fluxes, there was a much stronger correlation of benthic flux to the OW to 4 cm pore-water gradient (Table 5.2). Neither bulk density nor any other sediment characteristic provided insight into the two most conspicuous outliers, H-50 and D-50 from COMUS 3. Nitrate flux has been shown to be a function of NO_3 concentration in the overlying water. This high correlation with pore-water gradient can be attributed to the consistently low concentration of NO_3 in pore-waters, thus the overlying water concentrations control NO_3 benthic flux.

Ammonium benthic fluxes showed the strongest correlation to pore-water concentration gradients (Figure 5.20). Examination of points that deviated from the curve fit provided some insight into what factors caused variation in this the correlation. Stations B-50 (COMUS 3) (which showed the highest densities of macroinfauna among stations for either cruise (Figure 5.14)) and C-50 (COMUS 3) both had decapods present. The larger burrows of the decapods (in contrast to the ubiquitous polychaetes) combined with the higher sediment deposition at these stations, resulted in higher fluxes and pore-water gradients. Station E-50 (COMUS 1) had the highest deposition rate measured on either cruise, and also had a significant flocculent layer (personal observation). Ammonium remineralization occurs primarily in the uppermost flocculent layer (at the sediment-water interface), which is not adequately sampled when cores are sectioned at 1 cm resolution (Kemp et al. 1982). Neither PO_4 nor SiO_4 benthic fluxes were correlated with pore-water gradients of respective nutrient concentrations. Examination of the other factors for the stations with extreme deviations from the linear model did not reveal any anomalies that could account for the high variability.

Diffusive fluxes of nutrients across the sediment-water interface are influenced, in addition to concentration gradients, by sediment porosity (Ø) (Berner 1980). Expected fluxes can be calculated using the equation $J = -Ø\ D\ dC/dz$, where J is the diffusive flux, Ø is the sediment porosity, D is the nutrient specific diffusion coefficient, and dC/dz is the nutrient pore-water concentration gradient (Berner 1980; Li and Gregory 1974). When the observed fluxes were compared to expected fluxes calculated from the pore-water gradients (Li and Gregory 1974), even less correlation was found than when observed fluxes were compared to only the pore-water gradients. In most cases, expected fluxes remained at least one order of magnitude lower than the actual measured fluxes and the r^2 values were even lower than those observed in Figure 5.20. The activity of organisms in the benthos is equally as influential in determining nutrient fluxes (Berner 1980; McCaffrey et al. 1980). The macroinfaunal densities

and biomass of the stations do not account for the incongruence of the observed and expected fluxes. More focus is needed on the utility of an advective model to calculate expected benthic fluxes that may reflect patterns of observed fluxes. Aller and Aller (1992) also stressed the importance of meiofauna, which can increase nutrient flux by 20-40% from porosity-tortuosity changes. Berner (1980) noted the difficulty of understanding diagenesis in the zone of bioturbation due to the multi-faceted chemical and physical changes caused by the presence of burrowing organisms.

5.6.2 Temporal Differences

Significant differences in benthic nutrient fluxes between COMUS 1 and COMUS 3 occurred for NO_3 and PO_4, but not for NO_2, NH_4, and SiO_4 (Table 5.4, Figure 5.21). Nitrate uptake is a function of NO_3 concentration in the overlying water (Figure 5.22), and therefore the significant temporal difference can be explained by the seasonal supply of this nutrient to the study area by the river (Turner and Rabalais 1991). Higher river discharge during COMUS 3 supplied greater amounts of NO_3 to the plume region of the shelf causing significantly greater rates of benthic uptake.

There was also a seasonal difference in benthic PO_4 regeneration rates, associated with differences in river discharge. However, PO_4 regeneration rates did not show a correlation to PO_4 concentrations in the overlying water (Figure 5.22). This lack of correlation to benthic PO_4 flux was also observed by Nixon et al. (1980) for Narragansett Bay. However, PO_4 regeneration does show a high correlation to indices of sediment input (Figure 5.18). This indicates that a difference in riverine input is also driving the difference in PO_4 flux, since PO_4 is adsorbed onto particles that are transported to the seabed. However, there was no significant difference in the total phosphorus concentrations in the sediments between the two cruises. In addition, PO_4 fluxes in November were higher than those in June, suggesting that the mean bottom temperature differences of 22.4°C (COMUS 1) and 20.7°C (COMUS 3) may have influenced rates of PO_4 regeneration. This is in agreement to results found by Nixon et al. (1980) in a cold temperate system.

Another possible explanation for the temporal difference in PO_4 flux is the flooding in the midwestern portion of the Mississippi River drainage basin two months prior to COMUS 1. Heavy agricultural runoff could have loaded the shelf sediments with phosphorus, thus accounting for the greater PO_4 fluxes on the first cruise.

The general lack of any temporal difference in the regeneration rates of NH_4 and SiO_4 indicates that there is a steady supply of these nutrients to the water column and/or to the pore waters from the seabed. Rates of benthic regeneration of NH_4 and SiO_4 were similar during both cruises, indicating less dependence on river supply for exchange across the sediment-water interface. Thus the benthic regeneration rates of 150 and 300 $\mu mol\ m^{-2}\ h^{-1}$ of NH_4 and SiO_4 respectively provide a consistent supply of these nutrients to the shelf ecosystem. Many researchers have observed that benthic nutrient regeneration serves as a buffer of nutrient availability from periodic allochthonous delivery of nutrients (Hartwig 1974; Rowe et al. 1975; Nixon et al. 1976; Rowe et al. 1977; Propp et al. 1980; Flint and Kamykowski 1984). The lack of difference in NH_4 and SiO_4 regeneration rates, with respect to the differences in riverine input, suggests that benthic regeneration of these nutrients accommodates the seasonal demand for nutrients in the water column.

5.6.3 Spatial Trends

The conceptual model of the Mississippi River plume area presented in Figure 5.1 shows three distinct areas:

Turbid Zone- High deposition and high benthic regeneration;
Second Zone- Moderate deposition and moderate benthic regeneration;
Third Zone- Low deposition and low benthic regeneration.

Spatial groupings of benthic nutrient fluxes based on cluster analyses were used to test this conceptual model (Figures. 5.23 - 5.27). Values of benthic flux for stations in each spatial group were averaged and included on the maps. The high rates of benthic flux at South Pass (SP) resulted in this station being grouped separately from the other stations. Average rates of benthic fluxes in the other groups indicate that rates decrease for each respective nutrient with increased distance from the mouth of Southwest Pass. Station SP, which was sampled directly in the mouth of South Pass (3 m depth), was typical of a Turbid Zone station. The patterns established in the dispersal system of Southwest Pass represent trends of the Second and Third Zones (with decreased flux rates at increased distance from Southwest Pass). Thus the spatial zonation followed the general pattern suggested in the conceptual model.

Patterns of benthic NO_3 uptake (Figure 5.23) divide into three main regions of the shelf based on cluster analysis. Stations SP and D-50 each constituted a unique cluster due to extreme uptake rates of -454.3 and -71.5 μmol m^{-2} h^{-1} respectively. The next group has an average rate of -25.9 μmol m^{-2} h^{-1} and consists of stations that are adjacent to and distant from D-50. Although this does not correspond to the linear nature of the conceptual model, NO_3 uptake did not show a correlation to deposition, and therefore other factors such as bottom currents may have supplied D-50 with higher concentrations of NO_3 than the surrounding stations. Examination of benthic parameters reveals that NO_3 regeneration rates are driven primarily by the NO_3 concentrations in the overlying water. This is reflected in the correlation of fluxes to the nutrient gradient from the overlying water to the pore-waters, since all pore-water concentrations were below limits of detection (Table 5.3). Total nitrogen concentrations in the sediments do not seem to influence the groupings, as only G-50 and H-50 show significantly lower concentrations (Figure 5.12).

Nitrite (Figure 5.24) on the other hand, shows a more specific link of nutrient flux to distance from Southwest Pass. The first two groups show a decreasing release of NO_2, while the third starts to show slight uptake. Again, the pattern seems to be linked to concentrations of NO_2 in the overlying water, just as they were for NO_3 (Table 5.3). Nitrate uptake is linked to denitrification in the sediments, and therefore NO_2 release occurs at those stations where NO_3 uptake is great, and decreases as NO_3 uptake decreases.

The pattern of NH_4 fluxes decreases with increased distance from Southwest Pass with the exception of one station (Figure 5.25). F-20 is grouped with stations B-50 and C-50, which are near Southwest Pass and the average rate of benthic NH_4 regeneration for this group is 299.1 μmol m^{-2} h^{-1}. The station F-20 also had high biomass (and density) of macroinfauna caused by a shallow burrowing worm eel present in core two (2) resulting in resuspension and increased NH_4 flux. F-20 had the highest macrofauna density and biomass among all stations during COMUS 1 (Figure 5.14). Macroinfaunal density did not make a significant contribution to the stepwise regression models with NH_4 fluxes, although animal excretions and subsequent burrow ventilation have been shown to enhance NH_4 fluxes (Aller 1980; Pelegrí 1994). In agreement with the conceptual model, proximity to the river (and

consequently, amount of deposition) seems to be directly associated with the magnitude of nitrogen flux across the sediment-water interface.

Phosphate and SiO_4 fluxes (Figs. 5.26 and 5.27, respectively) both clustered into two main groups with higher rates in regions proximal to the riverine source. These results are in closer agreement with the conceptual model (Figure 5.1) than the nitrogen flux rates, in that regeneration rates decrease with an increase in distance from the riverine source. The stations in each cluster were similar for both PO_4 and SiO_4ß with the exception of F-20 which was in the cluster of higher rates for SiO_4, but was in the distal cluster of lower rates for PO_4. This can be attributed to the presence of macrofauna at station F20, and their differential effect on SiO_4 compared to PO_4. Since PO_4 showed the highest correlation with sediment deposition, the stations in the proximal cluster follow the projected pattern of sediment dispersal from Southwest Pass (personal communication, Dr. B.A. McKee).

Benthic regeneration rates at South Pass were unique for all of the nutrients measured. Benthic fluxes of NO_3, NO_2, and NH_4 at SP were higher and consistent with the conceptual model. Nitrate uptake rates were higher, while rates of NO_2 and NH_4 release were greater at SP. However, PO_4 and SiO_4 benthic fluxes were uptake at SP compared to regeneration observed in the Southwest Pass dispersal area. Uptake rates at SP can perhaps be attributed to the extreme deposition observed in this area (personal communication, Dr. B.A. McKee), the high sediment load thus burying PO_4 and SiO_4 faster than they can be regenerated. This was also reflected in the lower pore-water concentrations for PO_4 and SiO_4 at SP.

Patterns of benthic nutrient regeneration on the Louisiana continental shelf are nutrient specific. Phosphate and SiO_4 fluxes are linked directly to deposition from the river, NH_4 fluxes seem dominated by *in situ* production, and NO_3 fluxes are a results of dissolved inputs (either from a riverine source or upwelling). Silicate fluxes varied by one-half between clusters, while NO_3, NH_4, and PO_4 all varied by an order of magnitude from the high to low grouping.

5.6.4 Deltaic versus Pelagic Systems

The seabed of deltaic systems receive inputs of terrigenous materials while deposits to sediments in pelagic shelves consists primarily from material produced *in situ* . A comparison of these two types of continental shelves provides insight into the relationship of benthic nutrient regeneration to the quantity and quality of deposited material (Figure 5.28). Average rates of NO_3 and NH_4 benthic fluxes show little difference among continental shelves and thus little direct link to riverine influence. Despite low riverine inputs of organic N to pelagic systems, the total inputs of organic N to pelagic systems may not be different from deltaic systems due to regional upwelling.

Phosphate and SiO_4, however, show greater benthic regeneration rates in deltaic systems (Figure 5.28). Since PO_4 is transported to the seabed via adsorption onto particles, more effective scavenging and transport of PO_4 occurs in continental shelves with higher suspended solids. The fact that SiO_4 shows higher regeneration rates in deltaic systems is related to the direct riverine input of SiO_4 from terrestrial sources. The difference observed for PO_4 and SiO_4 fluxes does not mean that a higher quality of deposition does not increase benthic regeneration rates, but rather that there could be a significant difference in the amount of PO_4 and SiO_4 reaching the benthos in deltaic systems. In agreement with the spatial

analyses, riverine deposition establishes the patterns of PO_4 and SiO_4 regeneration, while NO_3 and NH_4 benthic fluxes are controlled by other factors such as upwelling and *in situ* production.

5.7 Summary

Benthic nutrient regeneration of NO_3, NO_2, NH_4, PO_4, and SiO_4 was examined on the Louisiana continental shelf in November 1993 and June 1994. Temporal differences in these fluxes between cruises were examined, as well as any spatial trends occurring across the shelf. Pore-water gradients for all the nutrients were obtained and compared to the nutrient fluxes; sediment deposition was also compared to nutrient fluxes. Sediment characteristics and macroinfaunal densities and biomass were used in conjunction with these objectives to explain spatial and temporal variation.

Modeling of nutrient fluxes from pore-water gradients proved difficult, as correlations of regeneration to pore-water gradients were moderate for NO_3 and NH_4, and non-existent for PO_4, and SiO_4. Quality of deposition does provide a slightly better correlation to regeneration than quantity of deposition, but the precise index of quality does not fit our hypothesis. Nitrate and PO_4 were the only two nutrients that showed a significant difference in regeneration with respect to time. These differences are a result of different riverine inputs.

Pore-water modeling of nutrient fluxes and examining the influence of the quantity versus quality of deposition on benthic nutrient regeneration are complex issues, encompassing more than the preliminary parameters examined here. A more in depth analysis is needed to really look at these issues, in particular, data involving greater deposition rates. This research provides a starting point for further examination and perhaps experimentation on these benthic processes.

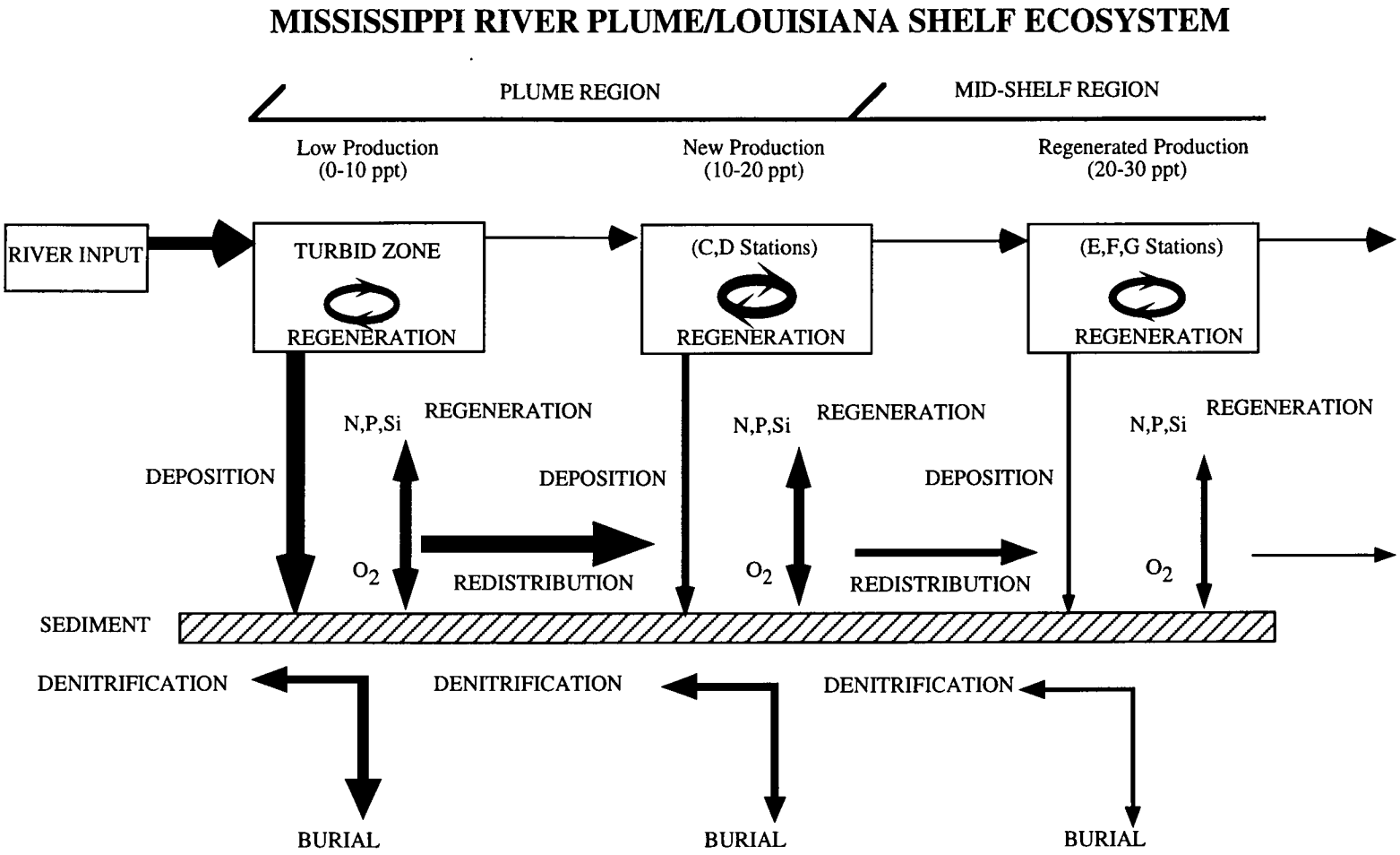

Figure 5.1. Conceptual model of the fate of organic matter in the plume and mid-shelf region of the Louisiana continental shelf (from Twilley et al. 1994).

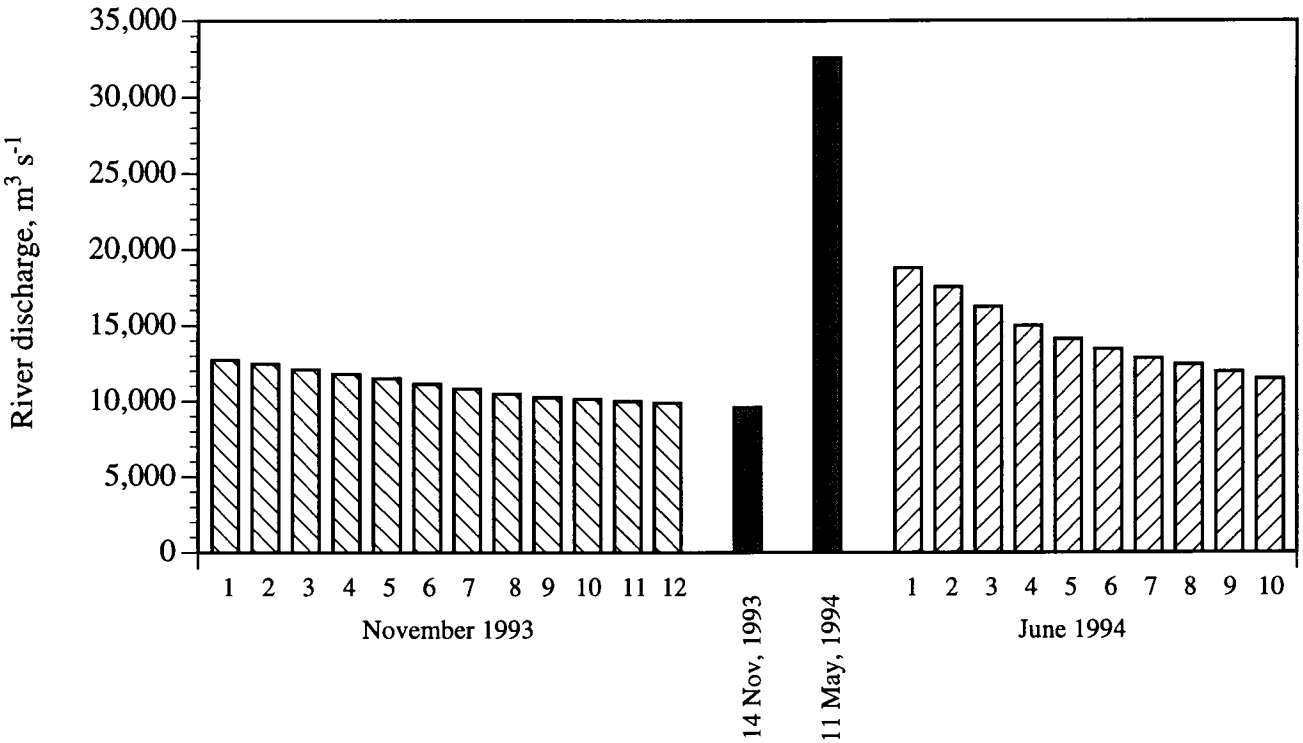

Figure 5.2. Histogram of the discharge of the Mississippi River at Tarbert Landing, Louisiana (USGS) for COMUS 1 and COMUS 3 in $m^3 s^{-1}$. The middle two bars indicate the lowest and highest river stages of the year, while their dates show their proximity to the respective cruises.

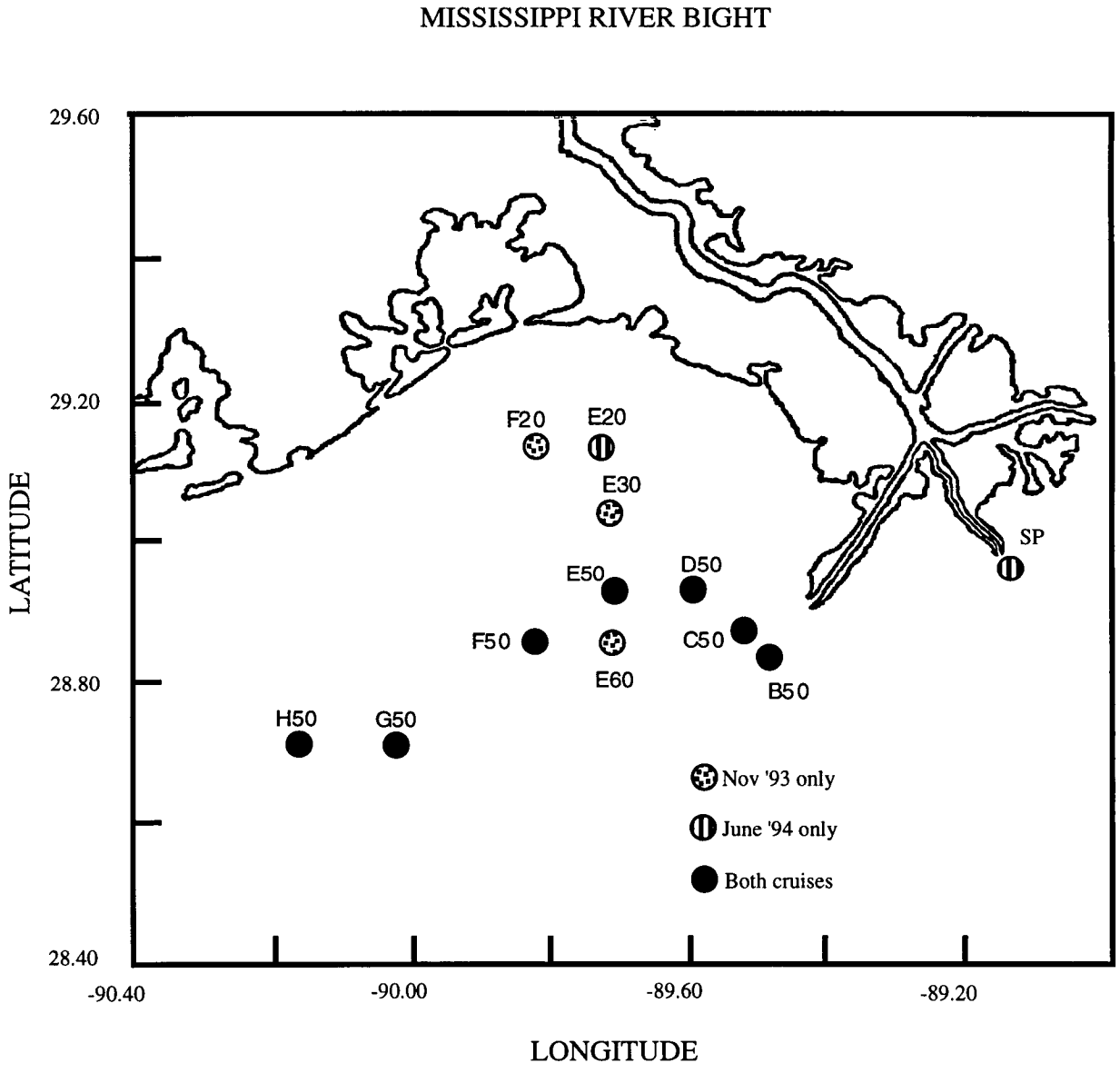

Figure 5.3. Sampling stations on the two cruises: COMUS 1 (November 1993) and COMUS 3 (June 1994).

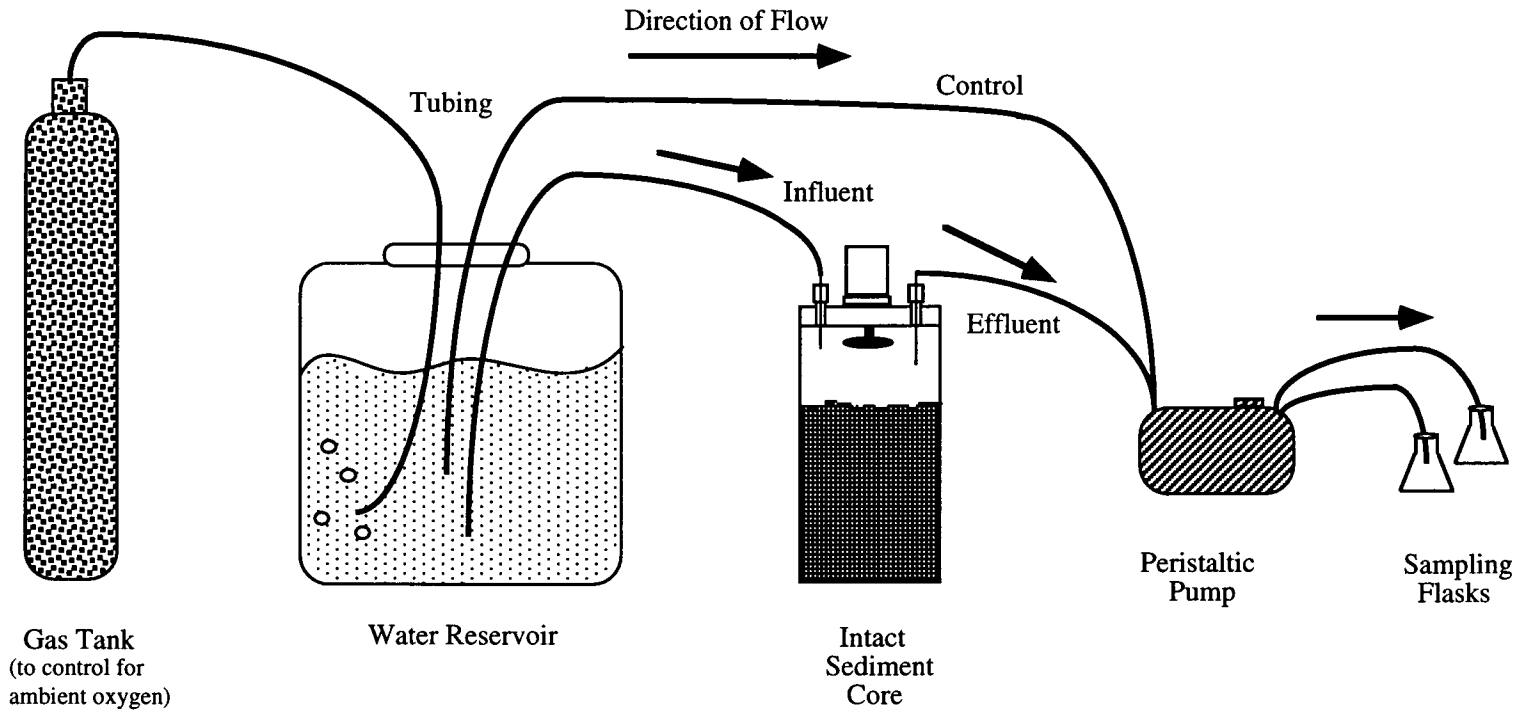

Figure 5.4. Core chemostat system used to determine benthic nutrient flux rates (Miller-Way and Twilley 1996).

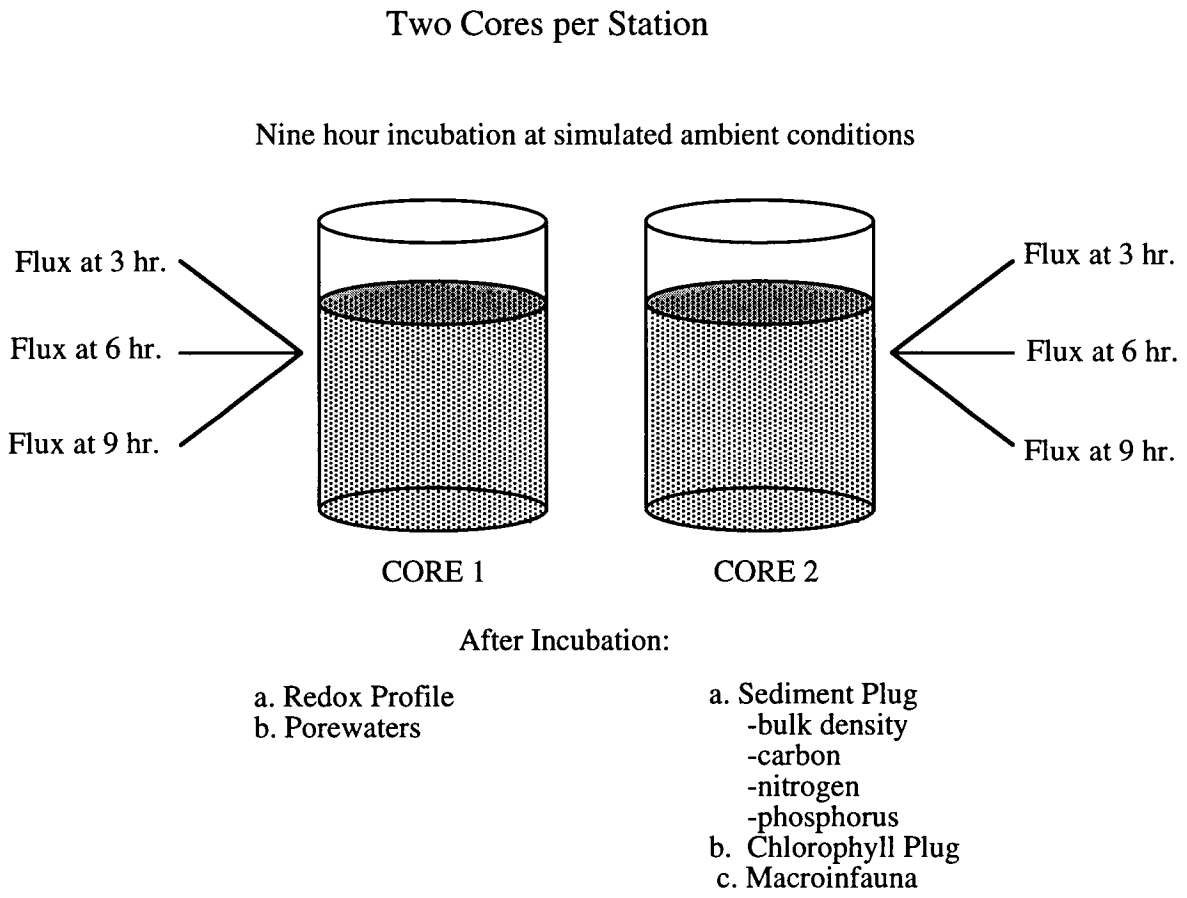

Figure 5.5. Sampling regime used to analyze each core during and after incubation.

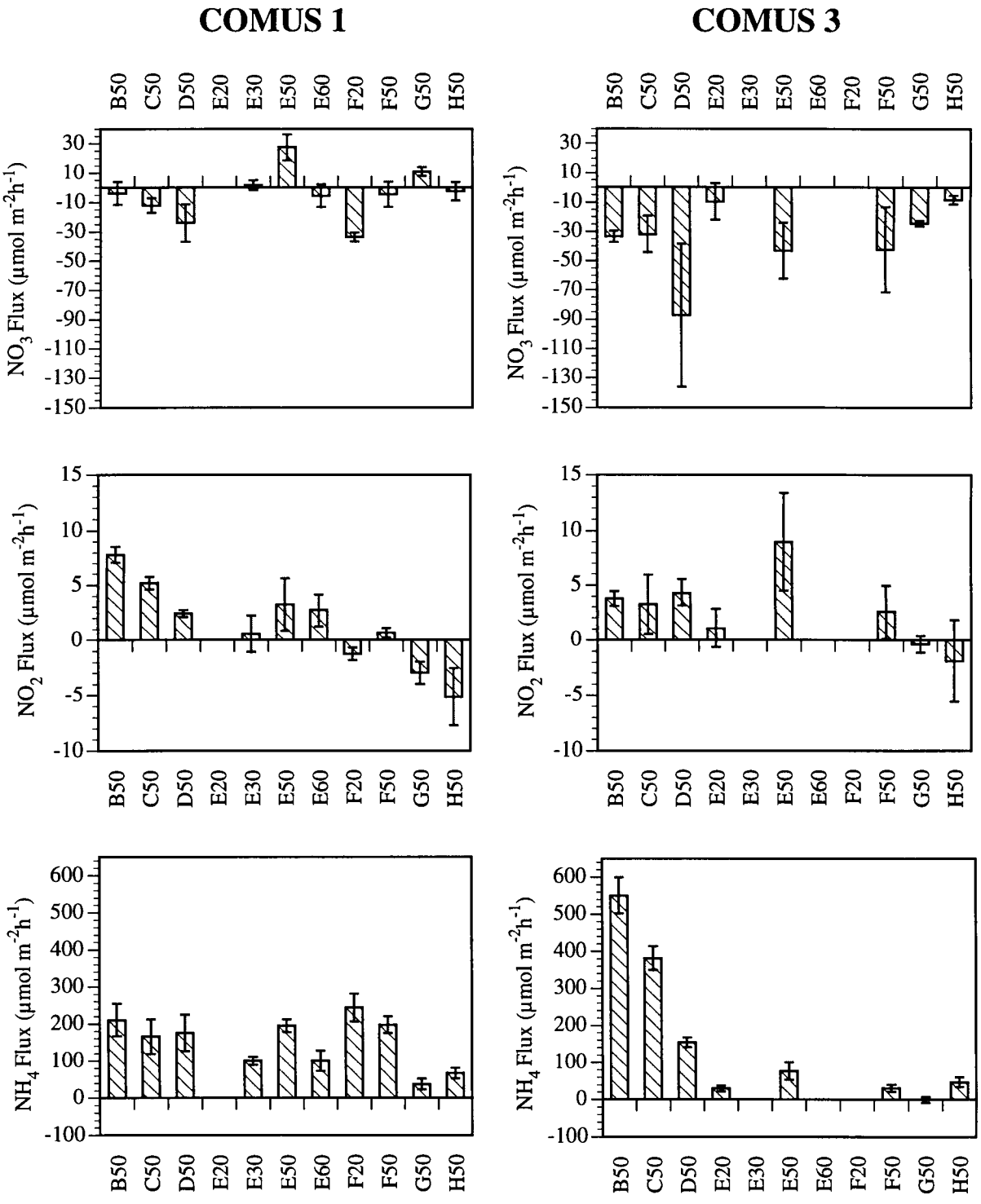

Figure 5.6a. Average flux per station for NO_3, NO_2, and NH_4 for each cruise (with standard error bars), excluding the station at South Pass (SP).

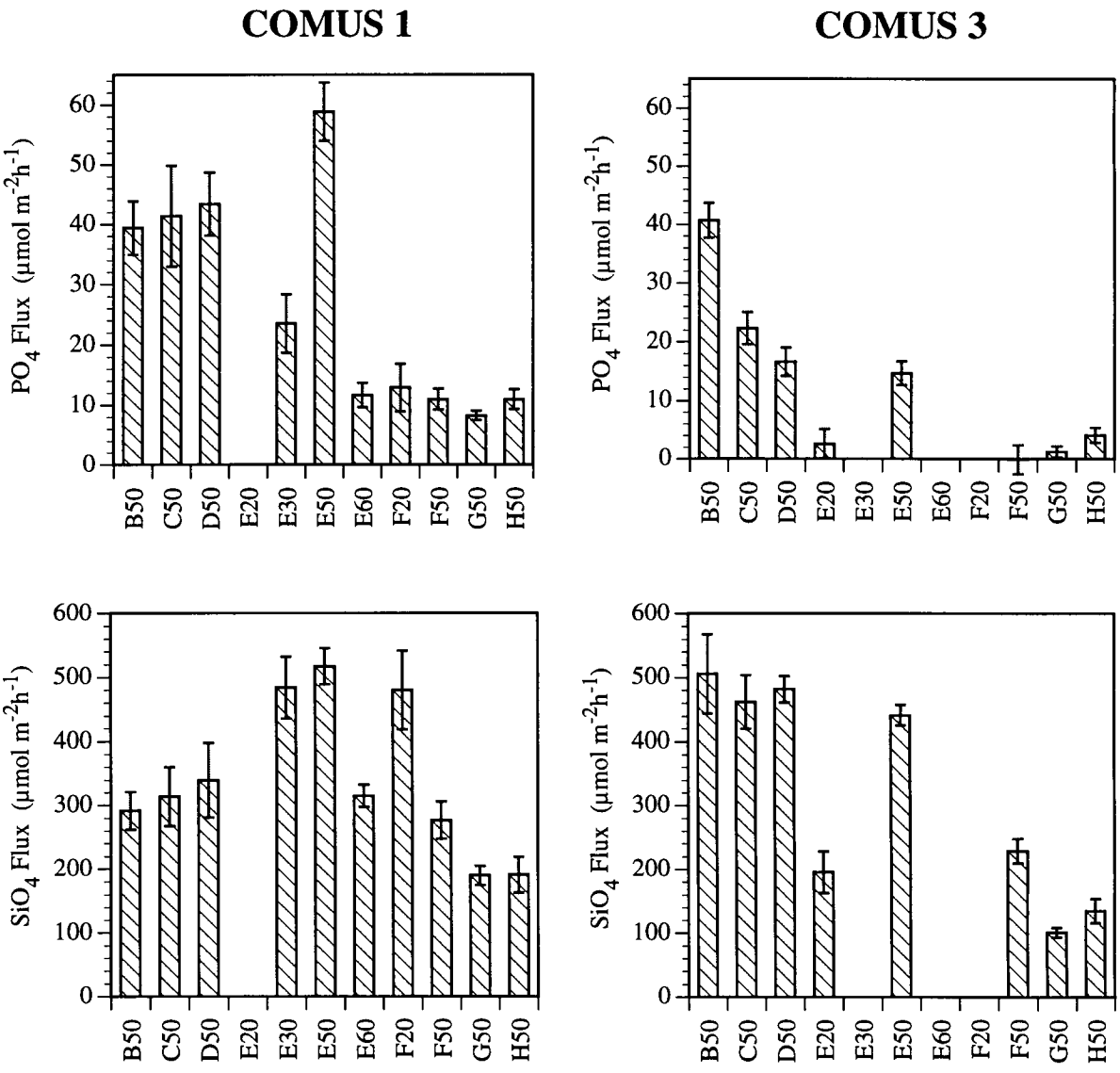

Figure 5.6b. Average flux per station for PO_4 and SiO_4 for each cruise (with standard error bars), excluding the station at South Pass (SP).

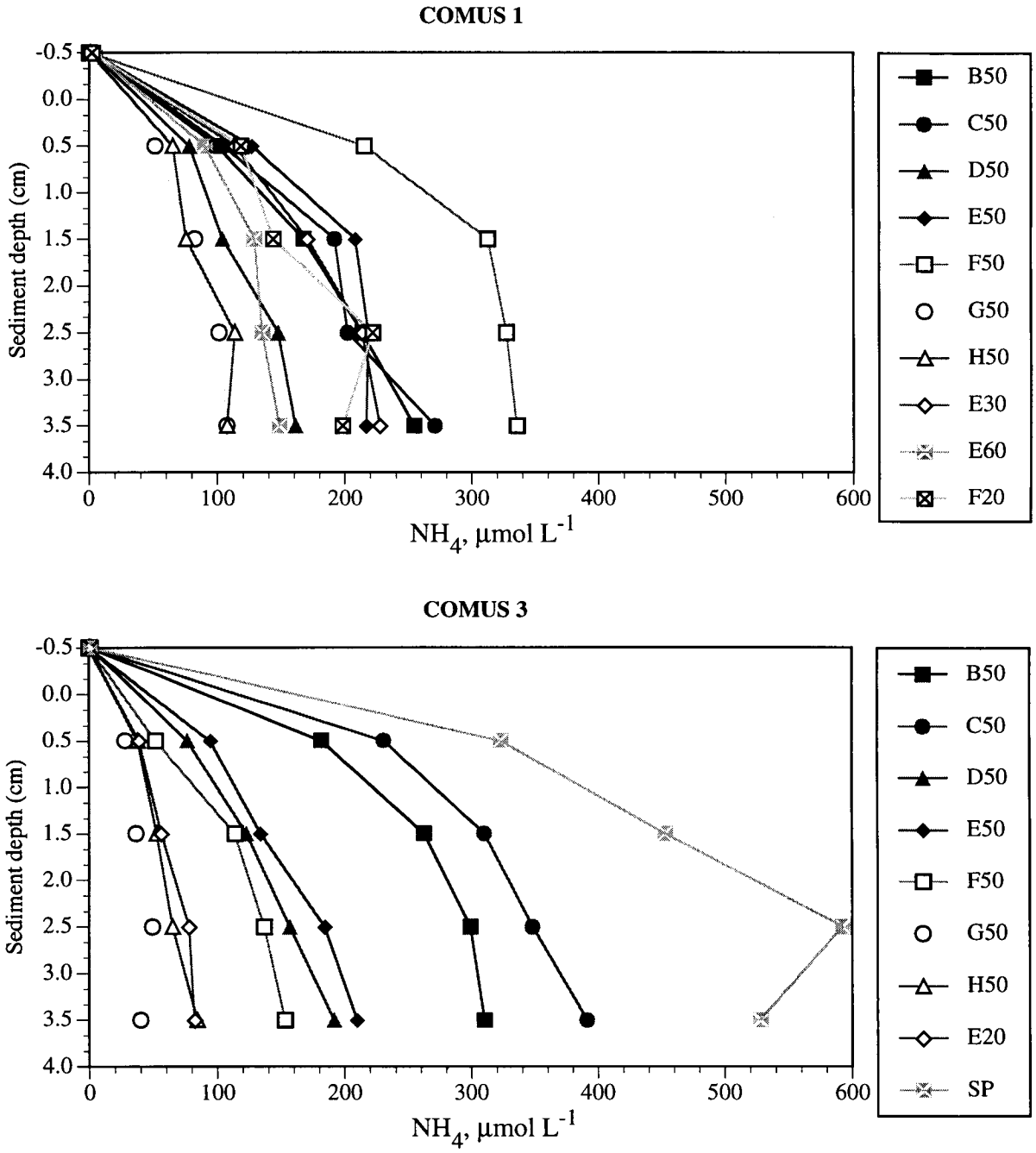

Figure 5.7. Pore-water profiles with depth for NH_4, from the overlying water (-0.5 cm) to a depth of 3.5 cm into the sediment. All values are in µmol L^{-1}. See Figure 5.3. for station locations.

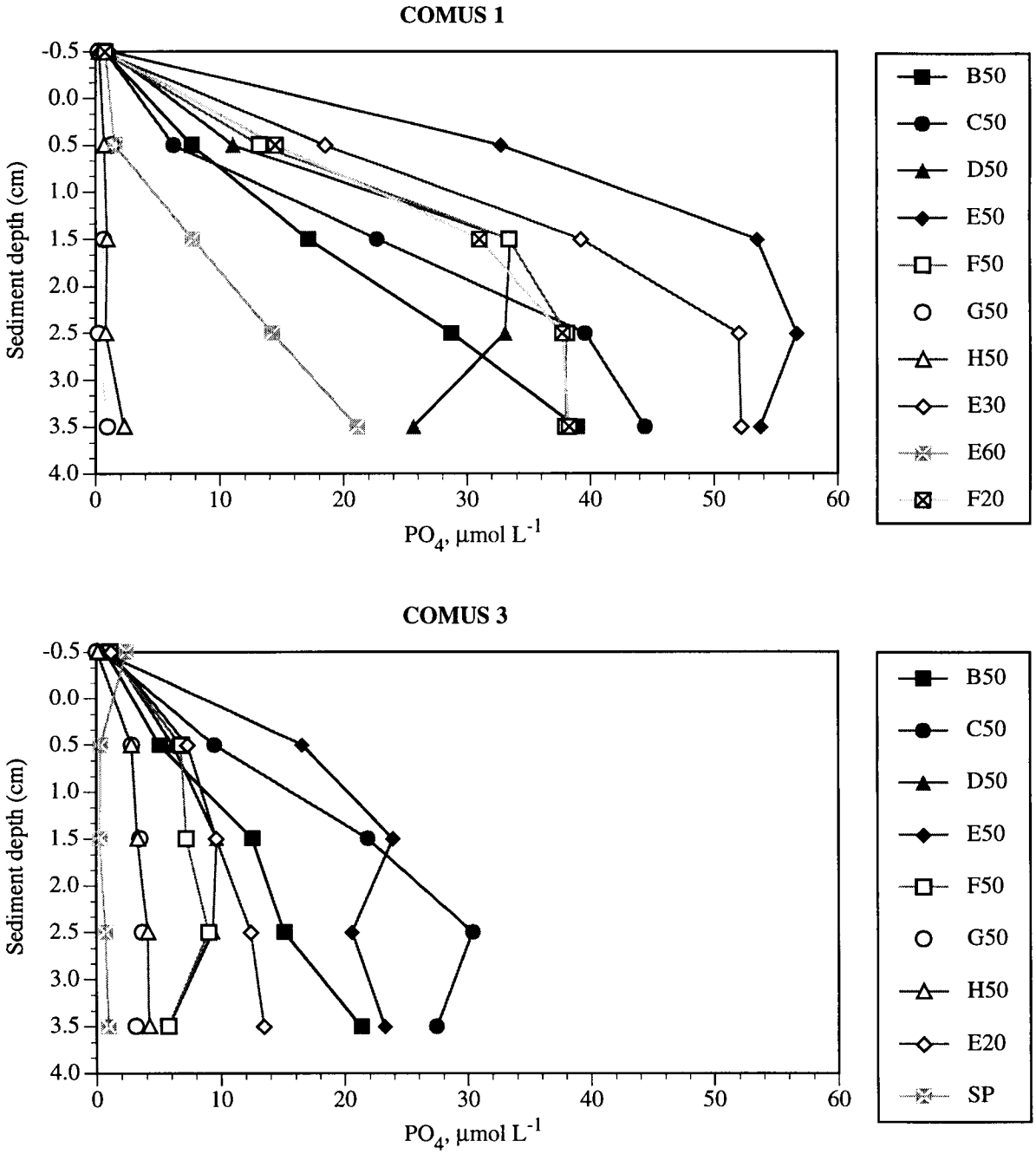

Figure 5.8. Pore-water profiles with depth for PO_4, from the overlying water (-0.5 cm) to a depth of 3.5 cm into the sediment. All values are in µmol L^{-1}. See Figure 5.3. for station locations.

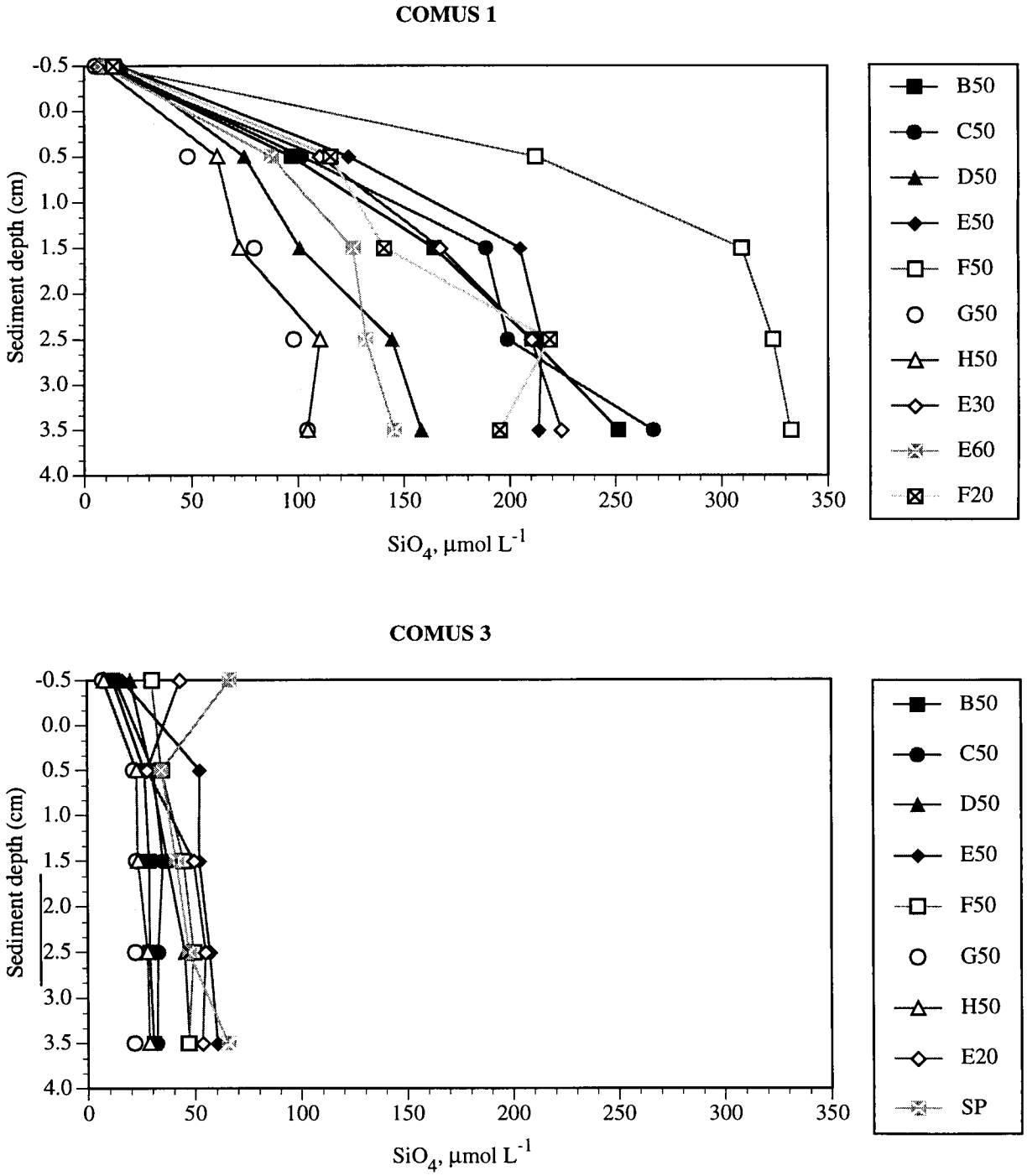

Figure 5.9. Pore-water profiles with depth for SiO_4, from the overlying water (-0.5 cm) to a depth of 3.5 cm into the sediment. All values are in µmol L^{-1}. See Figure 5.3. for station locations.

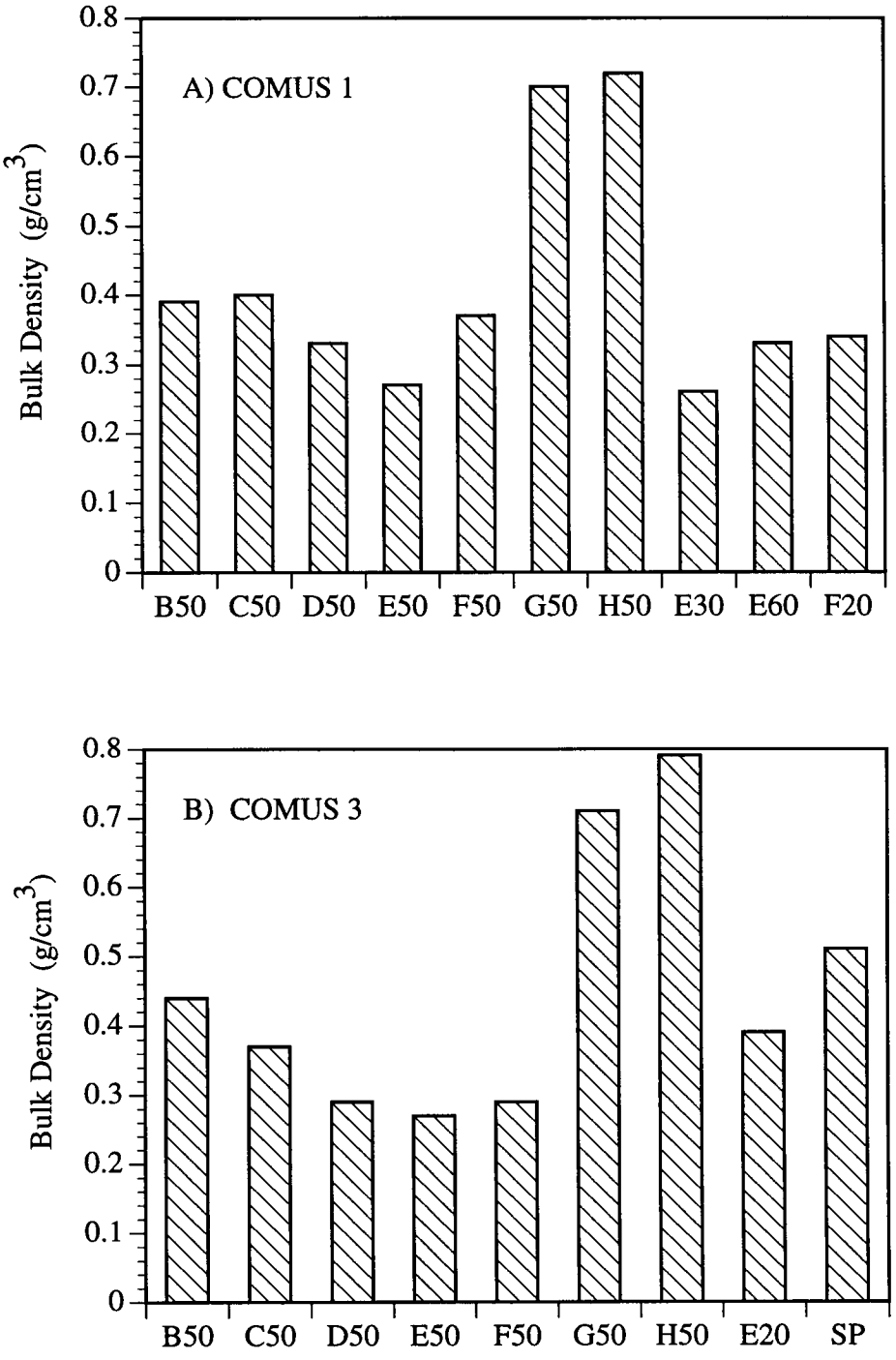

Figure 5.10. Sediment bulk density (g/cm^3) by station for A) COMUS 1 and B) COMUS 3.

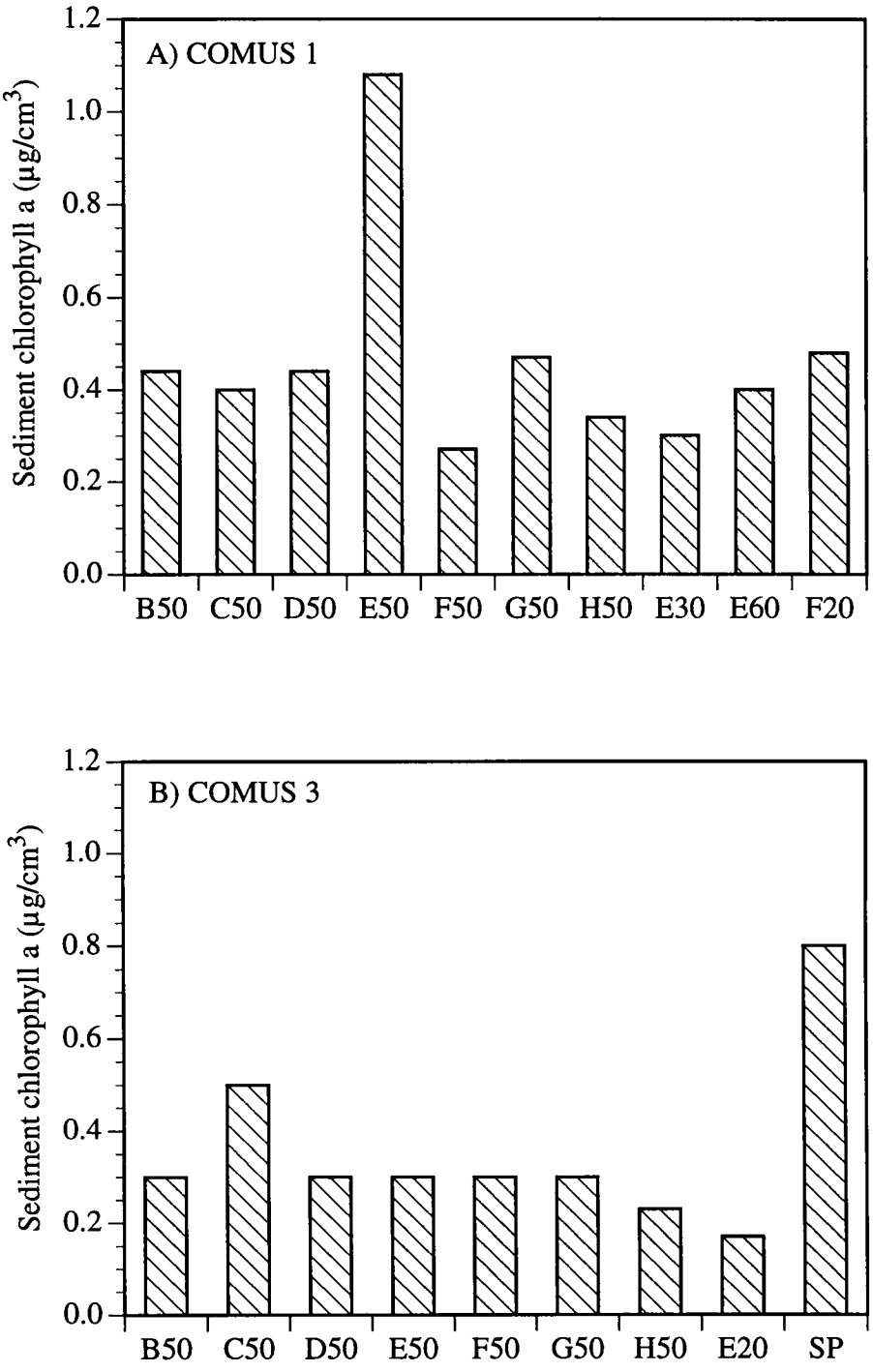

Figure 5.11. Sediment chlorophyll a concentrations (µg/cm^3 at 1cm depth) by station for A) COMUS 1 and B) COMUS 3.

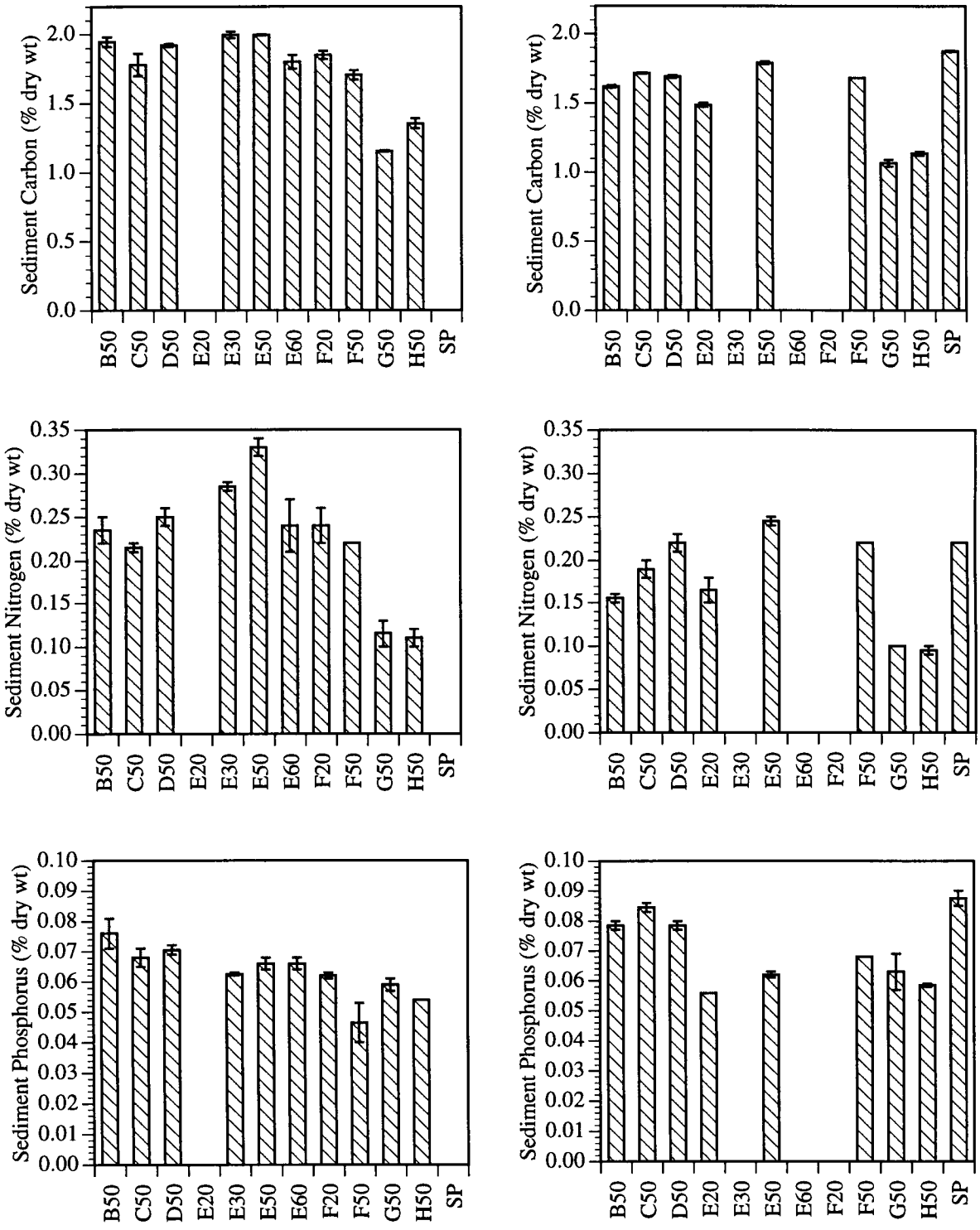

Figure 5.12. Mean concentrations of sediment carbon, nitrogen, and phosphorus with standard error bars by station for both cruises.

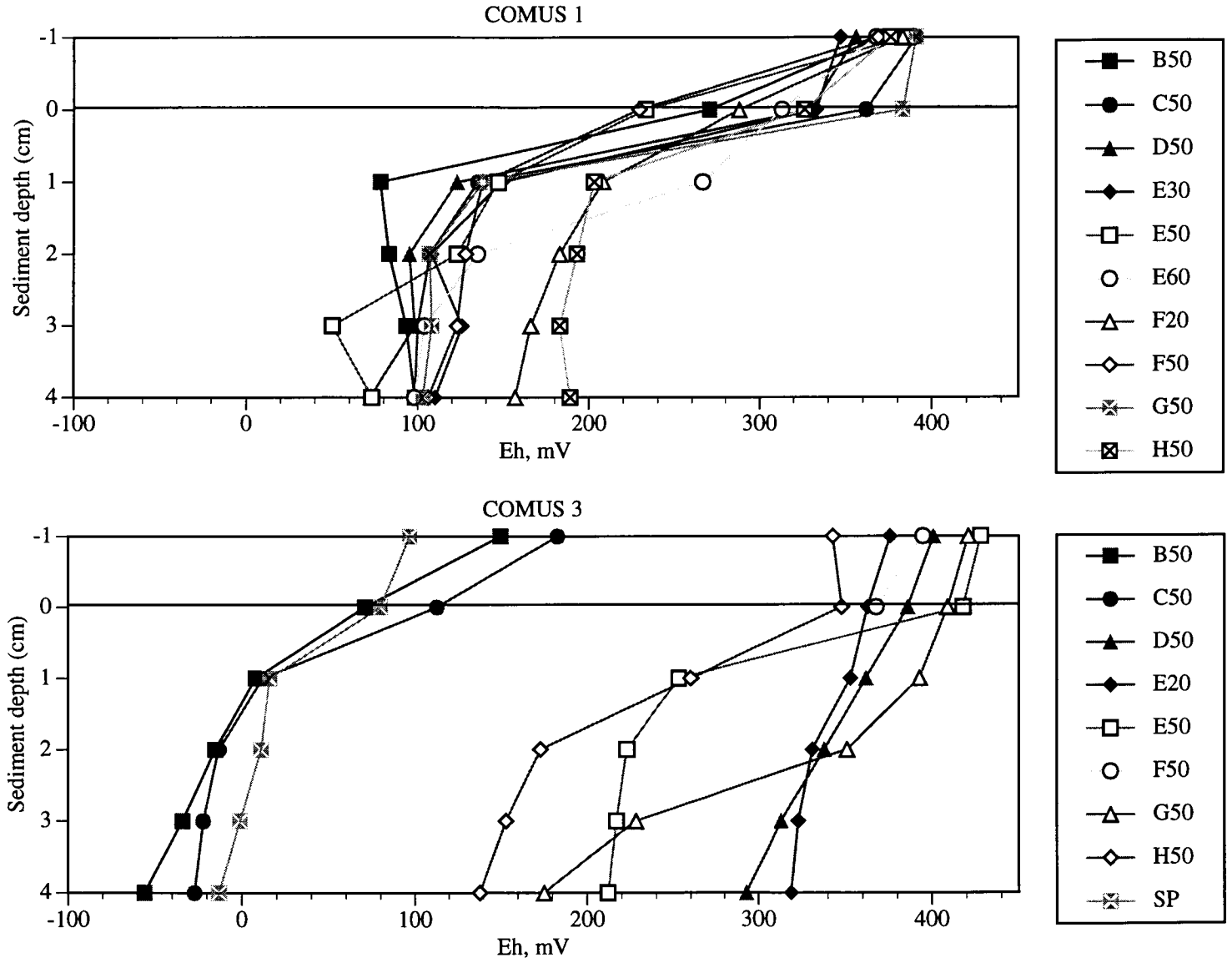

Figure 5.13. Redox profiles (Eh, mv) with depth in sediment (-1 corresponds to overlying water Eh, and 0 to the sediment-water interface Eh value).

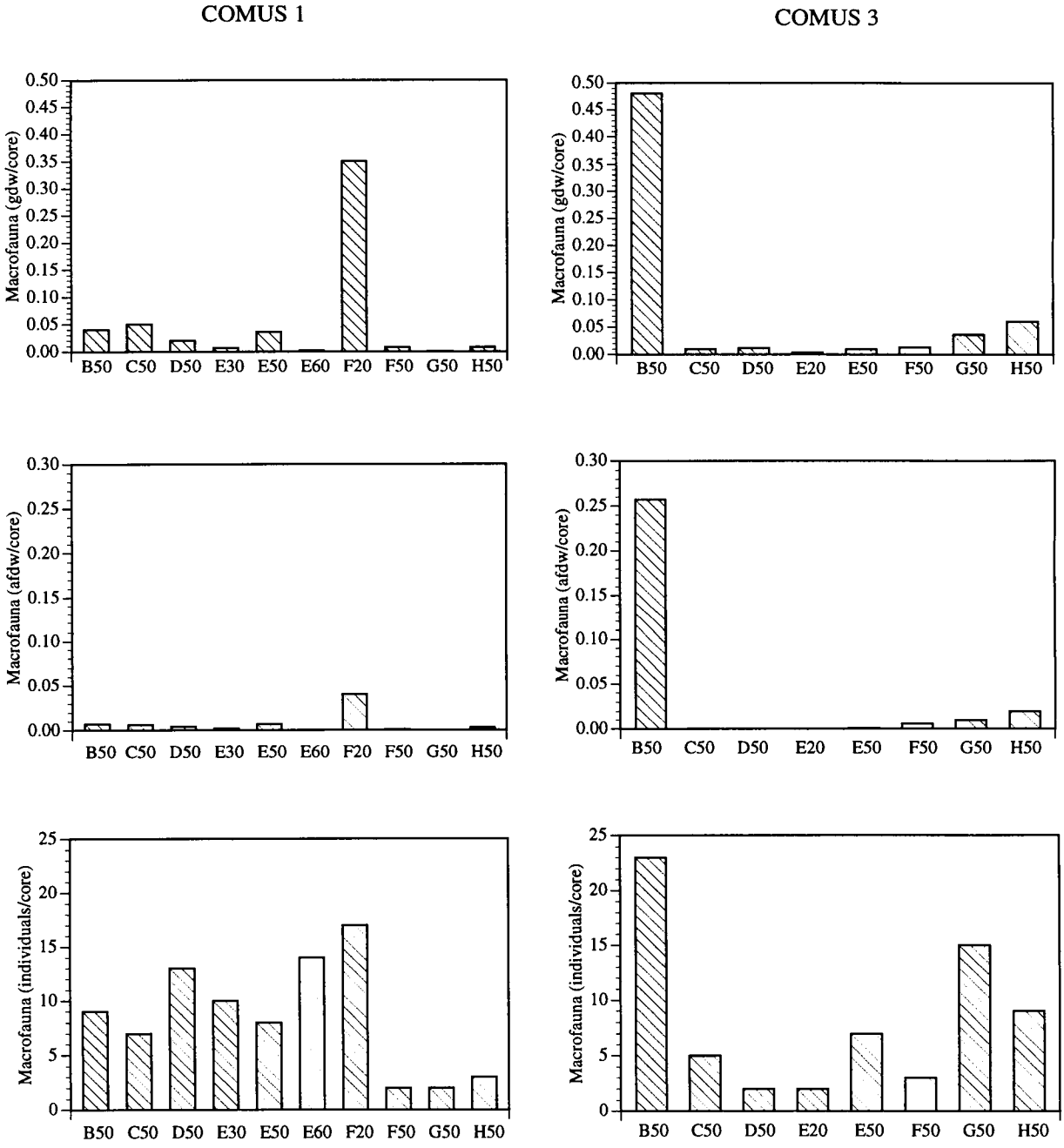

Figure 5.14. Dry weight (gdw), ash-free dry weight (afdw), and number of individuals per core of benthic macroinfauna by station for COMUS 1 and COMUS 3.

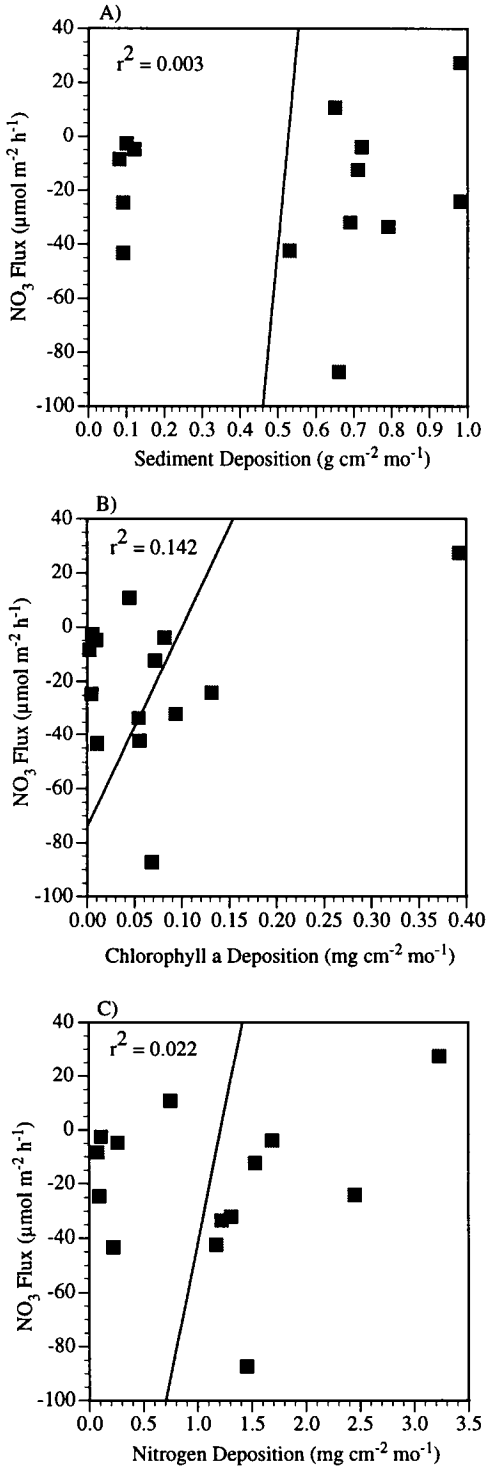

Figure 5.15. Linear correlations of mean NO_3 fluxes to three indices of input to the seabed: A) Bulk sediment input, B) Input of the component with the highest correlation, and C) Input of the component that was hypothesized to have the highest correlation (nitrogen).

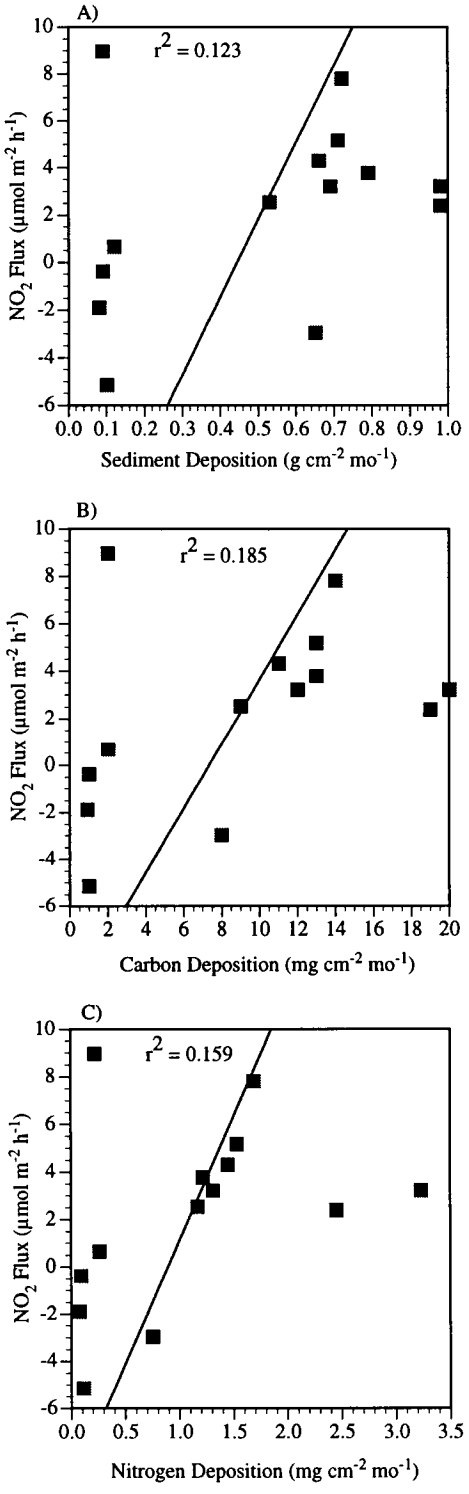

Figure 5.16. Linear correlations of mean NO_2 fluxes to three indices of input to the seabed: A) Bulk sediment input, B) Input of the component with the highest correlation, and C) Input of the component that was hypothesized to have the highest correlation (nitrogen).

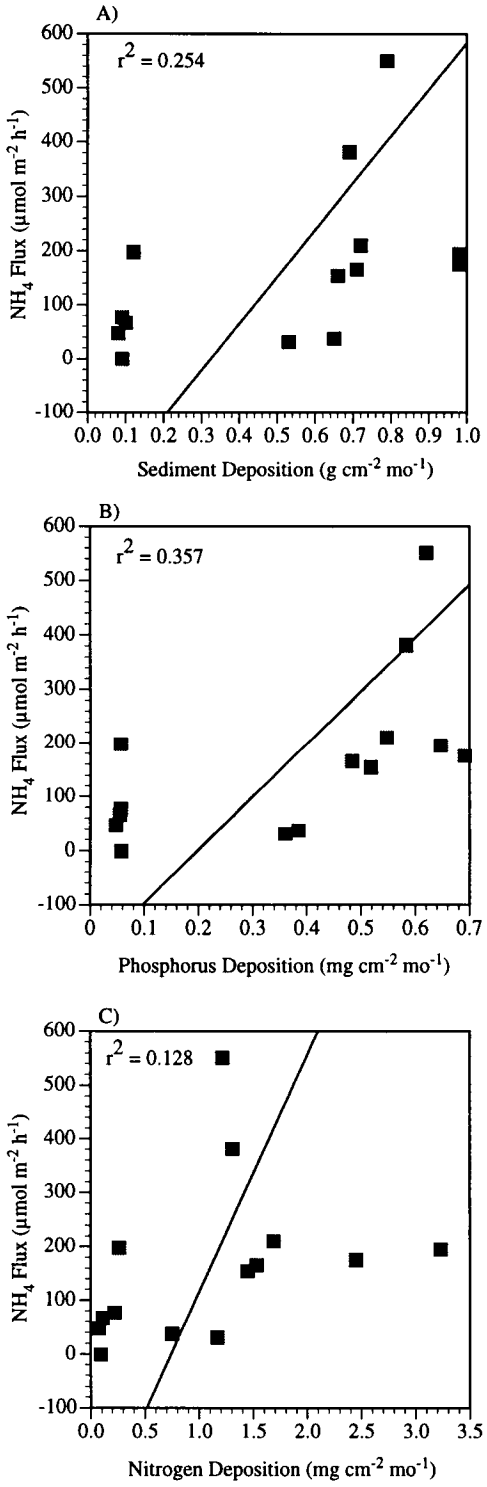

Figure 5.17. Linear correlations of mean NH_4 fluxes to three indices of input to the seabed: A) Bulk sediment input, B) Input of the component with the highest correlation, and C) Input of the component that was hypothesized to have the highest correlation (nitrogen).

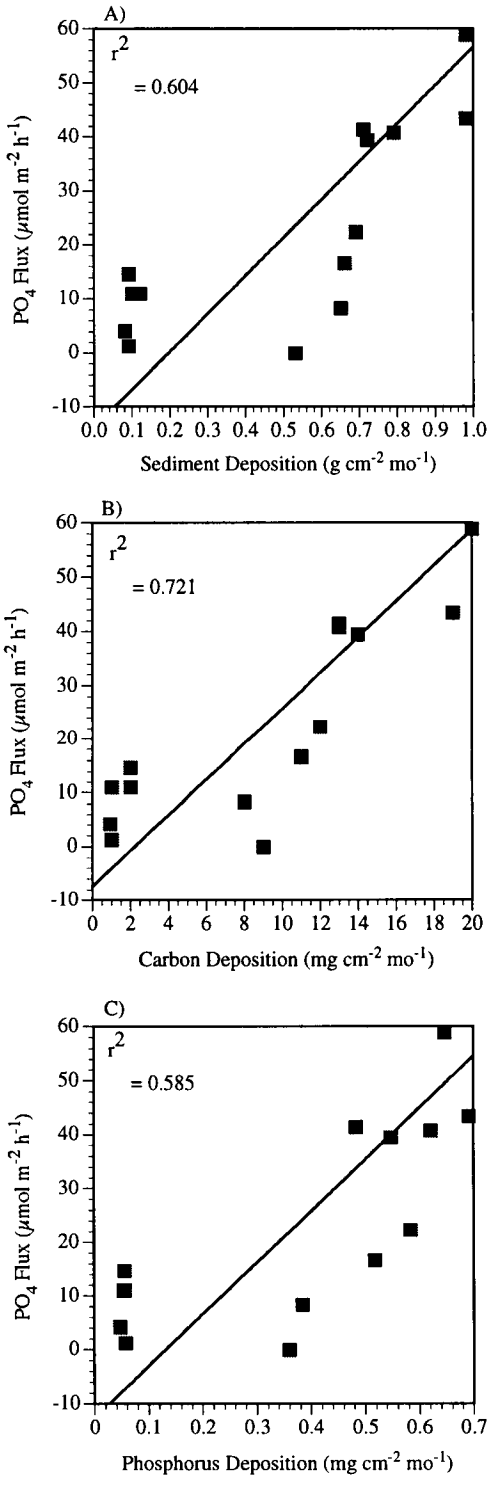

Figure 5.18. Linear correlations of mean PO4 fluxes to three indices of input to the seabed: A) Bulk sediment input, B) Input of the component with the highest correlation, and C) Input of the component that was hypothesized to have the highest correlation (phosphorus).

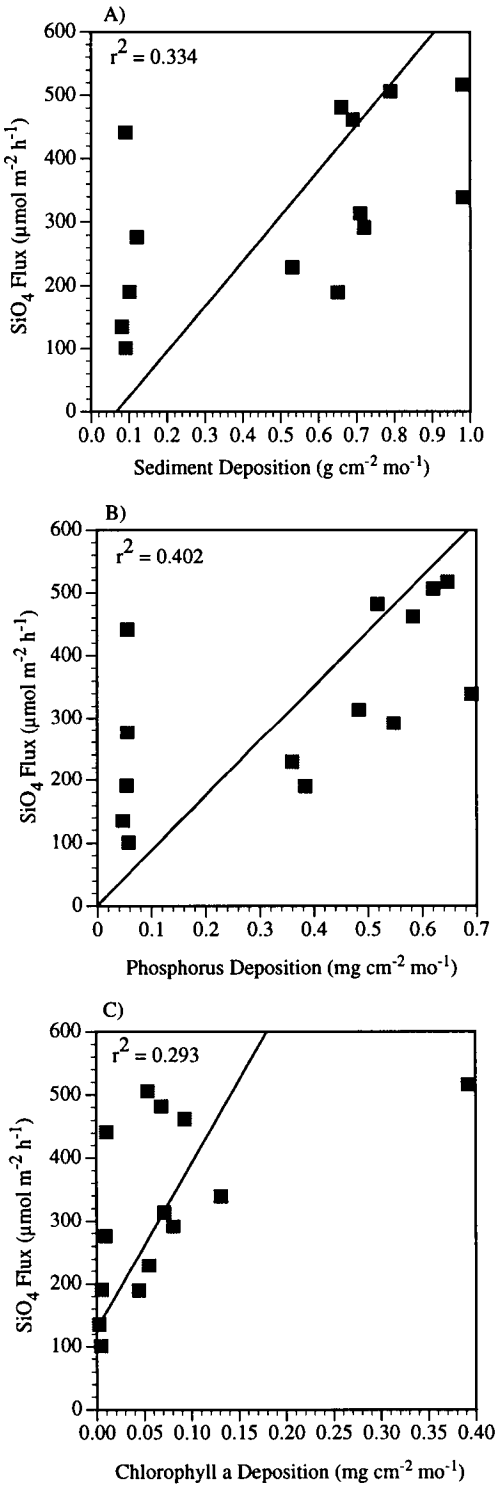

Figure 5.19. Linear correlations of mean SiO_4 fluxes to three indices of input to the seabed: A) Bulk sediment input, B) Input of the component with the highest correlation, and C) Input of the component that was hypothesized to have the highest correlation (chlorophyll a).

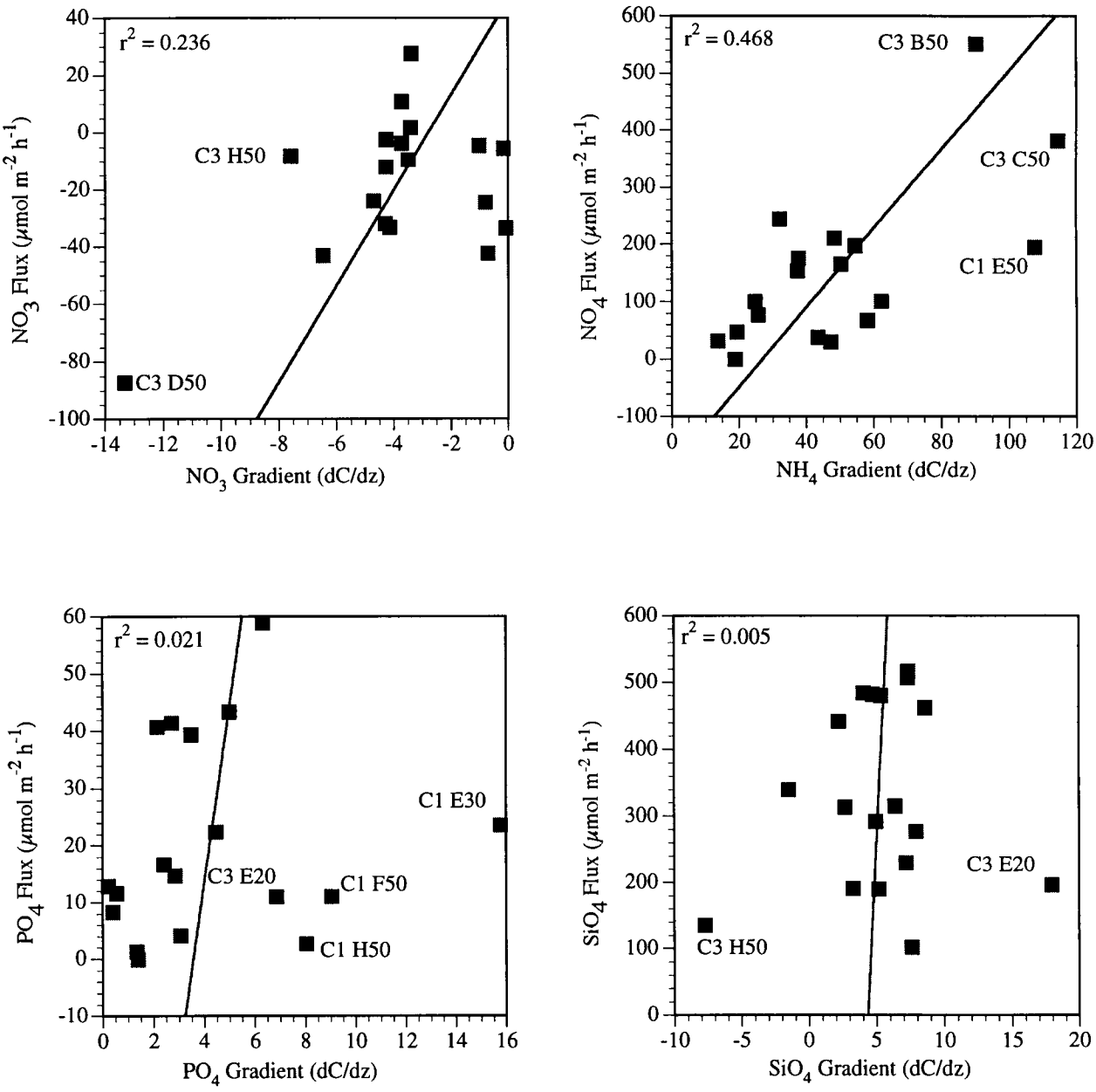

Figure 5.20. Linear correlations of nutrient flux to the pore-water gradient (from overlying water to 1cm for NO3, NH4, PO4, and SiO4.

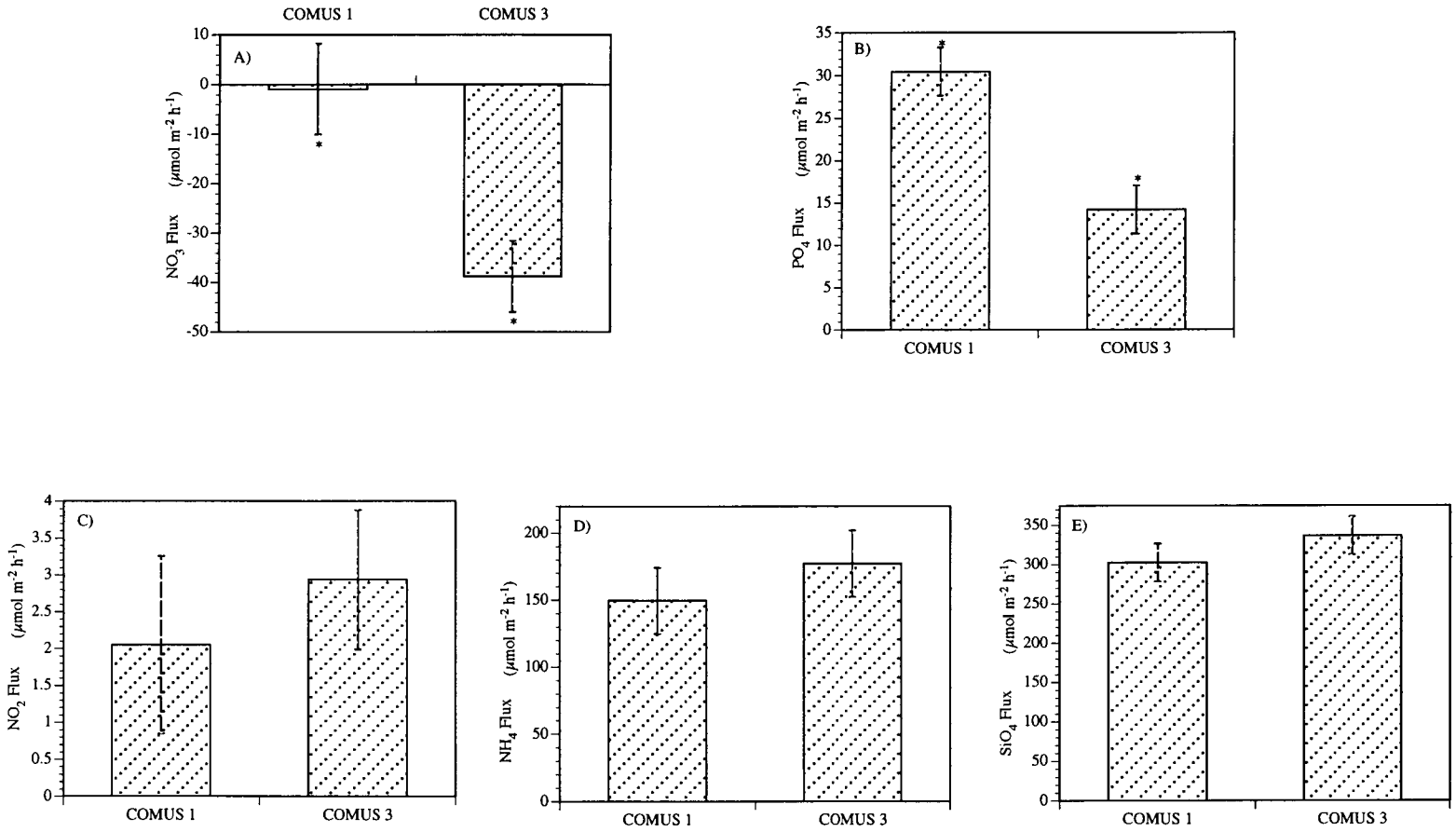

Figure 5.21. Average benthic fluxes (± standard error) for each cruise for A) NO_3, B) PO_4, C) NO_2, D) NH_4, and E) SiO_4. Only the seven stations sampled on both cruises were used for this comparison (*indicates significant difference at alpha=0.05).

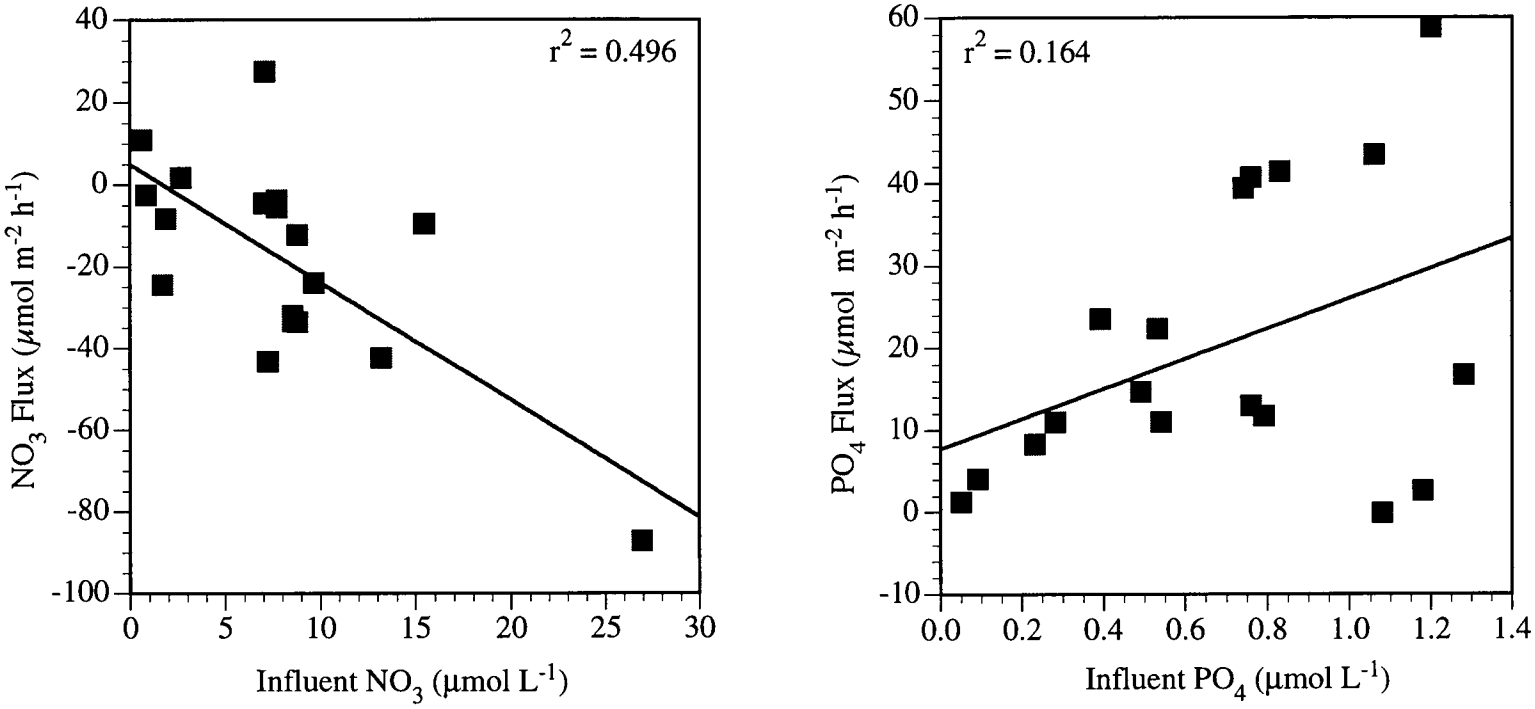

Figure 5.22. Linear correlations of influent nutrient concentrations and benthic fluxes for NO3 and PO4. Both graphs exclude station Sp (COMUS 3).

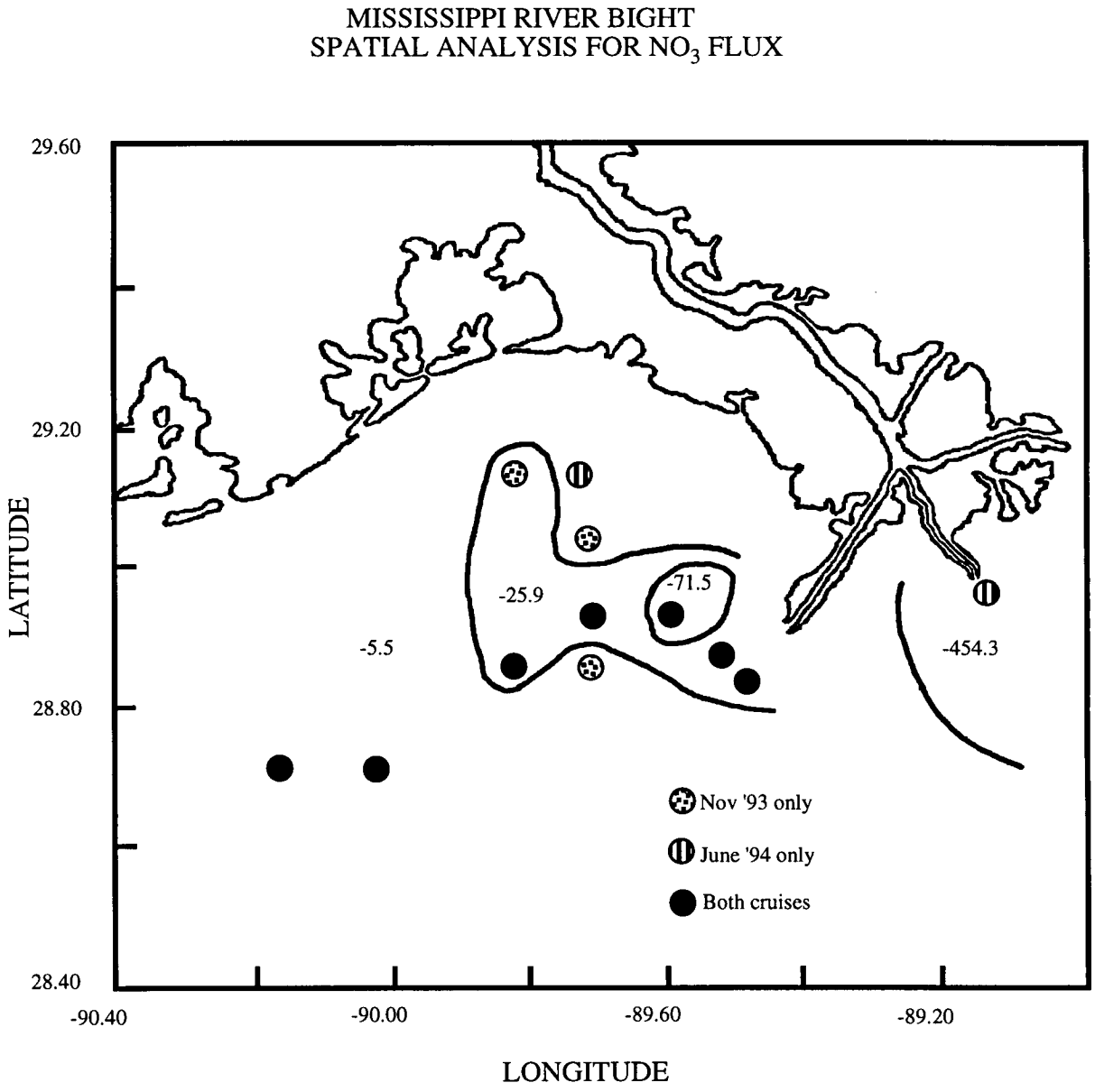

Figure 5.23. Spatial contours for NO_3 flux ($\mu mol\ m^{-2}\ h^{-1}$) as determined by cluster analysis. Numbers indicate average benthic flux for stations within each spatial group.

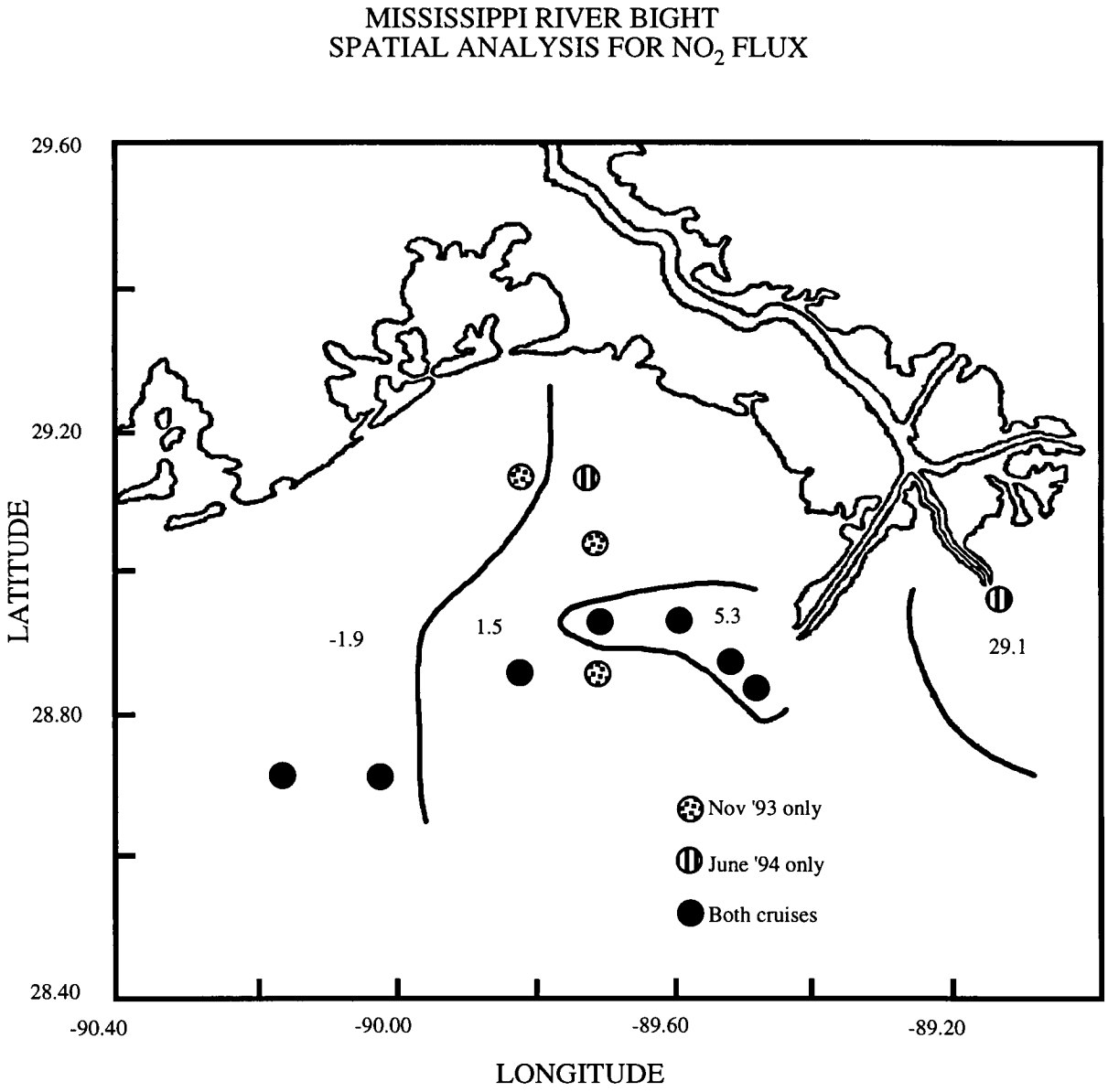

Figure 5.24. Spatial contours for NO_2 flux (μmol m^{-2} h^{-1}) as determined by cluster analysis. Numbers indicate average benthic flux for stations within each spatial group.

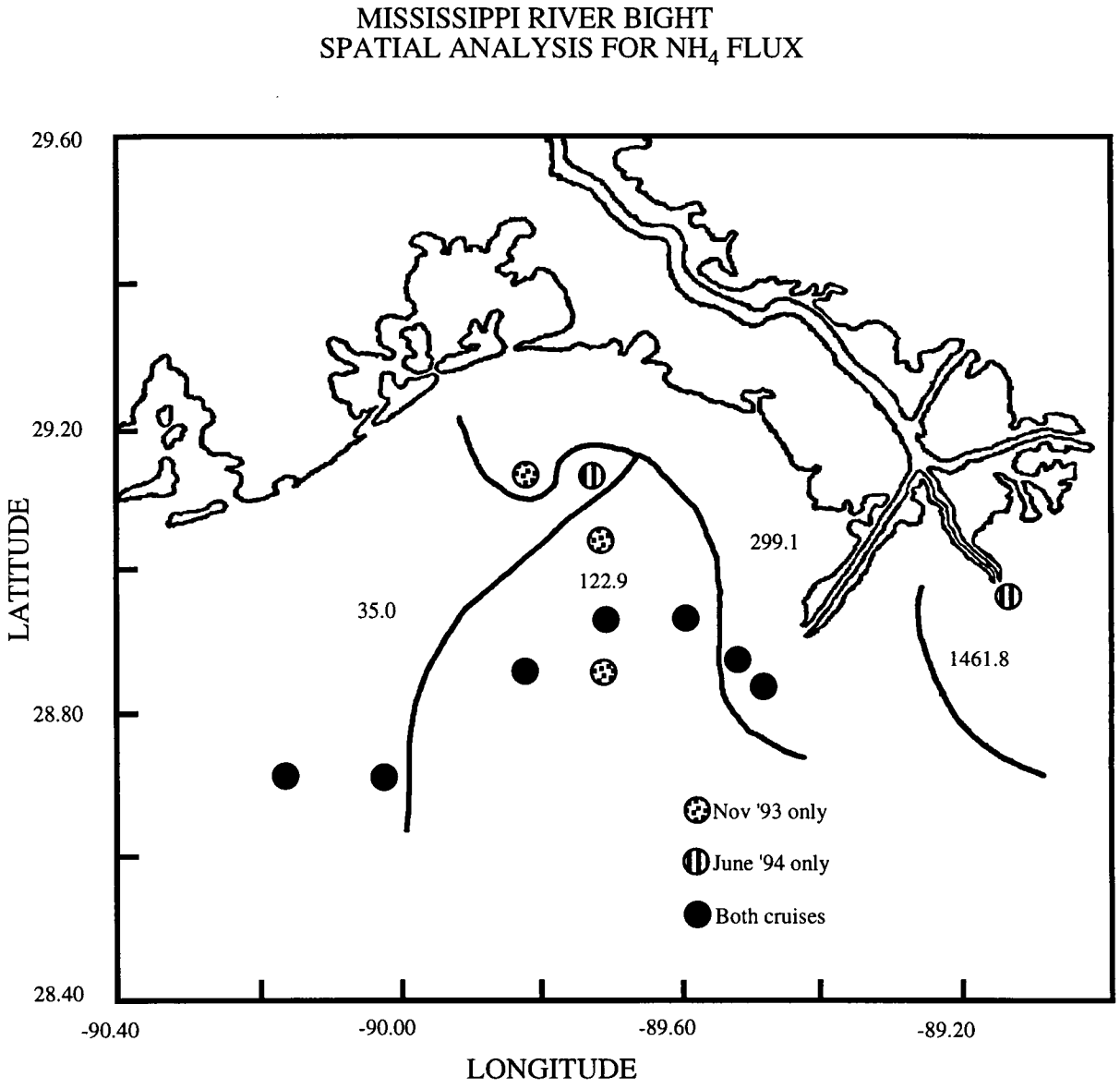

Figure 5.25. Spatial contours for NH_4 flux ($\mu mol\ m^{-2}\ h^{-1}$) as determined by cluster analysis. Numbers indicate average benthic flux for stations within each spatial group.

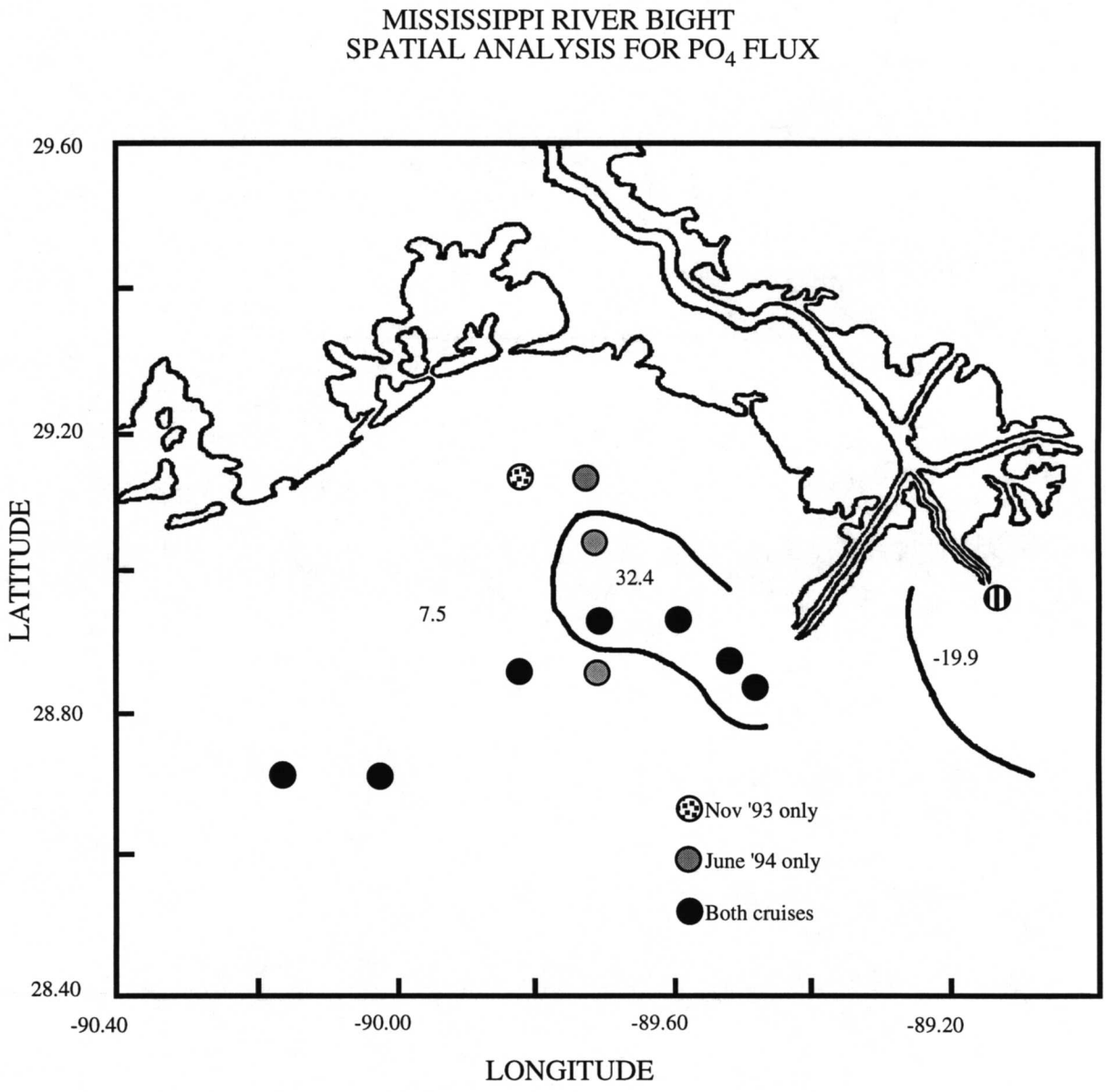

Figure 5.26. Spatial contours for PO_4 flux ($\mu mol\ m^{-2}\ h^{-1}$) as determined by cluster analysis. Numbers indicate average benthic flux for stations within each spatial group.

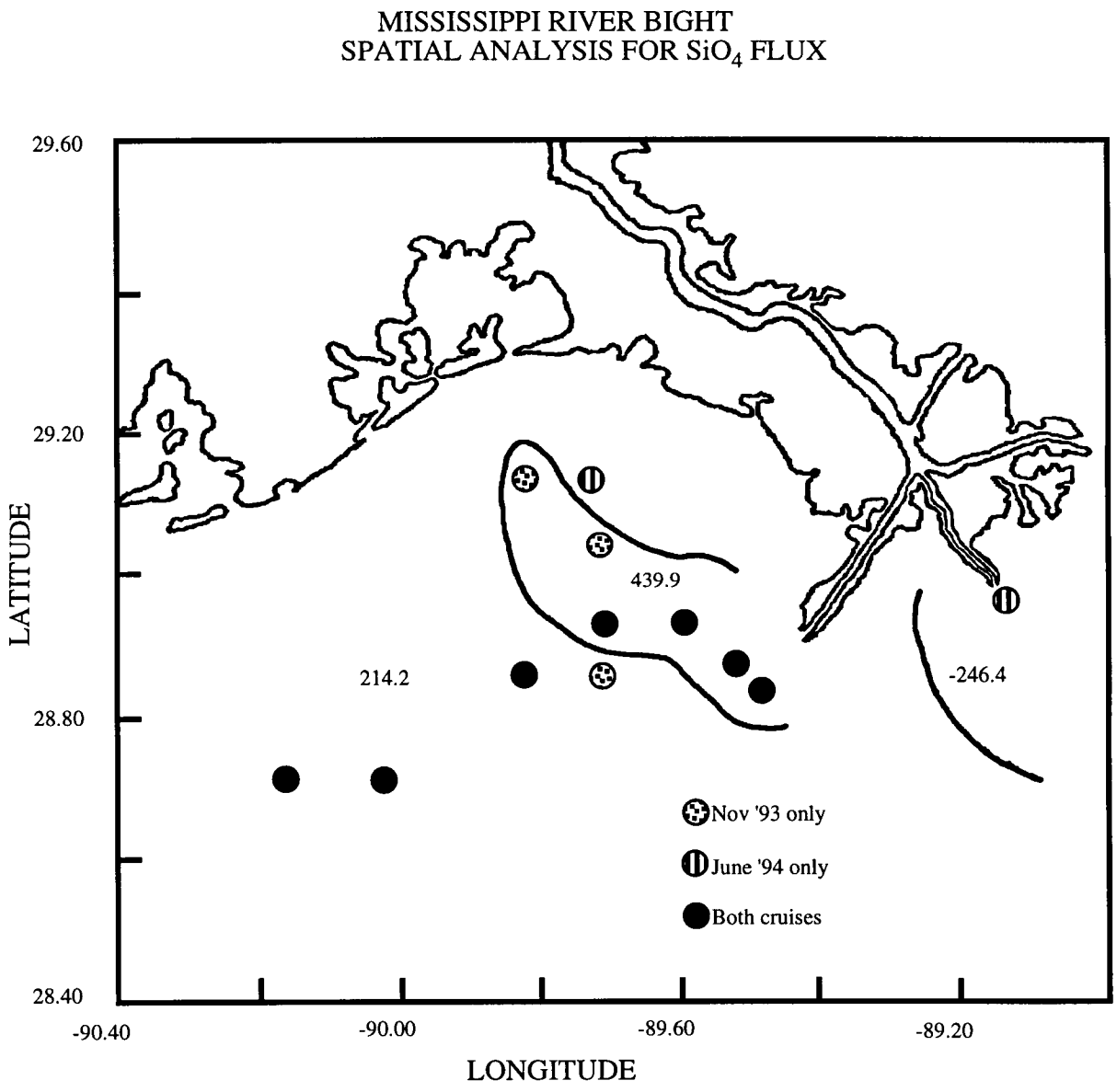

Figure 5.27. Spatial contours for SiO_4 flux (μmol m^{-2} h^{-1}) as determined by cluster analysis. Numbers indicate avergae benthic flux for stations within each spatial group.

Table 5.1. Latitude and longitude of sampling stations with bottom CTD conditions for COMUS 1 and COMUS 3.

				Bottom Conditions		
Cruise	Station	Latitude	Longitude	Temperature	Oxygen (mg/l)	Salinity (psu)
COMUS 1	B50	28 50.47	89 29.07	20.00	2.90	36.49
COMUS 1	C50	28 25.48	89 31.68	20.00	3.00	36.75
COMUS 1	D50	28 56.03	89 35.58	20.00	4.00	not available
COMUS 1	E50	28 56.88	89 43.53	20.00	4.00	34.40
COMUS 1	F50	28 52.51	89 50.08	21.00	4.00	not available
COMUS 1	G50	28 43.19	90 01.97	24.50	5.92	35.18
COMUS 1	H50	28 42.97	90 10.08	25.00	5.34	33.46
COMUS 1	E30	29 02.44	89 43.60	26.00	3.50	34.20
COMUS 1	E60	28 51.65	89 43.52	20.35	4.35	not available
COMUS 1	F20	29 08.26	89 50.03	26.80	2.59	32.53
COMUS 3	B50	28 50.48	89 29.19	19.80	5.34	36.25
COMUS 3	C50	28 52.51	89 31.52	20.50	6.10	36.15
COMUS 3	D50	28 56.01	89 35.60	18.75	3.86	35.98
COMUS 3	E50	28 56.89	89 43.54	20.00	5.20	30.70
COMUS 3	F50	28 52.49	89 50.03	19.27	3.10	34.70
COMUS 3	G50	28 42.79	90.02.00	20.40	6.50	not available
COMUS 3	H50	28 42.80	90 10.22	20.80	5.80	not available
COMUS 3	E20	29 07.25	89 44.56	21.99	2.21	35.84
COMUS 3	SP	29 00.36	89 09.28	24.90	5.20	0.00

Table 5.2. Stepwise regression of nutrient fluxes to all nutrient and sediment parameters.

Nutrient Flux	Parameter	r-square
NO_3	Pore-water gradient (OW-4cm)	0.95
	Bulk Density	0.97
NO_2	Pore-water gradient (OW-1cm)	0.61
	Sediment phosphorus	0.84
	Pore-water gradient (OW-4cm)	0.93
	C:N ratio	0.96
	Sediment chlorophyll a	0.97
	Redox gradient (OW-1cm)	0.98
	Sediment nitrogen	0.99
	Sediment carbon	0.99
	Redox gradient (OW-4cm)	0.99
	Bulk density	1.00
NH_4	Pore-water gradient (OW-1cm)	0.68
	Bulk Density	0.75
	Redox gradient (OW-4cm)	0.80
	Pore-water surface value	0.86
	Sediment carbon	0.88
	Macroinfauna number	0.91
	Macroinfauna dry weight	0.93
	Redox gradient (OW-1cm)	0.94
	Sediment chlorophyll a	0.96
	C:N ratio	0.96
PO_4	Redox gradient (OW-1cm)	0.40
	Sediment chlorophyll a	0.50
	Sediment phosphorus	0.58
	Pore-water gradient (OW-4cm)	0.72
	Sediment nitrogen	0.76
	Macroinfauna ashed dry weight	0.80
	Sediment carbon	0.85
	C:N ratio	0.88
	Redox surface value	0.91
SiO_4	Pore-water gradient (OW-1cm)	0.30
	Sediment carbon	0.48
	Pore-water surface value	0.57
	Redox gradient (OW-4cm)	0.67
	Bulk density	0.76
	Pore-water gradient (OW-4cm)	0.79

Table 5.3. Stepwise regression of nutrient fluxes to only the depositional parameters.

Nutrient Flux	Parameter	r-square
NO3	Chlorophyll deposition	0.14
	Nitrogen deposition	0.30
NO2	Carbon deposition	0.19
	Bulk sediment deposition	0.31
	Nitrogen deposition	0.46
NH4	Phosphorus deposition	0.36
	Bulk sediment deposition	0.59
PO4	Carbon deposition	0.72
	Bulk sediment deposition	0.79
SiO4	Phosphorus deposition	0.40

Table 5.4. t-Test on fluxes between cruises COMUS 1 and COMUS 3.

Nutrient	DF	t-Test	Prob.>|t|	Cruise	Mean	Std. Error
NO3 Flux	66	3.256	0.0018*	COMUS 1	-0.9	9.1
				COMUS 3	-38.7	7.2
NO2 Flux	66	0.577	0.5657	COMUS 1	2.0	1.2
				COMUS 3	2.9	0.9
NH4 Flux	82	0.787	0.4338	COMUS 1	149.6	24.7
				COMUS 3	177.1	24.7
PO4 Flux	82	4.060	0.0001*	COMUS 1	30.4	2.8
				COMUS 3	14.2	2.8
SiO4 Flux	82	0.995	0.3227	COMUS 1	302.5	24.3
				COMUS 3	336.7	24.3

alpha = 0.05; * denotes significant difference

LITERATURE CITED

Alexander, C.R., D.J. DeMaster and C.A. Nittrouer. 1991. Sediment accumulation in a modern epicontinental-shelf setting: The Yellow Sea. Marine Geology 98:51-72.

Aller, R.C. 1980. Relationships of tube-dwelling benthos with sediment and overlying water chemistry. In K.R. Tenore and B.C. Coull, eds. Marine Benthic Dynamics. University of South Carolina Press.

Aller, R.C., J.E. Mackin, W.J. Ullman, C.H. Wang, S.M. Tsai, J.C. Jin, Y.N. Sui and J.Z. Hong. 1985. Early chemical diagenesis, sediment-water solute exchange, and storage of reactive organic matter near the mouth of the Chang Jiang, East China Sea. Cont.Shelf Res. 4:227-251.

Aller, R.C. and J.Y. Aller. 1992. Meiofauna and solute transport in marine muds. Limnology and Oceanography 37:1018-1033.

Aller, R.C., N.E. Blair, Q. Xia and P.D. Rude. Continent. Shelf Res. in press.

Anderson, R.F., G.T. Rowe, P.F. Kemp, S. Trumbore and P.E. Biscaye. 1994. Carbon budget for the mid-slope depocenter of the Middle Atlantic Bight. Deep-Sea Research 41:669-703.

Aspila, K.I., H. Agemian and A.S.Y. Chau. 1976. A semi-automatic method for the determination of inorganic, organic and total phosphate in sediments. Analyst 101:187-197.

Berner, R.A. 1980. Early Diagenesis: A Theoretical Approach, Princeton University Press.

Berner, R.A. 1982. Burial of organic carbon and pyrite sulfur in the modern ocean: its geochemical and environmental significance. American Journal of Science 282:451-473.

Berner, R.A. 1989. Biogeochemical cycles of carbon and sulfur and their effect on atmospheric oxygen over phanerozoic time. Palaeogeogr. Palaeoclim. Palaeoecol. 75:97-122.

Billen, G. 1978. A budget of nitrogen recycling in North Sea sediments off the Belgian Coast. Estuar. Coast. Mar. Sci. 7:127-146.

Billen, G., C. Lancelot and M. Meybeck. 1991. N, P, and Si retention along the aquatic continuum from land to ocean, 19-44. In R. Mantoura, J. Martin and R. Wollast, eds. Ocean Margin Processes in Global Change, pp 19-44.

Boynton, W.R., W.M. Kemp and C.W. Keefe. 1982. An analysis of nutrients and other factors influencing estuarine phytoplankton. In V.S. Kennedy, ed. Estuarine Comparisons. Academic Press, New York, pp. 69-90.

Boynton, W.R. and W.M. Kemp. 1985. Nutrient regeneration and oxygen consumption by sediments along an estuarine salinity gradient. Mar. Ecol. Prog. Ser. 23:45-55.

Boynton, W.R., W.M. Kemp and C.G. Osborne. 1980. Nutrient fluxes across the sediment-water interface in the turbid zone of a coastal plain estuary. In V. Kennedy, ed. Estuarine Perspectives. Academic Press, New York, pp.93-109.

Broecker, W.S., A. Kaufman and R.M. Trier. 1973. The residence time of thorium in surface waters and its implication regarding the fate of reactive pollutants. Earth and Planetary Science Letters 20:35-41.

Callender, R. and D.E. Hammond. 1982. Nutrient exchange across the sediment-water interface in the Potomac River estuary. Estuarine, Coastal and Shelf Science 15:395-413.

Canfield, D.E. 1989. Sulfate reduction and oxic respiration in marine sediments: implications for organic preservation in euxinic environments. Deep-Sea Research 36:121-138.

Carpenter, R. 1987. Has man altered the cycling of nutrients and organic C on the Washington continental shelf and slope? Deep-Sea Research 34:881-896.

Cauwet, G. and F.T. Mackenzie. 1993. Carbon inputs and distribution in estuaries of turbid rivers: the Yang Tze and Yellow rivers (China). Marine Chemistry 43:235-246.

Christensen, J.P. 1994. Sulfate reduction and carbon oxidation rates in continental shelf sediments, and examination of offshelf carbon transport. Continental Shelf Research 9:223-246.

Dagg, M., C. Grimes, S. Lohrenz, B. McKee, R.R. Twilley and J. Wiseman W. 1991. Continental shelf food chains of the northern Gulf of Mexico. In K. Sherman, L.M. Alexander and B.D. Gold, eds. Food Chains, Yields, odels, and Management of Large Marine Ecosystems. Westview Press, pp 67-106.

DeMaster D.J., B.A. McKee, C.A. Nittrouer, J. Qian and G. Cheng. 1985. Rates of sediment accumulation and particle reworking based on radiochemical measurements from continental shelf deposits in the East China Sea. Continental Shelf Research 4:143-155 .

Deuser, W.G. 1988. Whether organic carbon? Nature 332:396-397.

Dukat, D.A. and S.A. Kuehl. 1995. Non-steady-state ^{210}Pb flux and the use of $^{228}Ra/^{226}Ra$ as a geochronometer on the Amazon continental shelf. Marine Geology 125:329-350.

Eadie, B.J., B.A. McKee, M.B. Lansing, J.A. Robbins, S. Metz and J. H. Trefry. 1994. Records of nutrient-enhanced coastal ocean productivity in sediments from the Louisiana Continental Shelf. Estuaries 17:754-765.

Fisher, R.R., P.R. Carlson and R.T. Barber. 1982. Sediment nutrient regeneration in three North Carolina estuaries. Estuarine, Coastal and Shelf Science 14:101-116.

Flint, R.W. and D. Kamykowski. 1984. Benthic nutrient regeneration in south Texas coastal waters. Estuarine, Coastal and Shelf Science 18:221-230.

Gearing, P.I., F.E. Plucker and P.L. Parker. 1977. Organic carbon stable isotope ratios of continental margin sediments. Marine Chemistry 5:251-266.

Glibert, P.M. 1982. Regional studies of daily, seasonal and size fraction variability in ammonium remineralization. Mar. Biol. 70:209-222.

Hargrave, B.R. 1973. Coupling carbon flow through some pelagic and benthic communities. J. Fish. Res. Bd. Can. 30:1317-1326.

Harrison, W.G., D. Douglas, P. Falkowski, G. Rowe and J. Vidal. 1983. Summer nutrient dynamics of the Middle Atlantic Bight: nitrogen uptake and regeneration. Journal of Plankton Research 5:539-556.

Hartwig, E.O. 1974. Nutrient cycling between the water column and a marine sediment. I. Organic carbon. Marine Biology 34:285-295.

Hatton, R.S., DeLaune, R.D. and W.H. Patrick, Jr. 1983. Sedimentation, accretion and subsidence in marshes of Barataria Basin, Louisiana. Limnol. Oceanogr. 28:494-502.

Hedges, J.I. and D.C. Mann. 1979. The lignin geochemistry of marine sediments from the southern Washington coast. Geochimica et Cosmochimica Acta 43:1809-1818.

Hedges, J.I. and P.L. Parker. 1976. Land-derived organic matter in surface sediments from the Gulf of Mexico. Geochim. Cosmochim. Acta 40:1019-1029.

Hedges, J.I., W.A. Clark and G.L. Cowie. 1988. Fluxes and reactivities of organic matter in a coastal marine bay. Limnology and Oceanography 33(5):1137-1152.

Heinrichs, S.M. and W.S. Reeburgh. 1987. Geomicrobiol. J. 5:191-237.

Houghton, J.T., G.J. Jenkins and J.J. Ephraums. 1990. Climate Change, The IPCC Scientific Assessment. Cambridge University Press.

Ittekkot, V. 1988. Global trends in the nature of organic matter in river suspensions. Nature 332:436-438.

Ittekkot, V., S. Safiullah, B. Mycke and R. Seifert. 1985. Seasonal variability and geochemical significance of organic matter in the River Ganges, Bangladesh. Nature 317:800-802.

Kemp, W.M., R.L. Wetzel, W.R. Boynton, D.C.F. and J.C. Stevenson. 1982. Nitrogen cycling and estuarine interfaces: some current concepts and research directions, In V.S. Kennedy, eds. Estuarine Comparisons. Academic Press, New York, pp. 209-230.

Kemp, W.M. and W.R. Boynton. 1984. Spatial and temporal coupling of nutrient inputs to estuarine primary production: the role of particulate transport and decomposition. Bull. Mar. Sci. 35:522-535.

Klump, J.V. and C.S Martens. 1983. Benthic nitrogen regeneration. In E.J. Carpenter and D.G. Capone, eds. Nitrogen in the Marine Environment. Academic Press, New York, pp. 411-457.

Koike, I. and A. Hattori. 1978. Simultaneous determinations of nitrification and nitrate reduction in coastal sediments by a ^{15}N dilution technique. Applied and Environmental Microbiology 35:853-857.

Kuehl, S.A., D.J. DeMaster and C.A. Nittrouer. 1986. Nature of sediment accumulation on the Amazon continental shelf. Continental Shelf Res. 6:209-226.

Li, Y.H. and S. Gregory. 1974. Diffusion of ions in seawater and in deep sea sediments. Geochimica et Cosmochimica Acta 38:703-714.

Lohrenz, S.E., M.J. Dagg and T.E. Whitledge. 1990. Enhanced primary production at the plume/oceanic interface of the Mississippi River. Continental Shelf Research 10:639-664.

McCaffrey, R.J., A.C. Myers, E. Davey, G. Morrison, M. Bender, N. Luedtke, D. Cullen, P. Froelich and G. Klinkhammer. 1980. The relation between pore-water chemistry and benthic fluxes of nutrients and manganese in Narraganstt Bay, Rhode Island. Limnology and Oceanography 25:31-44.

McKee B.A., C.A. Nittrouer and D.J. DeMaster. 1983. The concepts of sediment deposition and accumulation applied to the continental shelf near the mouth of the Yangtze River. Geology 11:631-633.

McKee B.A., D.J. DeMaster and C.A. Nittrouer. 1986. Temporal variability in the partitioning of thorium between dissolved and particulate phases on the Amazon shelf: implications for the scavenging of particle-reactive species. Continental Shelf Research 6:87-106.

Malcolm, R.L. and W.H. Durum. 1976. Organic carbon and nitrogen concentrations and annual organic carbon load of six selected rivers of the United States. USGS Water Supply Paper 1817-F.

Miller-Way, T. 1994. The role of infaunal and epifaunal suspension feeding macrofauna on rates of benthic-pelagic coupling in a southeastern estuary. Ph.D. Dissertation. Louisiana State University.

Miller-Way, T. and R.R. Twilley. 1996. A chemostat microcosm system designed for experimental manipulations in the study of benthic exchange processes. Marine Ecology Progress Series 140:257-269.

Milliman, J.D. 1991. Flux and fate of fluvial sediments and water in coastal seas. In R. F. C. Mantoura, J. M. Martin and R. Wollast, eds. Ocean Margin Processes in Global Change. John Wiley & Sons, pp 69-89.

Milliman, J.D. and R.H. Meade. 1983. World-wide delivery of river sediment to the oceans. The Journal of Geology 91:1-21.

Müller, P.J. and E. Suess. 1979. Productivity, sedimentation rate, and sedimentary organic matter in the oceans -- I. Organic carbon preservation. Deep-Sea Research 26A:1347-1362.

Newman, J.W., P.L. Parker and E.W. Behrens. 1973. Organic carbon isotope ratios in quaternary cores from the Gulf of Mexico. Geochimica cosmochim. Acta 37:225-238

Niino, H. and K.O. Emery. 1961. Sediments of shallow portions of east China Sea and South China Sea. Geol. Soc. Am. Bull. 72:731-762.

Nishio, T. I Koike and A. Hattori. 1982. Denitrification, nitrate reduction, and oxygen consumption in coastal and estuarine sediments. Appl. Environ. Microbiol. 43:648-653.

Nittrouer C.A., R.W. Sternberg, R. Carpenter and J.T. Bennett. 1979. The use of lead-210 geochronology as a sedimentological tool: Application to the Washington continental shelf. Marine Geology 31:297-316.

Nittrouer C.A., D.J. DeMaster, S.A. Kuehl and B.A. McKee. 1987. Association of sand with mud deposits accumulating on continental shelves. In R.J. Knight and J.R. McLean, eds. Shelf Sands and Sandstones, Canadian Society of Petroleum Geologists, Calgary, Canada, pp.17-27.

Nixon, S.W., C.A. Oviatt and S.S. Hale. 1976. Nitrogen regeneration and the metabolism of coastal marine bottom communities. In J.M. Anderson and A. Macfadyed, eds. The role of terrestrial and aquatic organisms in decomposition. Proceedings of the 17th symposium of the British Ecological Society, Blackwell Scientific Publications, England, pp 269-283.

Nixon, S.W., J.R. Kelly, B.N. Furnas, C.A. Oviatt and S.S. Hale. 1980. Phosphorus regeneration and the metabolism of coastal marine bottom communities. In K.R. Tenore and B.C. Coull, eds. Marine Benthic Dynamics. University of South Carolina Press.

Nixon, S.W. 1981. Remineralization and nutrient cycling in coastal marine ecosystems. In B.J. Neilson and L.E. Cronin, eds. Estuarine and Nutrient. Humana Press. Clifton, N.J, pp. 111-138.

Nixon, S.W. and M. Pilson. 1983. Nitrogen in estuarine and coastal marine ecosystems. In E. Carpenter and D. Capone, eds. Nitrogen in the Marine Environment. Academic Press, New York, pp. 565-648.

Parsons, T.R., Y. Maita and C.M. Lalli. 1984. A manual of chemical and biological methods for seawater analysis, Pergamon Press.

Pelegrí, S.P. 1994. Effects of bioturbation by the benthic infauna on nitrification and denitrification processes in freshwater and marine sediments. Aarhus Universitet, Denmark.

Pennock, J.R. 1987. Temporal and spatial variability in phytoplankton ammonium and nitrate uptake in the Delaware estuary. Est.Coast. Shelf Sci. 24:841-857.

Prahl, F.G. and R. Carpenter. 1984. Hydrocarbons in Washington coastal sediments. Estuar. Coast. Shelf Sci. 18:703-720.

Prahl, F.G., J.R. Ertel, M.A. Goni, M.A. Sparrow and B. Eversmeyer. 1994. Terrestrial organic carbon contributions to sediments on the Washington margin. Geochimica et Cosmochimica Acta 58:3035-3048.

Propp, M.V., V.B. Rarasoff, I.I. Cherbadgi and N.V. Lootzink. 1980. Benthic-pelagic oxygen and nutrient exchange in a coastal region of the Sea of Japan. In K.R. Tenore and B.C. Coull, eds. Marine Benthic Dynamics. University of South Carolina Press, pp 265-284.

Romankevich, E.A. 1984. Geochemistry of Organic Matter in the Ocean. Springer-Verlag, New York.

Rowe, G.T. 1978. Benthic nutrient regeneration and high rate of primary production in continental shelf waters: Rowe replies. Nature 274:189-190.

Rowe, G.T., C.H. Clifford and K.L. Smith. 1977. Nutrient regeneration in sediments off Cape Blanc, Spanish Sahara. Deep-Sea Research 24:57-63.

Rowe, G.T., C.H. Clifford, K.L. Smith and P.L. Hamilton. 1975. Benthic nutrient regeneration and its coupling to primary productivity in coastal waters. Nature 255:215-217.

Santschi P.H., D.M. Adler, M. Amdurer, Y.H. Li and J. Bell. 1980. Thorium isotopes as analogues for particle-reactive pollutants. Earth and Planetary Science Letters 47:327-335.

Sarmiento, J.L. and E.T. Sundquist. 1992. Revised budget for the oceanic uptake of anthopogenic carbon dioxide. Nature 356:589-593.

Shultz, D.J. and J.A. Calder. 1976. Organic carbon $^{13}C/^{12}C$ variations in estuarine sediments. Geochimica et Cosmochimica Acta 40:381-385.

Showers, W.J. and D.G. Angle. 1986. Stable isotopic characterization of organic carbon accumulation on the Amazon continental shelf. Continental Shelf Res. 6:227-244.

Smith, S.V. and J.T. Hollibaugh. 1993. Coastal metabolism and the oceanic organic carbon balance. Rev. Geophys. 31:75-89.

Spitzy, A. and V. Ittekkot. 1991. In R.F.C. Mantoura, J.M. Martin and R. Wollast, eds. Ocean Margin Processes in Global Change, pp. 5-18.

Stein, R. 1991. Accumulation of Organic Carbon in Marine Sediments. Springler-Verlag, Berlin.

Strickland, J.D.H. and T.R. Parsons. 1972. A practical handbook of seawater analysis. Bull. Fish. Res. Bd. Can. 169:1-310.

Tans, P.P., I.Y. Fung and T. Takahashi. 1990. Observational constraints on the global atmospheric CO_2 budget. Science 247:1431-1438.

Tan, F.C., D.L. Cai and J.M. Edmond. 1991. Carbon isotope geochemistry of the Changjiang estuary. Estuarine, Coastal and Shelf Science 32:395-403.

Thayer, G.W., J.J. Govoni and D.W. Connally. 1983. Stable carbon isotope ratios of the planktonic food web in the northern Gulf of Mexico. Bull. Mar. Sci. 33:247-256.

Trefry, J.H. and B.J. Presley. 1982. Manganese fluxes from Mississippi Delta sediments. Geochimica cosmochim. Acta 46:1715-1726.

Turner, R.E. and N.N. Rabalais. 1991. Changes in Mississippi River water quality this century. BioScience 41:140-147.

Twilley, R.R., T. Miller-Way and B. McKee. 1994. Synoptic investigations of benthic-pelagic coupling within the Louisiana shelf ecosystem. NOAA Nutrient Enhanced Coastal Ocean Productivity (NECOP) Program.

Walsh, J.J., T.E. Whitledge, F.W. Barvenik, C.D. Wirick and S.O. Howe. 1978. Wind events and food chain dynamics within the New York Bight. Limnol. Oceanogr. 23:659-683.

Whitfield, M. 1969. Eh as an operational parameter in estuarine studies. Limnol. Oceanogr. 14:547-558.

Wollast, R. 1991. The coastal organic carbon cycle: fluxes, sources, and sinks. In R.F.C. Mantoura, J.M. Martin and R. Wollast, eds. Ocean Margin Processes in Global Change. John Wiley & Sons, pp 365-381.

Zeitzschel, B. 1980. Sediment water interactions in nutrient dynamics. In K.R. Tenore and B.C. Coull, eds. Marine Benthic Dynamics. University of South Carolina Press, Columbia, SC, pp. 195 -218.

Zhang, S., V. Ittekkot and W.B. Gan. 1992. Organic matter in large turbid rivers: the Huanghe and its estuary. Marine Chemistry 38:53-68.

The Department of the Interior Mission

As the Nation's principal conservation agency, the Department of the Interior has responsibility for most of our nationally owned public lands and natural resources. This includes fostering sound use of our land and water resources; protecting our fish, wildlife, and biological diversity; preserving the environmental and cultural values of our national parks and historical places; and providing for the enjoyment of life through outdoor recreation. The Department assesses our energy and mineral resources and works to ensure that their development is in the best interests of all our people by encouraging stewardship and citizen participation in their care. The Department also has a major responsibility for American Indian reservation communities and for people who live in island territories under U.S. administration.

The Minerals Management Service Mission

As a bureau of the Department of the Interior, the Minerals Management Service's (MMS) primary responsibilities are to manage the mineral resources located on the Nation's Outer Continental Shelf (OCS), collect revenue from the Federal OCS and onshore Federal and Indian lands, and distribute those revenues.

Moreover, in working to meet its responsibilities, the **Offshore Minerals Management Program** administers the OCS competitive leasing program and oversees the safe and environmentally sound exploration and production of our Nation's offshore natural gas, oil and other mineral resources. The MMS **Royalty Management Program** meets its responsibilities by ensuring the efficient, timely and accurate collection and disbursement of revenue from mineral leasing and production due to Indian tribes and allottees, States and the U.S. Treasury.

The MMS strives to fulfill its responsibilities through the general guiding principles of: (1) being responsive to the public's concerns and interests by maintaining a dialogue with all potentially affected parties and (2) carrying out its programs with an emphasis on working to enhance the quality of life for all Americans by lending MMS assistance and expertise to economic development and environmental protection.